Author:
Ponce Garcia, Fernando Manuel

Title:
Understanding the role of ATM in neutrophil development and activity

Understanding the role of ATM in neutrophil development and activity

Fernando Manuel Ponce Garcia
School of Cellular and Molecular Medicine
May 2022

A dissertation submitted to the University of Bristol in accordance with the requirements for award of the degree of Doctor of Philosophy (PhD) in the Faculty of Life Sciences.

Word count: 28,546

Abstract

Neutrophils are the most abundant white blood cell and the first line of defence against pathogens. Their development is characterised by the compaction and lobulation of their nuclei. They have a wide variety of mechanisms to clear out pathogens and defects in their development or activity result in severe immunodeficiency. To better understand neutrophil function, we analysed ataxia-telangiectasia (A-T), a genetic recessive disease caused by mutations in ataxia telangiectasia mutated (ATM) gene. A-T patients suffer from increased susceptibility to bacterial infections and malignancies. ATM is involved in chromatin double strand break repair and has been shown to be necessary for the development of B- and T-cells. However, little is known about the role of ATM in neutrophil biology. Based on the immunodeficiency observed in A-T patients, we hypothesised ATM might regulate neutrophil development and/or function.

We established a CRISPR/Cas9 ATM knockout ($ATM^{-/-}$) and inducible ATM shRNA knockdown cell line, which we differentiated into a neutrophil-like cell. We tested the antimicrobial capacity of the cell line as well as primary neutrophils treated with an ATM inhibitor and found a decreased ability to kill *Staphyloccocus aureus* in both systems. To understand the mechanism behind this phenotype, we compared differentiation from precursors as well as different antimicrobial responses in both WT and $ATM^{-/-}$ cells. We found increased expression of CD11b and decreased expression of C-type lectin receptors, indicating developmental disturbances as well as reduced production of reactive oxygen species (ROS) and NETs. Increased CD11b surface marker expression was confirmed in neutrophils from A-T patients. These differences were related to dysregulated transcription and nuclear organisation in ATM deficient cells, implicating ATM in neutrophil chromatin regulation. In conclusion, we identified ATM as a regulator of neutrophil development and antimicrobial activity, and a potential therapeutic target in immunodeficiency or inflammatory disease.

Acknowledgements

I want to thank my supervisor Dr Borko Amulic for giving me the opportunity to do research under his supervision, for all the support given throughout the PhD and all the constructive criticism that has helped me become a better scientist.

I want to thank members of the Amulic lab for all the help and support during the PhD and those long Friday days of Barth experiments and a good bar billiards game to end the day. To my friend Drinalda who started with me this journey in Amulic lab and for all the insightful chats we had in the office. To Chris and Will who become my coffee mates and for all the science chats we had in the office. To Sarah who always was there to give some help and for her help in proofreading this dissertation. Finally, to new and previous members of the lab (Katy, Sam, Jamie, Rachel, Nawamin, Chinelo and Claire) for all the good times in the lab.

I want to thank the F-floor immunology group, for all the advice and insightful discussion held during the meetings. To my friend Luis for always being there for a chat and a nice walk for coffee and pastry deal.

I want to thank my internal progression panel, Professor Rafael Carazo and Professor Ash Toye, for all their support and advice during the PhD.

I want to thank Dr Seana for all her help with the experiments with S. aureus and Professor Ruth Massey for providing S. aureus.

I want to thank my family for all the support they have gave me through the PhD even when they are miles away, they always gave me the courage to keep going and had good words to lift my mood.

I want to thank my partner Selene, for always encouraging me to be better and I don’t have enough words to thank her for everything she has done for me during this time, and I can only say we will keep going and breaking more barriers.

I want to thank my Master's and Mexican friends for all those days of fun and barbecues were things seem to be better even if it was a rough time.

I want to thank Cheryl and CMM admin team for all their support and for giving me the opportunity to demonstrate, which allowed me to become a better researcher and learn how to communicate better with students.

Finally, I want to thank CONACyT for sponsoring me for doing this PhD.

Author's declaration

I declare that the work in this dissertation was carried out in accordance with the requirements of the *University's Regulations and Code of Practice for Research Degree Programmes* and that it has not been submitted for any other academic award. Except where indicated by specific reference in the text, the work is the candidate's own work. Work done in collaboration with, or with assistance of, others, is indicated as such. Any views expressed in the dissertation are those of the author.

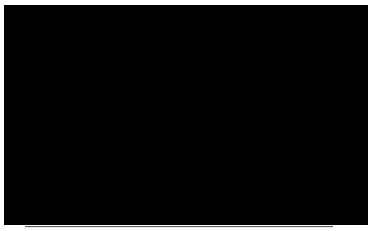

SIGNED:…… DATE:……22 May 2022……

This PhD was funded by CONACyT (Consejo Nacional de Ciencia y Tecnología, México); CVU 748193. The funder had no role in the study design, data collection, data analysis, or preparation of this report.

Table of contents

List of figures

Chapter 1

Chapter 4

Chapter 5

List of tables

Appendix

List of abbreviations

AQP9, Aquaporin 9
ARG1, Arginase
A-T, Ataxia telangiectasia
ATM, Ataxia telangiectasia mutated
AUC, Area under the curve
BM, Bone marrow
CD11b, ITGAM
CD62L, L-selectin
CD66b, CEACAM8
CGD, Chronic granulomatous disease
CLEC4E, Mincle
CLEC5A, C-type lectin domain family 5 member A
CLEC6A, Dectin-2
CLEC7A, Dectin-1
CLP, Common lymphoid progenitor
CLR, C-type lectin receptor
CMP, Common myeloid progenitor
ConA, Concanavalin A
COPD, Chronic obstructive pulmonary disease
CSF, Colony stimulating factor
CSF3R, Granulocyte-colony stimulating factor receptor
CSR, Class switch recombination
CSTG, Cathepsin G
DAMPs, Damage-associated molecular patterns
DDR, DNA damage response
DMF, N,N-Dimethylformamide
DMSO, Dimethyl sulfoxide
dPLB, Differentiated PLB
DSB, Double strand break
ECAR, Extracellular acidification rate
fMLP, N-formylmethionine-leucyl-phenylalanine
G-CSF, Granulocyte colony stimulating factor
GMP, Granulocyte monocyte progenitor
gRNA, Guide RNA
H_2O_2, Hydrogen peroxide
H3, Histone 3
HDAC, Histone deacetylase
HRP, Horseradish peroxidase
HSA, Human serum albumin
HSC, Haematopoietic stem cell

IFN, Interferon
ILs, Interleukins
IL5-R, Interleukin 5 receptor
KU55933, ATM inhibitor
LPS, Lipopolysaccharides
LRRK2, Leucine rich repeat kinase 2
MFI, Mean fluorescence intensity
MOI, Multiplicity of infection
MPO, Myeloperoxidase
NADPH, Nicotinamide adenine dinucleotide phosphate
NE, Neutrophil elastase
NET, Neutrophil extracellular trap
NHEJ, Non-homologous end joining
NOX2, NADPH oxidase 2
OCR, Oxygen consumption rate
OXPHOS, Oxidative phosphorylation
PAD4, Peptidyl arginase deaminase 4
PAMPs, Pathogen-associated molecular patterns
PKC, Protein kinase C
PMA, Phorbol 12-myristate 13-acetate
PPP, Pentose phosphate pathway
PRRs, Pattern recognition receptors
ROS, Reactive oxygen species
RPMI, Roswell park memorial institute
shRNA, Short hairpin RNA
SOD, Superoxide dismutase
TDB, Trehalose-6,6-dibehenate
TEM, Transmission electron microscopy
TLR, Toll-like receptor
TNF, Tumour necrosis factor
US, Unstimulated

CHAPTER 1: Introduction

1.1 Innate immunity and inflammation

Innate immunity is essential for living beings; it mounts a rapid response to defend the organism against pathogens in the first hours of infection and amplifies the signalling to promote activation of adaptive immunity[1]. The skin, leukocytes and other soluble factors comprise the innate immune system[1–3].

Pathogens can enter the body either when the skin gets damaged or via the nasal and oral cavities. The epithelial barrier protects the surface of the gastrointestinal tract as well as the respiratory tract[4]. The mucus in the respiratory and gastrointestinal tract can trap microorganisms, thus usually preventing their migration and growth. The epithelial cells also release fatty acids and lysozymes that are toxic to the pathogens and produce cytokines to recruit innate immune cells[4,5].

1.1.1 Innate immune cells

Haematopoietic stem cells give rise to leukocytes which are formed by the common lymphoid and myeloid progenitors[2,6]. The common lymphoid progenitor (CLP) gives rise to B and T-cells which are part of the adaptive immunity, moreover, natural killer cells also arise from this lineage but are considered part of the innate immune system[1,6]. The common myeloid progenitor (CMP) gives rise to monocytes and granulocytes which are part of the innate immune system[3,4]

Myeloid cells are the first line of defence after the physical barriers are compromised. They can recognise a variety of pathogen-associated molecular patterns (PAMPs) through different receptors and can engulf and phagocytose them[1,5]. Myeloid cells are divided in monocytes and granulocytes. The latter gets their name due to the fact that these cells contain a variety of granules in their cytoplasm[6].

Mononuclear myeloid cells include monocytes and macrophages, the former can be found travelling through the bloodstream, while the latter are long-lived and reside in tissues[3]. They are the main producers of cytokines among the myeloid cells[6].

Neutrophils or polymorphonuclear (PMN) cells are the most abundant of all granulocytes and are short-lived[7]. They migrate to tissues in response to an injury and are able to phagocytose and destroy pathogens[8,9]. Eosinophils and basophils are the less abundant ones of these white cells; eosinophils have the ability to phagocytose and together with basophils are involved in recognition of pathogens (e.g. parasites) and release a variety of granules[1,3,4]. Together, granulocytes have a variety of receptors that allow them to recognise different pathogens and further amplify the immune response whilst recruiting adaptive immunity[2,6].

1.1.2 Pattern recognition receptors

Cells from the innate immune system have a variety of receptors that allow them to recognise different molecules presented by viruses, bacteria, fungi and parasites, as well as signals from injured tissues. These pattern recognition receptors (PRRs) can identify a variety of pathogen-associated molecular patterns (PAMPs) that are different from self-antigens and can also recognise damage-associated molecular patterns (DAMPs) released by injured tissues. The major classes of PRRs are summarised below:

Toll-like receptors (TLR): They recognise a variety of ligands from either PAMPs or DAMPs through their leucine-rich repeat (LRR) domain, leading to enhanced transcription of cytokines to increase the immune response[1,10,11]. TLRs 1, 2, and 4-6 are membrane-bound and recognise different PAMPs from bacteria, fungi and protozoa[3]. On the other hand, TLRs 3, 7 and 9 are localised intracellularly, mainly in phagosomes and endosomes, where they recognise nucleic acids from a virus[2]. Once activated most of the TLRs signal via the adaptor protein MyD88 which activates downstream kinases to further activate the transcription factor NF-κβ[10,12], while TLRs 2 and 4 need an adaptor to recruit MyD88[2]. TLRs are also involved in the recognition of cellular damage, and they can recognise high-mobility group protein 1 (HMGP1), heat shock proteins (HSPs) and RNA and DNA released by damaged cells[2].

C-Type Lectin Receptors (CLR): This is a family of calcium-dependent carbohydrate-binding receptors that binds preferentially mannose and galactose carbohydrates through their QPD (Gln-Pro-Asp) and EPN (Glu-Pro-Asn) motifs[13,14]. This family of receptors can be found as soluble or transmembrane proteins[14,15] that recognise a

variety of PAMPs and DAMPs[14,16] which make them play a role in multiple physiological functions, from behaving as opsonins and growth factors to modulating the immune response[13,15,16]. Dectin-1 (CLEC7A) is the most characterised CLR and is expressed mainly on myeloid cells: neutrophils, monocytes, macrophages, dendritic cells and can also be found on B and T-cells[13]. CLEC7A binds β-1,3-linked glucans found in bacteria, fungi and plant cell walls[13,17]. It signals directly via tyrosine kinase Syk to activate NF-κβ to promote inflammation. In addition, it is involved in the neutrophil respiratory burst, and can activate Nlrp3 to induce production of IL-1β through the inflammasome[4,13,17].

The C-type lectin receptors Mincle (CLEC4E) and Dectin-2 (CLEC6A) are found as transmembrane proteins in macrophages, neutrophils and Kupffer cells[14,18]. They recognise α-mannans found in fungi, bacteria, and plant walls[6,14,19]. Moreover, CLEC4E can recognise cholesterol crystals, lipopolysaccharides (LPS) and *Mycobacterium tuberculosis* cord factor trehalose-6,6-dibehenate (TDB)[14,15], while CLEC6A also recognise *M. tuberculosis*, fungi such as *Aspergillus* and *Candida*, and *Lactobacillus* amongst others[16,18,20]. These receptors bind Fc- receptor γ-chain to signal via Syk and activate NF-κβ to promote an inflammatory response[14,19,21]. Similarly to CLEC7A, when activated they induce phagocytosis, production of ROS and activation of the inflammasome[14,16,18,19].

MDL-1 (CLEC5A) is another member of the CLR family found in the plasma membrane of neutrophils, monocytes and macrophages[22] and recognise fucose and mannose residues from viral glycans, as well as disaccharides of bacterial cell walls[22–24]. It binds DAP10 adaptor to signal downstream to promote inflammatory responses via NF-κβ signaling and can also induce activation of the inflammasome via Nlrp3[14,22]. CLEC5A has been shown to interact with *Listeria monocytogenes* and *Staphyloccocus aureus*, as well as playing a role in the inflammatory response against the lectin Concanavalin-A (ConA)[23].

NOD-like Receptors (NLR): These, like TLRs, contain an LRR domain but are all found intracellularly; ligands for these receptors are the result of phagocytosis and breakdown of the bacterial cell wall[4]. The receptors NOD1 and 2 mainly bind peptidoglycan and signal to activate NF-κβ and Map kinase like TLRs; absence of these receptors has been related to impaired antimicrobial capacity[25]. Another

subfamily of the NLR is NLRP, which also contain a NOD and a pyrin domain, and are important in assembly of the inflammasome, a multiprotein complex that is needed to activate the enzyme caspase-1[26]. Caspase-1 in turn will cleave the pro-forms of IL-1β and IL-18 into their active forms, leading to the recruitment of immune cells[25,26].

Retinoic acid-inducible Gene 1-like Receptors (RLR): These receptors recognise viral RNA and are located in the cytosol of cells[3,27]. There are three different RLRs - RIG-1, MDA5 and LGP2. They signal through recruitment of the adaptor protein MAVS, which in turn activates the transcription factors IRF3 and 7 to induce production of type 1 interferons[27,28]. RIG-1 also plays a role in the inflammasome while interacting with ASC protein[28].

1.1.3 Cytokines

Activation of the above described PRRs can lead to production and secretion of cytokines. Cytokines are proteins or glycoproteins used by cells to signal during immune responses[3,6]. Depending on the outcome of the signal, cytokines can be defined in some of the following ways:

Colony stimulating factors (CSF): They are involved in the differentiation of bone marrow cells into the different subtypes of immune cells. Gradients of these CSFs will also aid in the retention and release of immune cells from the bone marrow[1,6].

Interleukins (ILs): The majority of these cytokines are produced by T cells, however monocytes, neutrophils, endothelium and epithelium can also release them to signal for cells to divide and differentiate[3,4].

Chemokines: They are chemotactic proteins involved in regulating the movement of leucocytes through the bloodstream and into tissues[9,29].

Tumour necrosis factor (TNF): Important in the promotion of inflammation and cytotoxic reactions. TNF-α and β are mainly produce by macrophages and B-cells and can function as a priming signal for activation of some immune cells[9,30].

Interferons (IFNs): This family of cytokines is involved in viral infections. Viral infected cells, macrophages and NK cells release IFN-α and β to limit the spread of the

infection, while T- cells release IFN-γ enhancing activity of macrophages, neutrophils and NK cells[6,29].

1.2 Neutrophil biology

Neutrophils are the first line of defence against infections and the bridge that connects innate and adaptive immunity[7,31]. Over a billion neutrophil are made every day in the bone marrow and they represent 60-80% of all circulating leukocytes[31]. Life is not viable if there are no neutrophils[32]. Neutrophils carry a large amount of antimicrobial peptides in their granules[33] and can release reactive oxygen species (ROS) intracellularly into the phagosome were they are mixed with antimicrobial peptides[31,34], or also can release ROS into the extracellular space[35]. This can kill pathogens but also injure the host, therefore neutrophil development and release to the blood stream are tightly regulated to avoid any host damage and to allow proper antimicrobial activity[31].

1.2.1 Neutrophil development

The bone marrow of healthy individuals can release up to $1x10^9$ neutrophils every day[7]. Neutrophils are produced in the process termed haematopoiesis; this process gives rise to erythrocytes, platelets, B and T-cells, monocytes, and granulocyte cells[3,30]. More specifically, granulopoiesis refers to production of granulocytes. Heamatopoietic stem cells (HSCs) described as CD34+[36] have the ability to differentiate in all blood cell types, moreover, the lineage commitment depends on different transcription factors, including CCAAT/enhancer-binding proteins (C/EBP-α, -β, -γ, -δ, -ε, -ζ), Gfi-1, GATA-1 and 2 and PU.1[30,37–39]. HSCs differentiate into CLP and CMP where they commit to either lymphoid or myeloid lineage[30].

CMP gives rise to the granulocyte monocyte progenitor (GMP), which in turn commits to either granulocyte or monocyte lineage[7,30,40]. Once in the GMP stage, C/EBP-α and PU.1 promote differentiation into monocytes[7,30,41–43]. Granulopoiesis starts after GMP cells have committed to the granulocyte lineage, where they differentiate into neutrophil, eosinophil or basophil[9,30,36], this differentiation process happens in 6.5 days[31,44]. During the myeloblast stage, low concentrations of PU.1 and higher of C/EBP-α promote transition to the promyelocyte stage (**Figure 1.1**)[7,38,42,43]. It can be said that neutrophil differentiation starts at the myeloblast stage[45,46].

There is a tight balance between granulopoiesis, retention in the bone marrow and release of neutrophils into the bloodstream and it can be described as steady-state or emergency granulopoiesis; the former is described as homeostatic granulopoiesis in healthy individuals, while the latter happens upon severe infection or inflammatory responses[3,30,40,46]. The choice of granulopoiesis depends on the strength, type and duration of activating factors[7,9,46]

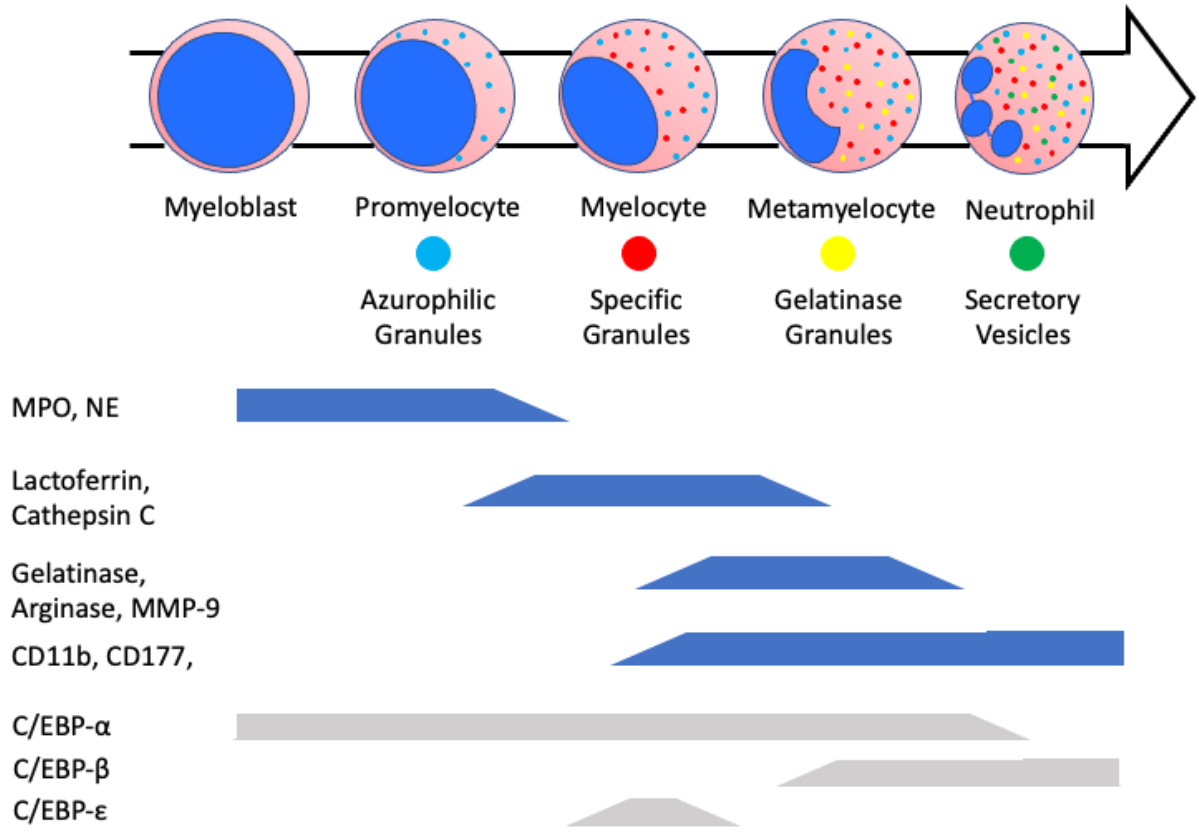

Figure 1.1: Neutrophil development schematic. Development stages starting with myeloblast stage. Promyelocyte stage shows increased expression of azurophilic (primary) granule components. Specific (secondary) granule proteins are expressed at the end of the promyelocyte stage and continue being expressed through the Myelocyte stage. Gelatinase (tertiary) granules are produced during the metamyelocyte stage. Finally secretory vesicle proteins are expressed through the metamyelocyte and neutrophil stage. Most prominent proteins of each granule and transcription factors are shown below the schematic and bars show the times they are highly expressed. Adapted from Yin et al.[33], Borregaard et al.[47], Sollberger et al.[46], Rosales[40].

During steady-state granulopoiesis, C/EBP-α is required in early stages of neutrophil development, it is involved in the transition from CMP to GMP[41,42]. C/EBP-ε and Gfi-1 are required for maturation and generation of neutrophils and eosinophils from GMP

cells[33,37,41,42,46], acetylation of C/EBP-ε and downregulation of GATA-1 induce differentiation into a neutrophil[7,33,37,46], whereas expression of GATA-1 promotes differentiation into an eosinophil[45,48]. Gfi-1 and C/EBP-ε control the transition from promyelocyte to myelocyte stage (**Figure 1.1**)[7,33,46,47] .

During emergency granulopoiesis, induction of C/EBP-β drives neutrophil differentiation, this transcription factor has been shown to promote granulopoiesis even in the absence of C/EBP-α during emergency granulopoiesis[7,46,49]. Retention and release of neutrophils in the bone marrow is regulated by a complex interaction between chemokines and receptors, this will be explained in more detail in section (**1.2.3**)

1.2.2 Ultrastructural changes in developing neutrophils

Neutrophil development is characterised by changes in the structure and compaction of their nucleus. Myeloblast and promyelocyte stages are characterised for having a nucleus with open chromatin covering most of the cytoplasm[44]. Transmission electron microscopy images have shown presence of various mitochondria in the cytoplasm, nucleoli in the nuclei and azurophilic granules in promyelocyte cells[38,44].

Later on, differentiation into myelocyte and metamyelocyte stages shows a reduction in nuclear size, however, chromatin has an open conformation and nucleolar structures can still be found[44]. Finally, across the band cell and mature neutrophil stages, there is a reduction in nuclear size together with lobulation of the nucleus an increase in chromatin compaction (**Figure 1.1**)[50,51]. These cells lack nucleoli structures and have fewer mitochondria[38]. These changes have been related to changes in the structure of nuclear lamina, showing high expression of Lamin A/C and low expression of Lamin B1 and 2 during myeloblast and promyelocyte stages[52,53]. Mature neutrophils show a shift in the conformation of their nuclear lamina, showing decreased expression of Lamin A/C and an increase expression of Lamin B2 and lamin B receptor[52,54,55].

1.2.3 Neutrophil granules

Neutrophils store a variety of antimicrobial substances in their granules, ready to be released into the extracellular space or the phagosome[31]. Depending on the content

and time of their production they are called primary (azurophilic), secondary (specific), tertiary (gelatinase) or secretory vesicles[7,56–58]. The 'target by timing' model is the most accepted hypothesis of how granules are made[57]. This model suggests that proteins in granules are transcribed at a specific time of granulopoiesis, rather than being made at similar times and then sorted into different granules[56,59]

Azurophilic granules are formed during the myeloblast and promyelocyte stages (Figure 1)[37,56], myeloperoxidase (MPO), neutrophil elastase (NE), cathepsin G (CTSG), and CD63 being the predominant contents of this granule[47,60,61]. They are the last granules to be mobilised upon activation and can be secreted to the extracellular space from the plasma membrane or fused with the phagosome to release the antimicrobial substances[31,39,40,62]. α-Defensins and azurocidin are also components of the primary granules and have a broad microbicidal capacity, they can also function as chemoattractant for monocytes, $CD4^+$ and $CD8^+$ T cells[7].

Specific granules are generated during the myelocyte and metamyelocyte stages of granulopoiesis[37,63]. Lactoferrin (LTF), neutrophil gelatinase-associated lipocalin (NGAL), NOX complex proteins and CEACAM8 (CD66b) are the main components of these granules[40,60,63,64]. These granules are easier to mobilise compared to azurophilic granules, and their antimicrobial peptides can be released extracellularly or mixed with azurophilic granules in the phagosome[31,40,58,65]

Gelatinase granules are formed during the metamyelocyte and band cell stage[56,66]. They are the first granules to be mobilised upon contact with the endothelium[33]. They contain membrane receptors such as ITGAM (CD11b), CD177, fMLF-R and antimicrobial peptides; arginase 1, gelatinase and MMP-9[56,60,66]. These granule proteins are involved in the attachment and rolling process of neutrophils[7,39]

Secretory vesicles are the last ones to be formed and contrary to the granules, they do not come from the Golgi[47,58], they are made by endocytosis of the plasma membrane[44,60]. They contain membrane receptors (eg. CD10, CD11b, CD15, CD16, and MMP-25)[64,65,67,68]. They release their content easily after sensing a chemotactic gradient to aid in the attaching of neutrophils to the endothelium[7,39].

1.2.4 Neutrophils and cytokines

Neutrophils are regulated by gradients of chemokines and cytokines throughout their life span[7,39]. During their maturation in the bone marrow (BM), neutrophil express the chemokine receptor CXCR4 which binds to CXCL12 to retain the neutrophil in the BM[9,69]. G-CSF is the main growth factor involved in the maturation of neutrophils[7,29,70] and is also involved during emergency granulopoiesis to increase neutrophil numbers[7,30,69]. Neutrophils are released into the bloodstream by increasing expression of the membrane receptor CXCR2; which in turn cause downregulation of CXCR4 leading to their release from the BM[7,8,70]. Once in the blood stream, gradients of cytokines will guide the neutrophil to sites of infection or injury, and further prime neutrophils to carry out their antimicrobial activity (e.g. phagocytosis, respiratory burst, degranulation and release of neutrophil extracellular traps (NETs)[6,31,39].

During inflammation, neutrophil behaviour is dictated by the cytokines surrounding them. TNF-α directs the neutrophil to sites of inflammation through upregulation of intracellular adhesion molecules, and primes them for degranulating and to sustain respiratory burst[7,29]. CXCL8 (IL-8) is the most common chemoattractant for neutrophils, it also enhances adhesion to the endothelium and promotes degranulation and the respiratory burst[29,69,71]. Leukotriene B_4 (LTB_4), C5a and fMLF increase expression of adhesion molecules facilitating migration through the endothelium, these chemokines also prime neutrophils for an enhanced respiratory burst, degranulation and (NETs) release[33,68].

However, during inflammation, neutrophil can also transcribe cytokines *de novo* to further signal for either an anti-inflammatory or pro-inflammatory outcome[68]. CXCL8 (IL-8) is the most abundant cytokine produced by neutrophils and is released after exposure to various stimuli, including LPS, IL-1 and TNF[29], this allows recruitment and activation of neutrophils to enhance the inflammatory response[32,69,72]. During inflammation, neutrophils enhance T-cell activity and promote proliferation of B-cell by releasing the pro-inflammatory cytokines IL-1α and IL-1β[29,65], moreover, activation by TLR2 agonist induce IL-6 release which also enhance B and T-cell activity[29,72]. Neutrophils have been shown to promote NK cells cytotoxicity and cytokine

production, as well as, proliferation of cytotoxic T-cells and T-helper cells, via IL-12 and MIP1-α[29,72,73] On the other hand, neutrophils are also capable to produce anti-inflammatory cytokines to suppress an inflammatory signal[74]. Release of IL-6 can also work as an anti-inflammatory signal by inhibiting the production of IL-1α and TNF-α [29,72,74].

1.2.5 Neutrophil receptors

Neutrophil express a wide variety of receptors on their plasma membrane to recognise different PAMPs and DAMPs. The adhesion receptors L-selectin (CD62L) and ITGAM (CD11b) are involved in the interaction with the endothelium, mediating the rolling process of neutrophils[39,40,75]. The chemokine receptors BLT1, C5aR and chemoattractant receptor FPRs are involved in migration and priming of neutrophils upon contact with gradients of LTB4, C5a and fMLF[76]. C-type lectins such as CLEC5A, Dectin-1 (CLEC7A) and Mincle (CLEC4E) are non-opsonic receptors that recognise PAMPs like β-glucan and trehalose dimycolate from fungal and bacterial walls[16,21,75], while CD16, CD11b and C5aR recognise opsonised bacteria and fungus promoting phagocytosis of the pathogens by neutrophils[3,31,65,75].

1.2.6 Neutrophil respiratory burst

The neutrophil respiratory burst is defined by the release of reactive oxygen species (ROS) to the extracellular space or the phagosome to kill pathogens. The oxidative burst is catalysed by the multicomplex membrane associated enzyme NADPH oxidase[35]. The complex consists of the electron transferring oxidase $gp91^{phox}$ and $p22^{phox}$ (cytochrome b_{558}), and phosphoproteins ($p40^{phox}$, $p47^{phox}$ and $p67^{phox}$) and two GTP-binding proteins (Rac2 and Rap1a)[34,35,77]. In unprimed cells, the heterodimer of $gp91^{phox}$ and $p22^{phox}$ are bound to the membranes of specific granules, secretory vesicles and plasma membrane[35,64,77], while the trimeric complex of phosphoproteins is found in the cytosol[35,77]. Upon activation, $p47^{phox}$ gets phosphorylated and binds to $p22^{phox}$, simultaneously Rac2 gets activated by the exchange of GDP to GTP and binds $gp91^{phox}$ forming the NADPH complex[35,78,79], allowing the production and release of superoxide anions (O^{-}_{2}) into the extracellular space or into the phagosome[34,35].

NADPH is the electron donor for the production of superoxide anion (O_2^-) from O_2[35,80]. Superoxide is not a strong oxidant but is rapidly dismutated to hydrogen peroxide (H_2O_2) by the enzyme superoxide dismutase (SOD)[35,68,77]. Moreover, MPO can convert H_2O_2 into hypochlorous acid (HOCl), a stronger oxidant that is mainly produced in the phagosomes of neutrophils, and in the extracellular space[34,81]. MPO can directly convert superoxide into singlet oxygen[35,40,61]

These reactive oxygen derivatives diffuse through pathogen membrane and damage their DNA and proteins[35,40]. Deficiencies in NOX2 cause severe bacterial and fungal infections as seen in the rare genetic disease chronic granulomatous disease (CGD), where components of the NOX2 complex have mutations and their neutrophils fail to produce ROS[35,68,81,82].

1.2.7 Neutrophil extracellular traps

Another way neutrophils can stop the spreading of pathogens is through a particular form of cell death were neutrophils release their chromatin associated with antimicrobial peptides from their granules[67,83]; these structures resemble a net and therefore are termed neutrophil extracellular traps (NETs)[83]. They prevent dissemination of pathogens[84,85] and have also been suggested to kill microbes by the antimicrobial activity of the histones and granular enzymes covering the DNA[86]. Production of ROS is required for the formation and release of NETs against most of the stimuli[81,86], and CGD neutrophils do not form NETs[81]. In addition to ROS, neutrophil elastase (NE) is required for NET formation as it is involved in cleaving histones during nuclear decompaction and is part of the released NET where it function as an antimicrobial peptide[83,85,87]. NET formation is also regulated by microbe size: neutrophils will try to phagocytose the pathogen, however, in the case of large pathogens such as filamentous fungi, which are too large to be engulfed, neutrophils decrease phagocytic activity and trigger NET formation, thus preventing pathogen dissemination[13,88,89].

Excessive production of NETs and faulty clearance can be detrimental to the host; histones are toxic to endothelial cells[39], additionally, NETs have been implicated in the development of some diseases such as cancer, vasculitis, and systemic lupus erythematosus (SLE)[40]. For instance, NETs have been shown to interact with platelets

in the bloodstream causing thrombus formation[90], moreover, SLE patients develop autoantibodies against histones, neutrophil peptides and DNA and these autoantibodies make neutrophils more prone to NET[39,40,86]. Similarly, a study made by Albrengues and colleagues[91] showed that NET formation caused by sustained inflammation was able to modify laminin and awaken dormant cancer cells.

1.2.8 Neutrophils in health and disease

Neutrophil activity can also be deleterious for the host and excessive activity has been related to the development of systemic lupus erythematosus, rheumatoid arthritis and type 1 diabetes[35]. During severe pneumonia, dysregulation in cytokine production and clearance of the pathogen cause an overflow of neutrophils into the airways causing the development of acute respiratory distress syndrome (ARDS)[92]. During hyperglycaemia and hyperlipidaemia, neutrophils respond to high levels of glucose in blood and become primed; which can lead into stronger pro-inflammatory responses[8]. This could be seen by increased CD11b expression, elevated ROS production and MPO release; which may contribute to cardiovascular and adipose tissue inflammation, and diabetes[8].

On the other hand, neutrophil activity is necessary for a proper antimicrobial response, and it has also been involved in inflammation resolution[93]. In controlled pulmonary infection, neutrophils are recruited to the airways and resolution of inflammation is initiated by neutrophil apoptosis and clearance by macrophages[92], which then polarises macrophages into an anti-inflammatory state. Moreover, neutrophils are required for proper innate immune response, this can be seen in patients with severe congenital neutropenia, who suffer from life-threatening bacterial and fungal infections[32].

1.3 Ataxia telangiectasia

Ataxia Telangiectasia (A-T) is an autosomal recessive genetic disorder, considered to be a primary immunodeficiency disease (PID), with an incidence of 1 in 40,000-100,000 births. It is caused by a biallelic inactivation of the *Ataxia Telangiectasia Mutated* (*ATM*) gene, located on chromosome 11q22c[94], which codes for a kinase that is important in the DNA Damage Response (DDR).

A-T has broad phenotypic heterogeneity and is characterised by immunodeficiencies[95], cerebellar dysfunction[95], oculocutaneous telangiectasia, predisposition to lymphomas and leukaemias[96], and metabolic disorders[95,96]. A-T patients also suffer from other abnormalities such as growth failure, insulin resistance, diabetes, lung disease, cutaneous abnormalities and cardiovascular disease[95,96]. A-T patients have a poor prognosis, and their life expectancy is around 25 years, with the two most common causes of death being chronic obstructive pulmonary disease (COPD) and malignancies[95].

The early signs of ataxia and ocular telangiectasia as well as high levels of α-fetoproteins, carcinoembryonic antigen expression and low serum immunoglobulins can help lead to an early diagnosis of A-T[95–98]. Currently there is no treatment for this disease and early diagnosis aids providing of palliative care to the patients[99].

The majority of the mutations in the ATM gene lead to a truncated protein which causes complete inactivation or elimination of the protein; other missense or splicing variations lead to a residual ATM kinase activity. These cases cause milder phenotypes and patients are diagnosed during their adulthood. Most of the ATM variants are nonsense mutations (90%) while 10% are missense[99].

The major clinical manifestations in patients with ATM mutations are neurodegenerative processes[98]. The onset of spinocerebellar neurodegeneration occurs around 6 to 18 months of age[95]. and is related to atrophy of the cerebellar vermis, especially Purkinje cells and granule neurons[100].

A-T patients show a significant increased risk of developing cancer. The most prevalent type of cancer among A-T patients are leukaemias and lymphomas occurring at a young age[95,97,101]. However, adults are also susceptible to lymphomas as well as solid tumours including liver, breast, gastric and oesophageal carcinomas[101]. Another cause of susceptibility to malignancies is due to the Epstein-Barr Virus (EBV), this being due to immunodeficiency and poor DNA repair[95,96]. Treatment of malignancies can be difficult since chemotherapy can worsen the immunodeficiency phenotype[98].

A minority of A-T patients suffer from insulin resistant diabetes; however, non-diabetic patients may have increased glycaemia and decreased insulin sensitivity[97,102]. A study carried out by Connelly et al tested A-T patients against healthy controls using a glucose oral test and found that A-T patients were associated with dysglycaemia and reduced insulin sensitivity[103]. This suggests that ATM might play a role in glucose and insulin signalling pathways.

1.3.1 Immunodeficiency in A-T patients

Some studies suggest that 80% of A-T patients suffer from infections, especially in the sinopulmonary region with onset in the early years of life[97,98]. Some complications that patients develop are otitis, pneumonia and mucocutaneous infections (e.g. *S. aureus, Candida*)[97,98], along with autoimmunity, hepatosplenomegaly and in rare cases neutropenia[86,97,104].

Generally these patients have low numbers of B and T cells (lymphopenia), deficiency in antibody production and hypogammaglobulinemia[95] Approximately 70% of A-T patients present primary immunodeficiencies (PID) due to impaired antigen receptor recombination, class switch recombination (CSR) and antibody production[95].

1.3.2 Innate immunity and inflammation in A-T

Few studies have been done regarding the innate immune system of patients with A-T and it remains unclear if innate deficiencies exist in these patients. Clinical studies have shown similar blood number of neutrophils between healthy donors and A-T patients[95,97]. One study found that neutrophils from A-T patients have an increased production of the chemokine IL-8 and a longer lifespan[82]. A second study performed RNAseq in peripheral blood mononuclear cells from A-T patients and found that signature genes for inflammation, malignancy and cell growth were enriched in these cells, furthermore, they found an association with patients that had elevated IL-8 levels in serum with a higher risk of malignancy after 6 years[105]. It has been shown that approximately 10% of A-T patients suffer from non-infectious chronic cutaneous granulomas. Treatment of these granulomas rely on steroids and inhibitors of tumour necrosis factor (TNF-α)[98].

1.4 Ataxia telangiectasia mutated

Ataxia telangiectasia mutated (ATM) kinase is a member of the phosphatidylinositol 3-kinase-related kinase (PIKK) family and is involved in the coordination of DNA damage response (DDR)[106–108]. Under normal conditions, ATM is found in a dimeric or multimeric inactive state. Following interaction with the MRE11-RAD50-NBS1 (MRN) complex after sensing of double-strand breaks (DSBs), activation of ATM occurs through autophosphorylation at serine 1981 of each subunit promoting dissociation from the dimeric state to an active monomeric state[106,109]. Moreover, ATM can also be active in its dimeric form when ROS crosslinks cysteine residues forming disulphide bonds and activates ATM independently of DDR[110–112]. ATM is the apical kinase for the response to DSBs; it coordinates DNA repair mainly in heterochromatic regions through non-homologous end joining (NHEJ) processes preferentially in G1, although it can also act throughout the cell cycle by promoting homologous recombination (HR)[107,113–116] (**Figure 1.2**).

Ataxia-Telangiectasia (A-T) patients bear mutations in the ATM gene causing impaired DDR signalling[108]. ATM-deficient cells are impaired in establishing cell/cycle checkpoints (G1/S-G2/M)[107], and therefore these cells show increased susceptibility to ionising radiation and genome instability[106]. In addition to disruptions in DDR, various structures are seen to be disturbed in the absence of ATM; for example, numbers of mitochondria are increased in these cells apparently due to a defective destruction of abnormal mitochondria rather than an enhanced biogenesis[110]. In addition, the nuclear lamina has been observed to be affected in ATM-deficient cells, showing an increase in Lamin B protein but not in mRNA levels in A-T cells[106].

1.4.1 ATM role in DNA damage response

It is noteworthy that ATM is capable of regulating the chromatin compaction state through post-translational modifications in chromatin modifying enzymes, which reorganise chromatin architecture near the DSB to allow an efficient DNA repair[112]. ATM works throughout the cell cycle and mainly relies on non-homologous end joining (NHEJ) to fix DSB, however during S/G2 phase, ATM can also rely on homologous recombination (HR) to fix DNA damage[117]. During DDR, phosphorylation of KRAB

domain-associated protein 1 (KAP1) at serine824 disturbs its interaction with the chromodomain helicase DNA binding protein isoform 1 (CHD3.1) causing chromatin relaxation[112].

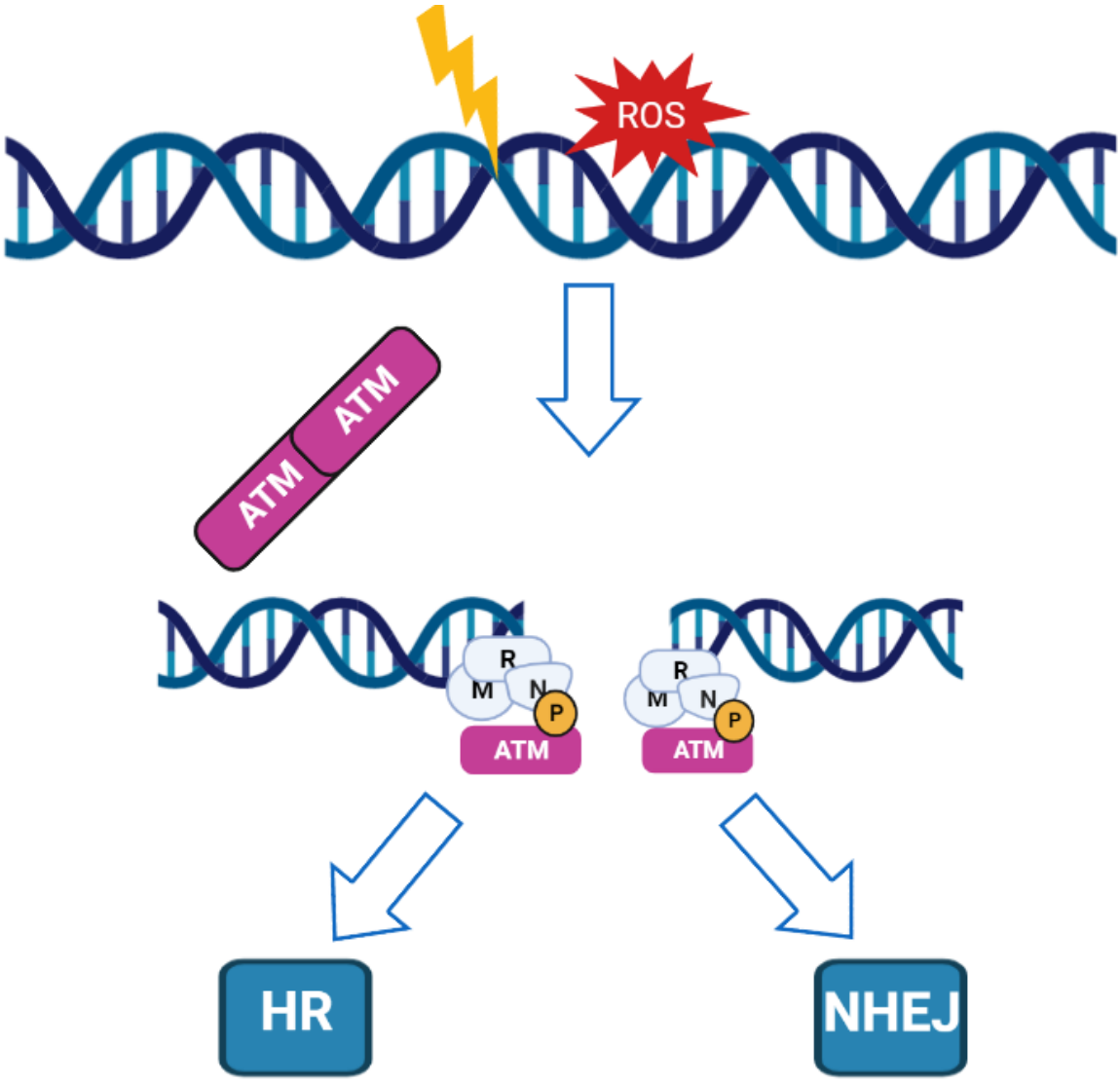

Figure 1.2: Schematic of ATM activation by DSBs. Ionising radiation and reactive oxygen species can cause double strand breaks in the DNA. MRE11-RAD50-NBS1 (MRN) complex binds to the site of break and phosphorylates ATM which gets activated and phosphorylates downstream substrates to carry on with the repair of the DNA damage, either by homologous recombination or non-homologous end joining. Adapted from Blackford et al.[107] and Berger et al.[112] Created using Biorender.

In neurons, SIRT1 is recruited to DSB foci to further stimulate ATM and histone deacetylase 1 (HDAC1). HDAC1 is required to keep a closed conformation at the

beginning of the process; this allows the broken DNA ends to be retained and halts transcription in the vicinity avoiding transcriptional stress[118,119].

1.4.2 ATM in chromatin remodelling

ATM has been implicated in regulation of chromatin state, independently of DNA damage[120]. For instance, in A-T cells defective activity of protein phosphatase 2A (PP2A) has been seen to increase histone deacetylase 4 (HDAC4) hypo phosphorylation, causing it to relocate in the nucleus and result in increased deacetylation and aberrant gene expression, due to condensation of chromatin and repression of transcription[106,121]. Another study showed that inhibition and depletion by siRNA of ATM lead to an increase in the repressive histone mark H3K9me3 and an increase in chromatin compaction in NIH3T3 cells[122]. Similarly, another group reported that, under hypoxic conditions, ATM interaction with the methyltransferase SUV39H1 increases the expression of the repressive mark H3K9me3[123]. ATM activity is required to activate downstream enzymes capable of modulating chromatin structure as seen in this section.

1.4.3 Non-canonical roles of ATM

There is evidence to show that ATM can be activated without DNA damage through other signals such as: chromatin hyperacetylation[109], direct binding to DNA[106], reactive oxygen species (ROS)[111] and interaction with Aurora B kinase[113,124,125]. Ji and colleagues[126] demonstrated ATM activation in the absence of DNA damage through chromatin opening by the SWI/SNF complex. This activation halts hepatic cell conversion of induced pluripotent stem cells (iPSC)[126]. In addition, ATM is also linked with recruitment of the polycomb repressive complex 1 and 2 (PRC1 and PRC2), as well as in microRNA(miRNA) biogenesis[110,112]. Tresini et al propose a model where the formation of R-loops activates ATM to mobilize the spliceosome machinery and regulate alternative splicing during transcriptional stress[127].

Aside from its canonical role in DDR and chromatin remodelling, it has been suggested that ATM is implicated in metabolic pathways such as the pentose phosphate pathway (**Figure 1.3**); this pathway is involved in the production of antioxidants (eg. superoxide

dismutase [SOD] and glutathione) as well as synthesis of nucleic acids[128]. Gregory et al found lower activity of glucose 6-phosphate dehydrogenase (G6PD) enzyme in ATM deficient cells[110,129]; this enzyme is essential to maintain redox homeostasis by producing NADPH in the oxidative part of pentose phosphate pathway[128]. New evidence suggests a background role for ATM in signalling processes in the cytoplasm and its involvement in proteasome degradation[110,130].

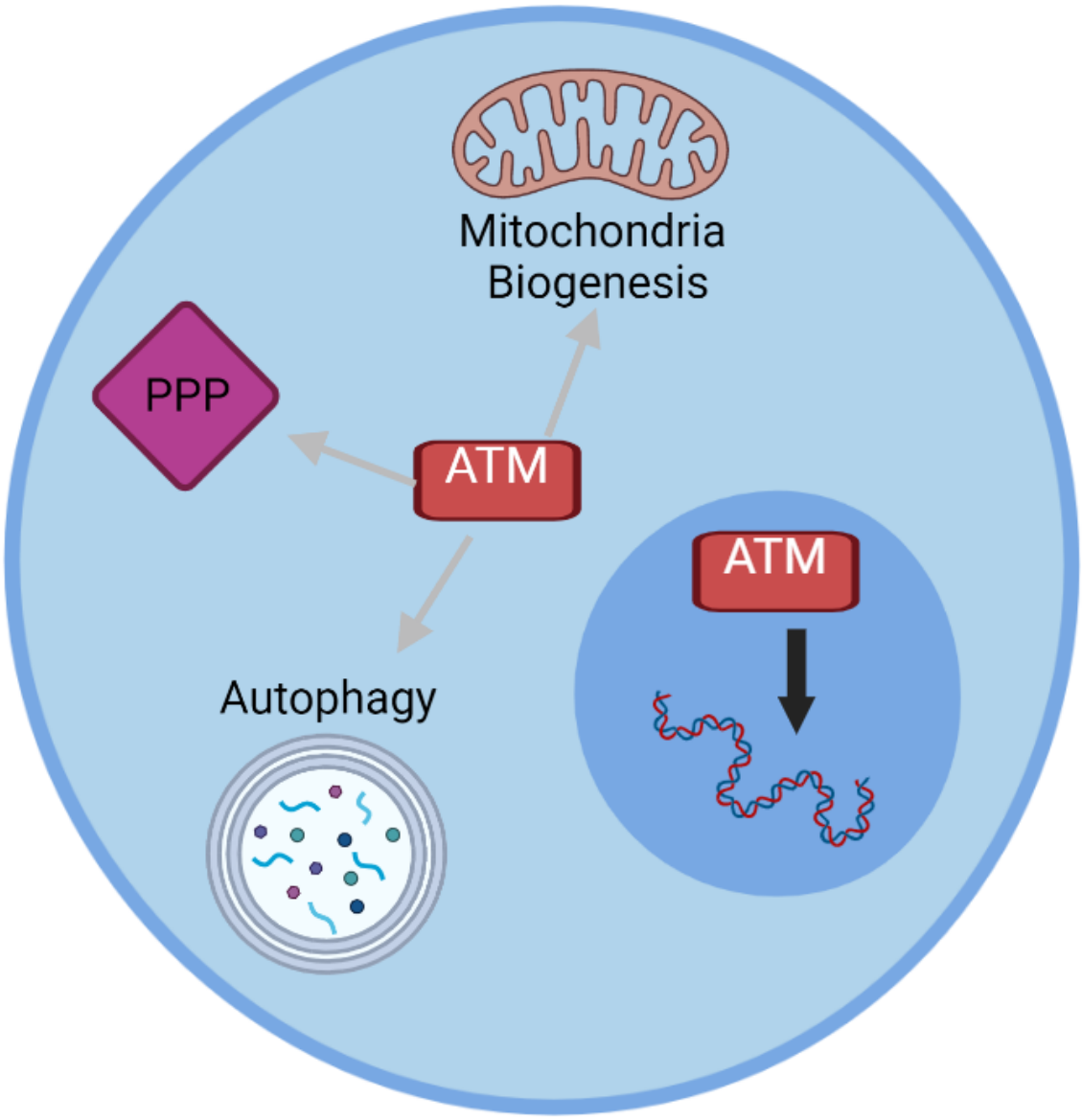

Figure 1.3: Schematic of ATM non-canonical roles. ATM can be found in the nucleus and the cytoplasm of the cell. In the nucleus it can remodel the chromatin in the absence of DNA damage. In the cytoplasm it can be activated by reactive oxygen species and be involved in homeostasis of mitochondrial biogenesis, promote autophagy and pentose phosphate pathway. Adapted from Stracker et al[106] and Shiloh et al[110]. Created using Biorender.

1.4.4 ATM DDR in innate immunity

Different roles for DDR and ATM have been reviewed by Neves-Costa and Moita[131]. DNA damage in early stages of *Caenorhabditis elegans* development, prime the adult tissue to further tolerate and increase survival against lethal conditions[131]. Similarly, they reviewed studies where ATM is involved in cytokine inhibition and downstream signalling of TLR activation by LPS[131]. Moreover, different roles for ATM in immunity and inflammation have been previously shown, with contrasting outcomes, from promoting secretion of pro-inflammatory cytokines to downregulating inflammatory mediators[82,131–134].

A study by Figueiredo and colleagues[132] showed treatment with anthracyclines, a DNA damage agent protect mice against severe sepsis. They found ATM was needed to promote disease tolerance in a sepsis model caused by cecal ligation and puncture. Treatment with anthracycline, a chemotherapy drug known to activate ATM through DNA damage, increased mice survival to sepsis. Disease tolerance was associated with decreased pro-inflammatory cytokine release and similar bacteria burden compared to PBS treated mice. The protective effect of anthracycline was decreased in mice lacking ATM, showing ATM was required for protection against sepsis in anthracycline treatment[132].

A study by Härtlova and colleagues[134] showed an increase in interferon production in cells lacking ATM, they demonstrated this was not directly caused by the loss of ATM, but by unrepaired DNA being released to the cytosol as ssDNA and recognised via STING, which further primed the immune system against viral infections[134]. On the other hand, a study made by Erttman and colleagues[133] showed enhanced bacterial susceptibility in mice lacking ATM. Enhanced ROS was seen in bone marrow derived macrophages from $ATM^{-/-}$ which cause impairment in inflammasome formation leading to reduce production of IL-1β[133].

Lastly, a role for ATM in neutrophil lifespan and cytokine production was studied by Harbort and colleagues[82]. They showed inhibition of ATM cause increased neutrophil lifespan and cytokine production (IL-8, MIP-1α, IL-1β, IL-6 and TNF) against LPS and IL-8 increase production was also seen in A-T peripheral blood neutrophils treated with LPS[82]. They further showed induction of DNA damage decreased IL-8 production

against LPS, Finally, they showed NADPH ROS production was required for ATM activation and regulation of IL-8 production, neutrophils from CGD patients showed increased IL-8 production compared to healthy controls. Similarly, neutrophils treated with a ROS scavenger also showed increased IL-8 production. They showed induction of DNA damage with etoposide in neutrophils treated with a ROS scavenger decrease IL-8 production[82]. This showed a role for ROS induced ATM activation in the regulation of pro-inflammatory cytokines by neutrophils. This is in our knowledge the first paper to study a role for ATM in neutrophil function.

In summary, ATM is a kinase involved in many pathways as explained in this section. The role of ATM in redox homeostasis plays an important role in safeguarding the integrity of DNA, however this has not been explored in neutrophils, where production of NADPH from the pentose phosphate pathway is also used for the production of superoxide instead of glutathione substrate. Moreover, ATM's role in chromatin remodelling has not been specifically related to differentiation in any cell. There is evidence ATM is involved in chromatin organisation[120,121], therefore, there is the possibility ATM could be involved in neutrophil development. Since chromatin changes are very prominent during neutrophil development, making this an excellent model for testing the role of ATM in chromatin organisation.

CHAPTER 2: Objectives and hypothesis

2.1 Objectives

- Investigate the role of ATM in neutrophil antimicrobial response
- Investigate the role of ATM in neutrophil development
- Determine the mechanism by which ATM regulates neutrophil antimicrobial activity

2.2 Hypothesis

ATM is an apical kinase in the DNA damage response that also has non-canonical roles in chromatin remodelling, mitochondrial homeostasis, and metabolism. A-T patients are susceptible to bacterial infections but the role of ATM in neutrophil activity has not been tested. We hypothesized that ATM regulates neutrophil antimicrobial responses. Neutrophils are known to reduce mitochondrial mass and to compact their chromatin through development to acquire their characteristic lobulated nucleus and low number of mitochondria. We hypothesised that ATM is required during neutrophil development for chromatin compaction and a proper mitochondrial biogenesis, as well as defective ATM might result in dysregulation of neutrophil antimicrobial capacities, contributing to the immunodeficiency seen in A-T patients.

CHAPTER 3: Methods

3.1 Healthy donor and patient blood

Blood collection from healthy donors was approved by NHS REC committee. Informed consent was obtained from all donors. A-T patient blood samples were obtained with approval from the ethical committee of Charité University Hospital, Berlin, Germany and informed consent was given by the patient or their parents in case of children. Blood samples were obtained by venous puncture and collected in EDTA tubes.

3.2 Neutrophil purification

3.2.1 Negative immunomagnetic selection

Whole blood (5ml) was processed using EasySep™ Direct Human Neutrophil Isolation kit (STEMCELL Technologies) and processed as per manufacturer protocol. Cells were counted using a haemocytometer.

3.2.2 Gradient purification

Human neutrophils were isolated using a double gradient step purification [82]. Whole blood was layered carefully on top of a layer of Histopaque-1119 (Sigma) in a ratio of 1:1. Cells were spun down at 800xg for 20 minutes with slow deacceleration. Four layers were visualised after centrifugation. the top two (plasma and PBMC layers) were discarded, the third (pink layer ”Neutrophils”) was collected in a new tube and discarded the last layer (red blood cells). We washed with PBS (Gibco) + 0.2% human serum albumin (HSA) (SEQENS) and spun down at 400xg for 5 minutes. Cells were resuspended in 1ml of PBS and layered carefully on top of a discontinuous percoll (G&E) gradient; 2ml were used for each layer, starting with highest concentration at the bottom (85%, 80%, 75%, 70%, 65%). Spun down at 800xg for 20 minutes with slow deacceleration. The first white layer was discarded, and the second layer was collected in a new tube, we washed once with PBS + 0.2%HSA. Spun down at 400xg for 5 minutes. Resuspend in 1ml of PBS and count neutrophil concentration with a haemocytometer.

3.3 Cell culture

PLB-985 cell line was cultured in growth medium Roswell Park Memorial Institue 1640 Medium (RPMI-1640) (Gibco) media supplemented with 10% Heat inactivated fetal bovine serum (FBS) (Gibco), 2mM L-Glutamine (Gibco), 100 units/ml Penicillin and 100µg/ml Streptomycin (Gibco). Cells were passaged twice a week to keep confluency of 1.5-2x10^6/ml.

HEK293Tcell line was cultured in Dulbecco's modified eagle medium (DMEM) (Gibco) supplemented with 10% FBS, 2mM Glutamine, 100units/ml Penicillin and 100 µg/ml Streptomycin. We kept cells at a confluency of 80%.

3.4 PLB differentiation

PLB-985 cell line was seeded in a 6 well plate at 1x10^6 cells per well in differentiation media; RPMI-1640 media supplemented with 2.5% FBS, 2mM Glutamine, 100units/ml Penicillin, 100µg/ml Streptomycin, 0.5% N,N-dimethylformamide (DMF) (Sigma) and 1x Nutridoma-CS (Sigma)[135]. On day 4 of differentiation wells were topped up with 2ml of differentiation media. On day 6, cells were collected from the wells and spun down at 400xg for 5 minutes. Cells were resuspended in 1ml assay media; RPMI-1640 w/o phenol red supplemented with 1% FBS, 0.5% DMF and 2mM Glutamine. Cells were layered carefully on top of 3ml of Histopaque-1077 (Sigma) and spun down at 800xg for 20 min with soft deacceleration. The white top layer was collected and placed in a new falcon tube. Cells were washed with 10ml assay media and spun down at 400xg for 5 minutes. Cells were resuspended in 1ml PBS and counted using a haemocytometer. We added 50ng/ml doxycycline (Sigma) to the media throughout the differentiation process for the PLB shRNA knockdown cell line.

3.5 Luminol measurement of neutrophil respiratory burst

Primary neutrophils or differentiated PLB (dPLB) cells were seeded at 1x10^5 cells per well in 100µl of ROS media: Hanks' buffered saline solution (HBSS) (Lonza) with 2mM $CaCl_2$ and 2mM $MgCl_2$, supplemented with 1mM N-2-hydroxyethyl piperazine-N-2-ethane sulfonic acid (HEPES) (Gibco) and 0.025% HSA in 96 well white plates (Sterilin). ATM inhibitor KU55933 (Sigma) was added to the media at a final concentration of 10µM before adding the cells to the media; cells were incubated in

media with inhibitor or dimethyl sulfoxide (DMSO)(Sigma) for 45 minutes before stimulation. We diluted horseradish peroxidase (HRP) (Sigma) and Luminol (Sigma) 1:200 in ROS media, and 11µl were added to each well for a final concentration of 1.2U/ml HRP and 50µM Luminol[88]. Cells were incubated at 37°C in 5%CO_2 for 15 minutes. Stimulation was carried out by adding 5µl of stimuli for a final concentration of; 100nM phorbol12-myristate 13-acetate (PMA)(Sigma), 50µg/ml concanavalinA (ConA) (Sigma), 50µg/ml trehalose-6,6-dibehenate (TDB) (Invivogen), MOI 20 *Staphylococcus Aureus* (JE2), MOI 5 *Candida albicans*. We recorded luminescence measurement every 2 minutes for 121 cycles with a gain of 3600 on a FLUOstar (BMG Labtech) plate reader.

3.6 Measurement of NET production

Cells were seeded at 1x10^5 cells per well in black/clear bottom 96 well plates in 100µl NET's media; RPMI-1640 w/o phenol red supplemented with 1mM HEPES and 0.05% HSA. Inhibitors were added to the media, and then cells were added and incubated for 45 minutes before stimulation. Stimuli were added in 5µl for a final concentration of 50nM PMA, 50µg/ml ConA, 50µg/ml TDB. The time course of NET production was analysed using an IncuCyte ZOOM (Essen Biosciences) cell imaging system. We added SYTOX™ Green (Invitrogen) at a final concentration of 1µM for detection of NET formation; images were acquired every 30 minutes using a green laser (400nm wavelength excitation) for 4 hours. Endpoint measurement of NETs was either acquired on EVOS (Invitrogen) confocal microscopy or Incucyte imaging system. 1µM SYTOX ORANGE and 250nM SYTO GREEN were added to the plate and left to incubate for 5 minutes at room temperature covered from light. Images were taken at 10x magnification using green and red channels; for Incucyte, a scan on demand was made to have a single time point acquisition. Images were analysed on FIJI software.

3.7 Cytokine production and analysis

Cells were seeded at a concentration of 1x10^5 cells/ml in 200µl of growth media in a flat bottom 96 well plate. We stimulated cells with either 100ng/ml lipopolysaccharides (LPS from E. coli) (Sigma), 25µg/ml Opsonised Zymosan (OZ) (Sigma), 100nM PMA, and 2ng/ml TNF (Peprotech) for 18 hours at 37°C 5% CO2. We collected the

supernatant and analysed IL-8 production using the Human IL-8/CXCL8 DuoSET ELISA kit (R&D Systems) following the manufacturer's instructions.

3.8 Metabolic analysis

Metabolic analysis was carried out on the extracellular flux analyser Seahorse XFe96 analyser (Agilent Technologies), and experiments were run as manufacturers protocol. Briefly, we seeded $4x10^5$ cells per well in Seahorse media: RPMI-1640 (Agilent Technologies) supplemented with 2mM Glutamine and with or without 5mM Glucose (Sigma). We prepared a 10x working solution of Oligomycin (Alfa Aesar) 25μM, carbonyl cyanide 4-(trifluoromethoxy) phenylhydrazone (FCCP) (Sigma) 5μM, Rotenone (Sigma) 10μM and Antimycin A (Alfa Aesar) 10μM, Glucose 100mM and 2-Deoxy-D-Glucose (2-DG)(Sigma) 500mM. We loaded 10x solutions into ports (A-D) (20μl A, 22.2μl B, 24.7μl C and 27.4μl D). We measured the metabolites in the media every 5 minutes; the first three reads are the basal state of the cell before any inhibitor or stimuli are injected. After each injection, we made three readings every 5 minutes, analysing two different values; Oxygen consumption rate (OCR) and extracellular acidification rate (ECAR). OCR allows analysis of mitochondrial metabolism, and ECAR allows analysis of glycolytic metabolism.

3.8.1 Mitochondrial stress test

This assay analyses a cell's oxidative phosphorylation (OXPHOS) capacity by quantifying the oxygen consumed by the mitochondria while being challenged with drugs that either block the proton flux or allow their free transfer. For this assay, we seeded the cells in Seahorse media with glucose and plated at the concentration stated before. The first three measurements represent the basal mitochondrial capacity of a cell. Then we injected 2.5μM Oligomycin, an inhibitor of Complex V of the electron transport chain that inhibits mitochondrial metabolism and allows measurement of ATP produced by the mitochondria. Then we injected 500nM FCCP, which uncouples mitochondrial membrane and allows measurement of maximal mitochondrial capacity. Finally, we injected 10μM Rotenone and 10μM Antimycin A; the former inhibits Complex I while the latter inhibits Complex III, which completely shuts down mitochondrial metabolism.

3.8.2 Glycolytic stress test

This assay analyses a cell's glycolytic capacity by quantifying the extracellular acidification rate caused by the release of lactate during glycolysis. PLBs were resuspended in Seahorse media without glucose and seeded in each well at the concentration previously stated. The first three measurements show basal acidification of the media. At this point, cells are on glucose-free media, and glycolysis is minimal. Then we injected 10μM glucose and measured it three times to analyse the cell's glycolysis. The second injection is 2.5μM Oligomycin which inhibits mitochondrial metabolism and allows measurement of the maximal glycolytic capacity of the cell. Finally, we injected 50μM of 2-DG, an analogue of glucose blocking down glycolysis.

3.9 CRISPR knockout generation in PLB

pLentiCRISPRV2 construct with a puromycin selection marker (GenScript) was used. We had two different guide RNA targeting the ATM gene, crRNA1: CCAAGGCTATTCAGTGTGCG and crRNA2: TGATAGAGCTACAGAACGAA. HEK293T cells were transfected with each of the constructs and the packaging plasmids (pMD2 and pPAX2) using lipofectamine 2000 (Invitrogen). After day 3 post-transfection, the supernatant containing the virus was collected, and aliquots were frozen down at -80ºC. PLB-985 were plated at $1x10^6$ cells in a 6 well plate with 3ml of medium and 500μl of the virus. On day 2 post-infection, we added puromycin at a final concentration of 2.5mg/ml to each well, including the uninfected one as control, 3 days later, we split the cells 1:3 in RPMI media supplemented with puromycin to dilute cell debris and allowed cells to grow better. When cells started to grow better, puromycin was removed, and cells were diluted in 35 ml of RPMI to a final 8 cells/ml concentration. Cells were plated in 96 well plates for the single-cell cloning step. After 2 weeks we looked for the wells where cells grew, took a mix of fast and slow-growing colonies and plated them in new 96 well plates (duplicate). Thirty-two clones were selected for ATM crRNA1 and crRNA2, one of the plates was frozen down at -80ºC, while we used the other to extract DNA of the cells for further sequencing.

To sequence our single clones, we followed Schmid-Burgk protocol[136]. Firstly, we amplified a locus-specific region (300bp-400bp) using primers targeting 150bp upstream and downstream of the gRNA site of recognition. Afterwards, we use our

locus-specific PCR product as a template to carry out a barcoding PCR using a combination of eight forward primers and 12 reverse primers mentioned in[136]. Finally, we use outknocker software[136] to analyse each single clone sequence to look for insertions or deletions in the specified region. Primers sequences are shown in table (**Table A5**)

3.10 Generation of inducible shRNA knockdown in PLB

We followed Frank and colleagues' protocol[137] to generate a doxycycline-inducible shRNA lentiviral vector. We used EZ-Tet-pLKO-Puro vector[137] as a template. Firstly, we digested 5µg of the vector with 20 units of the restriction enzymes NheI-HF and EcoRI-HF (NEB) in a 50µl digest reaction at 37ºC for 3 hours and enzymes were heat-inactivated at 80ºC for 20 minutes. The cut vector was then dephosphorylated for 30 minutes at 37ºC using 5 units of Antarctic Phosphatase (NEB) and the digest reaction supplemented with AP buffer; the reaction was stopped by heat-inactivation at 80ºC for 5 minutes and dephosphorylated cut vector was diluted with water to a final volume of 200µl. Next, we purify the dephosphorylated cut vector with polyethylene glycol (PEG) (Sigma) to size exclude the stuffer region. Then, we made a 2x mix of 12%(w/v) PEG-8000 and 20mM Magnesium Chloride and added 1:1 to the dephosphorylated cut vector. We mixed gently by inversion and left to incubate at room temperature for 1 hour. After incubation, we spun down the mix at 15,000xg for 40 minutes in a benchtop centrifuge, then we discarded the supernatant and added 500µl of 70% ethanol (Sigma) to wash the pellet and span down at 15,000xg for 10 minutes. Next, we aspirated the ethanol and repeated once more the wash step. After the second wash, we aspirated the ethanol, and the DNA pellet was allowed to air dry. Then, the pellet was resuspended in 50µl of RNase free water and quantified using a nanodrop (Thermo Fisher Scientific).

We chose sequences from the BROAD RNAi Consortium database (https://portals.broadinstitute.org/gpp/public/gene/search) for shRNA oligo design. We selected three different ATM shRNA target sequences: ATM shRNA1 (TRCN0000194969), ATM shRNA2 (TRCN0000039951) and ATM shRNA3 (TRCN0000194861). Oligos were designed as described in[137] and ordered from Eurofins Scientific (**Table A5**). We resuspended shRNA oligos at 100µM in duplex buffer (100mM Potassium Acetate, 30mM HEPES, pH7.5). We then mixed 20µl of

each oligo and annealed using a simpliamp thermal cycler (Thermo Fisher Scientific) with a program set to start at 95ºC and drop 5ºC/minute down to 12ºC. Next, we resuspend the annealed oligos to 360µl with water. We precipitated annealed oligos by adding 40µl of 3M sodium acetate and 1 ml 100% ethanol and incubated at -20ºC for 20 minutes. DNA was spun down for 30 minutes at 15,000xg in a benchtop centrifuge, washed twice with 70% ethanol and resuspended in 500µl water and quantified using a nanodrop. To phosphorylate oligos overhangs, we added 10 units T4 polynucleotide kinase (NEB) and 50µl T4 ligase reaction buffer (NEB) to the oligos mix and incubated at 37ºC for 30 minutes and heat-inactivated at 65ºC for 20 minutes.

Ligation was performed by adding 100ng of vector (digested and dephosphorylated), 800ng phosphorylated oligos and 5 units of T4 DNA ligase (Thermo Fisher Scientific) in 5x Rapid ligation buffer (Thermo Fisher Scientific) topped up to 20µl with water. We also use a vector-only reaction as a control for incomplete digestion or re-ligated vector derived colonies. First, we incubate the mix at 22ºC for 15 minutes. Next, 2µl of the reaction was transformed into 50µl NEB-stable competent E.coli (NEB) and incubated 30 minutes on ice, then heat shocked at 42ºC for 30s and return to ice for 1 minute. Then, 950µl of 10-β/stable outgrowth medium (NEB) was added and cells were allowed to recover with shaking 250rpm at 37ºC for 30 minutes. Then, 100µl were plated onto a LB-agar plate with 100µg/ml ampicillin and incubated overnight at 37ºC.

Colonies were PCR screened for successfully ligated clones. We used primers as stated in[137]: FWD-pLKO ATTAGTGAACGGATCTCGACGG and REV-pLKO AACCCAGGGCTGCCTTGG. We picked colonies with a 10µl pipette tip and mixed in a PCR tube with 8µl 5 Prime Master mix (Quantabio), 4µl FWD and REV primers mix and 8µl water. Thermal cycler program was set as follows: 1x [95ºC for 2 min], 35x [95ºC for 30s, 68ºC for 45s] and 1x [72ºC for 1 min]. Positive clones were miniprep using GeneJet Plasmid Miniprep kit (Thermo Fisher Scientific), and DNA was digested using the SpeI (NEB) restriction enzyme following the manufacturer's protocol. Briefly, 3µg DNA was digested with 10 units SpeI in 50µl cutsmart buffer for 1 hour at 37ºC, and we ran the digest in a 2% agarose gel. Confirmed positive clones were sequenced using FWD-pLKO ATTAGTGAACGGATCTCGACG primer. Lentiviral production and infection were carried out as described in (**3.9**).

3.11 Bacterial killing assay

To analyse the killing ability of differentiated PLB cells or human neutrophils, we seeded $2.5x10^6$ cells in 500µl HBSS without Ca^+ and Mg^+. In addition, ATM inhibitor KU55933 (Sigma) was added to neutrophils at 10µM and incubated for 45 minutes prior to mixing with bacteria.

Staphylococcus aureus strains (JE2, SH1000 and Newman) were obtained from Professor Ruth Massey (Bristol University) *S. aureus* was grown overnight at 37ºC with shaking 250 rpm in Tryptic soy broth (TSB). Then bacteria was diluted 1:20 in 5ml fresh TSB and left to incubate and shake at 37ºC for 60 to 90 minutes until OD600 was between 0.6-0.7. Bacteria were harvested at 2500xg for 10 minutes and washed three times with HBSS. We resuspend bacteria in 5ml HBSS and for a concentration ~$1x10^6$ cells/ml, diluted 1:500 in double strength buffer (HBSS + 2mM $CaCl_2$ + 2mM $MgCl_2$ + 10% pooled serum) and incubated at 37ºC with rotation to opsonise *S. aureus*.

We added 500µl *S. aureus* onto the 500µl of dPLB or primary neutrophil for an MOI 0.2[23], mixed and incubated with rotation at 37ºC for 4 hours. We removed 50µl aliquots at 0, 60, 120, 180 and 240 minutes, plated them in 96well plates, and performed ten-fold serial dilutions until 10^{-6} and plated out in duplicate in Tryptic soy agar plates. We incubated the plates for 16-18 hours at 37°C, and colonies were counted to calculate colony forming units (CFU).

3.12 Neutrophil panel staining for flow cytometry

We plated either 100µl of whole blood or $5x10^5$ neutrophils in a U-bottom 96 well plate to analyse neutrophil phenotype. First, we added 100µl PBS and spun down at 400xg for 5 min. Then, we added 25µl Fc Block and incubated on ice for 5 minutes, then added 25µl of antibody mix (CD10, CD11b, CD14, CD15, CD16, CD62L, CD63, CD66b, IL5-R, CXCR4, CXCR2 all of them 1:50 in MACS buffer), antibody manufacturer and concentration are shown in (**Table A4**). Samples were incubated on ice for 30 minutes covered from light. Next, we washed with 100µl MACS buffer, spun down at 400xg for 5 minutes, and repeated this step once more. If the initial sample was whole blood, made three washes in 100µl ACK lysis buffer to eliminate red blood cells, spun down at 400xg for 5 minutes and resuspended in 50µl 4%PFA. We

incubated at room temperature covered from light for 15 minutes. Washed twice and spun down at 400xg for 5 minutes. Finally, resuspended in 200µl MACS buffer and stored at 4°C covered in foil until analysis. We used the flow cytometer LSR Fortessa X20 (BD Biosciences), and gate for single events and side scatter area high (SSC-A high) to analyse neutrophil population. We acquired at least 10,000 events for neutrophil panel staining, pHrodo and bacteria engagement and degranulation. We analysed data on FlowJo (FlowJo LLC).

3.13 Bacterial engagement and degranulation

Bacteria were harvested at $1x10^9$cells/ml and heat-killed for 1 hour at 100°C. Bacteria were washed twice in HBSS w/o Ca+ and Mg+ and further opsonised with double strength buffer for 15 minutes at 37°C. Bacteria were washed three times in HBSS w/o Ca+ and Mg+ and resuspended in 1ml PBS with 1µl Cell Trace Violet (Invitrogen) for fluorescent tagging. We incubated at 37°C for 20 minutes, mixing occasionally. We spun down the cells at 2500xg for 10 minutes, washed once in PBS, and resuspended in 1ml of RPMI-1640 w/o phenol red with 2mM Glutamine (RPMI + Q).

We seeded either human neutrophils or dPLB at $2x10^6$ cells/ml in 500µl of RPMI + Q and add 5µl of bacteria for an MOI 100. We incubated the mix of cells and bacteria with rotation at 37°C for 1 hour, taking 100µl aliquots at 0, 10, 30, 45, 60 minutes, and plated them in a 96 well plate on ice with 50µl ROS stop buffer (1x PBS + 10mM EDTA). Next, we spun down the plate at 400xg for 5 minutes and resuspended the cells in 25µl Fc Block (1:200 in MACS buffer; PBS + 2mM EDTA + 1% bovine serum albumin (BSA) (Fischer Scientific)) and incubated on ice for 5 minutes. Then, we added 25µl antibody mix (CD66B, CD62L and CD11b 1:50 in MACS buffer) and incubated on ice for 30 minutes covered from light. Next, we washed the cells with 100µl MACS buffer and spun down at 400xg for 5 minutes and repeated once more the wash step. Then we added 50µl 4%PFA (Electron Microscopy Sciences) incubate at room temperature for 15 minutes covered from light to fix the cells. Later, washed with 100µl MACS buffer and span down at 400xg for 5 minutes. Finally, resuspend in 200µl MACS buffer and store at 4°C covered in foil until running samples in the flow cytometer.

3.14 pHrodo staining and phagocytosis analysis

To analyse phagocytosis in differentiated PLB and primary neutrophils, we stained heat-killed *S. aureus* with pHrodo™ Phagocytosis Particle Labeling Kit for Flow Cytometry (Invitrogen) following the manufacturer's protocol. Briefly, bacteria were harvested at $1x10^9$cells/ml and heat-killed for 1 hour at 100°C. Bacteria were washed twice in PBS and resuspended in 1ml double strength buffer and incubate at 37ºC for 15 minutes while rotating for opsonisation. Bacteria were washed twice in PBS and resuspended in 750µl component F (0.1M Sodium Bicarbonate, pH 9.3) and centrifuge at 15,000xg for 1 minute, resuspend in 750µl component F and add 37.5µl of 10mM pHrodo for a final concentration of 0.5mM, incubate at room temperature for 45 minutes covered from light. We then washed unbound dye by adding 750µl of wash buffer and spun down at 15,000xg for 1 minute. We resuspended in 1ml 100% methanol (Sigma) and flicked the tube carefully to disaggregate the pellet, then added 500µl of 100% methanol and vortex for 30 seconds and centrifuged at 15,000xg for 1 minute. Next, washed twice in 1ml of wash buffer and vortex to evenly disperse bacteria and centrifuged at 15,000xg for 1 minute. Finally, resuspended the bacteria in RPMI + Q.

We seeded either human neutrophils or dPLB at $2x10^6$ cells/ml in 500µl of RPMI + Q and added 20µl of pHrodo labelled bacteria for an MOI 100. We incubated the mix of cells and bacteria with rotation at 37°C for 1 hour, taking 100µl aliquots at 0, 10, 30, 45, 60 minutes, and plated them in a 96 well plate on ice with 50µl ROS stop buffer. Next, we washed the plate twice with 100µl MACS buffer, added 50µl 4% PFA, and incubated it for 15 minutes at room temperature covered from light. Finally, we washed twice with 100µl MACS buffer, resuspended in 200µl MACS buffer, and stored at 4ºC covered from light until samples were run on the flow cytometer.

3.15 RNA lysates and qPCR

We obtained RNA from PLBs using PureLink™ RNA mini kit (Invitrogen)and followed the manufacturer's protocol. We collected $3x10^6$ cells in a 1.5ml Eppendorf and washed twice with PBS, spun down at 400xg for 5 minutes between washes. We added 300µl RNA lysis buffer (Lysis buffer + 1% β-mercaptoethanol (Sigma)) and

froze down at -20°C. We thawed the samples on ice and added 300µl of 70%ethanol and vortex until clear. Next, loaded 600µl of the mix onto the cartridge, spanned down at 12,000xg for 30 seconds, discarded the flowthrough, and repeated this step until all the sample had been processed. Then, we added 500µl wash buffer I and centrifuge at 12,000xg for 30 seconds. Next, we added 500µl wash buffer II and centrifuge again, discarded the flowthrough and centrifuge again to dry the membrane. Then we added 30µl Rnase-free water to the centre of the membrane and incubated at room temperature for 1 minute. Finally, we centrifuged at 15,000xg for 2 minutes to elute the RNA. We quantified RNA using a nanodrop and adjusted the concentration to 200ng/µl.

Then we translate RNA into cDNA using the High-Capacity cDNA Reverse Transcription kit (Applied Biosystems) and followed manufacturers protocol. Briefly, we made a 2x master mix with 2µl 10x RT buffer, 0.8µl 25x dNTP Mix, 2µl 10x RT Random primers, 1µl MultiScribe™ Reverse Transcriptase and 4.2µl Nuclease-free water. We added 5µl of RNA (1000ng) with 10µl 2x Master mix and 5µl Nuclease free water for a final volume of 20µl. We use a thermal cycler programme for: 1x [25ºC for 10 minutes], 1x [37ºC for 120 minutes] and 1x [85ºC for 5 minutes]. We added 180µl of nuclease-free water to the reaction to adjust the concentration to 5ng/µl.

We then used Fast SYBR™ Green Master Mix (Applied Biosystems) reagent to perform our qPCR on a QuantStudio™ 3 System (Applied Biosystems). Primers are listed in table (**Table A5**), all the primers were designed using Primer3 software (https://primer3.ut.ee/) and ordered from Eurofins Scientific except MPO and LRRK2, which were ordered from Qiagen. We made a primer mix of forward and reverse with 10µl of each primer (5µM) in 180µl of nuclease-free water. We added 10µl of 2x FAST SYBR™ GREEN Master Mix into a qPCR 96 well plate. Then we added 4µl of cDNA (20ng), 1µl of primer mix (250nM) and 5µl of nuclease-free water for a final volume of 20µl. We centrifuged the plate and run the program: 1x [95ºC 2 minutes], 35x [95ºC for 15 seconds, 55ºC for 30 seconds and 75ºC for 30 seconds], 1x [75ºC for 2 minutes]. We also ran a melt curve phase to rule out any primer dimer or non-specific amplification.

3.16 Protein lysates and western blot

To analyse protein expression in PLB, we collected $3x10^6$ cells in a 1.5ml Eppendorf tube and washed them twice with 1ml PBS. Resuspended in 100µl 2x Laemmli sample buffer; 125mM Tris base (Sigma), 140mM sodium dodecyl sulfate (SDS) (Sigma) and 20% glycerol (Sigma), supplemented with protease and phosphatase (Thermo Scientific), neutrophil elastase inhibitor (Sigma) and cathepsin G inhibitor (Alfa Aesar). To lyse the cells, we either boiled at 100ºC for 10 minutes and using a syringe with a 25G needle, syringed the sample until no liquid can be seen and is all foam, or sonicated during three cycles of 15 seconds at 100% power using Q125 Sonicator (QSONICA).

Samples were centrifuged at 15,000xg for 3 minutes, quantified protein with a nanodrop and adjust to a final concentration of 4µg/µl with NuPAGE® 4xLDS sample buffer (Invitrogen), boiled the sample at 100ºC for 10 minutes, spun down in microfuge to collect drops of the lid and loaded 10µl of sample into the gel well. We resolved low molecular weight proteins (10 kilodaltons(kDa)-40kDa) in a NuPAGE® Novex® Bis-Tris 4-12% pre-cast gel (Invitrogen) and ran it in 1x NuPAGE® MES SDS running buffer at 200V constant for 35minutes. For mid molecular weight proteins (40kDa-120kDa), we used 4-12% pre-cast gel and ran it using 1x NuPAGE® MOPS SDS running buffer at 200V constant for 50 minutes. For high molecular weight proteins (120kDa-400kDa), we used NuPAGE® Novex® Tris-Acetate 3-8% pre-cast gel (Invitrogen) and ran it using 1x NuPAGE® Tris-Acetate running buffer at 150V constant for 70 minutes.

We then transferred proteins into a nitrocellulose or polyvinylidene fluoride (PVDF) membrane using either the semi-dry Power Blotter System (Invitrogen) or the dry transfer iBlot™ 2 Gel Transfer Device (Invitrogen). We then rinsed our membrane in 1x tris buffered saline + 0.1% Tween®20 (TBST) and blocked our membrane in 1% BSA in 1x TBST for one hour at room temperature with rocking. Next, we washed three times for 5 minutes with 1xTBST our membrane and then incubated overnight in primary antibodies diluted in 1%BSA in TBST with rolling at 4ºC. Next, we washed three times with 1x TBST and incubated for 1 hour in secondary antibodies diluted in 1%BSA in TBST while rocking. We develop the membrane using chemiluminescence

or fluorescent detection with the Odyssey®XF imaging system (LI-COR). We analysed the band intensity of the western blots using gel analysis on FIJI software.

3.17 Migration assay

Cells were resuspended in migration media; 1x HBSS supplemented with 0.5% BSA, with either 10µM ATM inhibitor KU55933 or DMSO at $1x10^6$ cells/ml. We plated 200µl ($2x10^5$ cells) in the upper chamber of a 24 well plate 6.5mm Transwell with 5µm pore (Corning). We added 500µl of migration media to the lower chamber and left it to incubate at 37º 5% CO2 for 45 minutes. Next, we added 100nM N-formylmethionine-leucyl-phenylalanine (fMLP)(Sigma) and incubated for 2 hours. Finally, we imaged four fields of the lower chamber using IncuCyte imaging system. We then collected the cells in the well and counted with a haemocytometer.

3.18 Proteomics sample preparation

We collected $4x10^6$ differentiated PLB and washed twice in 1ml PBS. The pellet was resuspended in RIPA lysis buffer (Sigma) supplemented with 10mM EDTA, 1x Halt phosphatase (Thermo Fisher Scientific), 2x protease inhibitor (Calbiochem), 2mM phenylmethanesulfonyl fluoride (PMSF) (Sigma), 50mM Tris (2-carboxyethyl) phosphine hydrochloride (TCEP)(Sigma). Samples were sonicated with three cycles of 15 seconds at 100%. Protein was quantified using Pierce™ BCA Protein Assay Kit-Reducing Agent Compatible (Thermo Fisher Scientific), and 50µg of protein were used for Tandem-Mass-Tag (TMT) mass spectrometry.

TMT labelling and high pH reversed-phase chromatography were performed by Dr Kate Heesom (Proteomics Facility, Bristol University). Briefly, samples were digested with trypsin and labelled with Tandem Mass Tag (TMT) six-plex reagents according to manufacturer's instructions. Next, the labelled samples were pooled, evaporated to dryness, resuspended in 5% formic acid, and desalted using a SepPak cartridge. The eluted sample was evaporated to dryness and resuspended in 20mM ammonium hydroxide pH 10 for fractionation. Next, the pooled sample was loaded into XBridge BEH C18 Column and eluted with an increasing gradient (0-95%) 20mM ammonium hydroxide in acetonitrile. The resulting fractions were evaporated to dryness and resuspended in 1% formic acid and analysed with a nano-LC MSMS system using an Orbitrap Fusion Tribrid Mass Spectrometer with ETD (Thermo Scientific).

Bioinformatic analysis was performed in R statistical computing environment by Dr Phil Lewis (Proteomics Facility, Bristol University)

3.19 Immunocytochemistry of tissue slides

Histological sections of lungs and livers were courtesy of Prof. Miguel Soares, Instituto Gulbenkian de Ciência. Histological sections were cut and mounted by the Histology Core, Bristol. Briefly, paraffin blocks were cut to 3µm, and tissue sections were mounted and dried on SuperFrost™ Plus Slides (Thermo Scientific).

Dewaxing of the sample was carried out by two changes of 5 minutes on histoclear (National Diagnostics). Rehydration was done by two changes of 5 minutes in 100% ethanol, then 5 minutes in 90% ethanol and 70% ethanol. We washed sections three times for 5 minutes in deionised water and a final wash in 1x TBS. We then incubated sections in pre-warmed citrate buffer (Sigma) supplemented with 0.05% Tween20 for 20 minutes at 95ºC for antigen retrieval. We let the section cool down at room temperature for 20 minutes and washed three times with deionised water and once with 1x TBS. Next, we drew a square around the section with a wax pen and added 200µl blocking buffer; 1%BSA, 5%Donkey serum (Sigma), 5% gelatin from cold-water fish skin (Sigma), 0.05% Tween20 in 1x TBS and incubated for 1 hour at room temperature. Then, we discarded the blocking buffer and added 200µl Calgranulin (inhouse antibody, Max-Planck, Berlin)[88] diluted 1:100 in diluent buffer; 1%BSA, 5%Donkey serum, 5% gelatin from cold-water fish skin, 0.05% Tween20, 0.05% TritonTM X-100(Sigma) in 1x TBS and incubated overnight at room temperature. The next day we washed the section three times with 1xTBST and added 200µl Alexa488 donkey-anti rat secondary antibody (Thermo Fisher Scientific) diluted 1:200 in diluent buffer and incubated for 2 hours at room temperature covered from light. We then washed once with deionised water, followed by adding 200µl of 1µg/µl 4’6-Diamidino-2-phenylindole dihydrochloride (DAPI) (Sigma) for five minutes. Finally, washed with deionised water, we mounted the section by adding 20µl Mowiol 4-88(Sigma) and covered it with a coverslip to avoid forming bubbles. Images were acquired at 40x magnification using a Leica DMI6000 Widefield microscope. We analysed images using FIJI software.

3.20 Transmission electron microscopy

We harvested $1x10^6$ cells and washed them twice in PBS. Pelleted cells were fixed, mounted and stained for transmission electron microscopy (TEM) by Mrs Judith Mantell and Dr Chris Neal (Wolfson Bioimaging Facility, Bristol University). Briefly, pelleted cells were fixed in glutaraldehyde and rinsed with sodium cacodylate. A second fixing step was performed with osmium tetroxide. Then, dehydration of the sample was done with ethanol and was embedded in epoxy resin. Next, the sample was cut to 60nm and stained. We acquired images using Tecnai 12-FEI 120kV BioTwinSpirit TEM, and analysis was done on FIJI software.

3.21 Immunofluorescence of coverslips

We rinsed and dried 13mm round coverslips (VWR) in 100% ethanol. Then we placed them in 24 well plates and seeded $1x10^5$ primary neutrophils or PLB in RPMI 1640. We incubated the plate for 15 minutes at 37ºC 5%CO_2 to allow neutrophils to attach to the coverslip. We washed twice with PBS and fixed with 4% PFA for 15 minutes, then we washed with PBS and stored at 4ºC until samples were stained. A-T neutrophils were stained and imaged in a SP8 confocal microscope by Christian Goosman (Max-Planck Institute for Infection Biology). Images were analysed using the MIA plugin on FIJI software, and a pipeline for 3D images analysis was made by Dr Dominic Alibhai (Wolfson Bioimaging Facility, Bristol University)

3.22 Data analysis

Data was transferred to GraphPad Prism and statistical analysis were carried out. Student's t-test was done between two groups, paired analysis was done for treatment with inhibitor and unpaired analysis for patients and PLB. Two-Way analysis of variance (ANOVA) statistical tests were performed between groups with multiple time-points . *p<0.05, **p<0.01, ***p<0.005, ****p<0.0001.

CHAPTER 4: ATM role in neutrophil antimicrobial activity

4.1 Introduction

AT disease is characterised by neurological disorders, predisposition to malignancies, immunodeficiency and recurrent sinopulmonary infections[138]. Immunological abnormalities are seen in two-thirds of all the patients, the most common ones are low levels of immunoglobulins and lymphopenia[98]. However, little research has been done on the innate immunity of this disease. A study in 2015[82] showed that cells from A-T patients overproduced pro-inflammatory cytokines (e.g. IL-8, IL-6 and TNF-α) and had a prolonged lifespan[82]. Erttman and collegues[133] showed that lack of ATM impaired inflammasome formation, decreasing the release of IL1-β and IL-18 cytokines and increasing the release of TNF-α and IL-6[133].

AT patients suffer from chronic lung infections[95], and a retrospective study done by Schroeder and Zielen[139] analysed clinical data of 127 A-T patients showing that the most prevalent pathogen obtained from lung samples during acute and chronic inflammation was *Staphylococcus aureus,* followed by *Pseudomonas aeruginosa* and *Streptococcus pneumoniae*[139]*.*

Staphyloccocus aureus is a gram-positive bacteria, that is found as a commensal and human pathogen[140]. *Staphylococcus aureus* is one of the pathogens responsible for causing bacteraemia, endocarditis and pleuropulmonary infections, and treatment is complicated due to its propensity to develop antibiotic resistance[141,142]. Methicillin-resistant S. aureus (MRSA) is a world-wide problem since its discovery in 1961[143]; half of the clinical isolates have become MRSA strains[140,143].

AT immunodeficiency caused by innate immunity has not been explored widely. Therefore, we decided to test different antimicrobial abilities that neutrophils possess against different pathogens to explore the possibility of an impairment in neutrophil function. This chapter aims to address the gap in the literature of the role of *ATM* in neutrophil antimicrobial activity.

4.2 Inhibition of ATM with small molecule KU55933 leads to impaired antimicrobial activity

A-T patients demonstrate immunodeficiency, but the role of ATM in neutrophil activity has not been tested. We wanted to test whether ATM regulates typical neutrophil functional responses. To test this, we took three approaches. First, we used a chemical inhibitor of ATM called KU55933. We purified primary neutrophils from the blood of three healthy donors using a negative selection kit. We incubated $2.5x10^6$ neutrophils in either vehicle control (DMSO) or 10μM ATM inhibitor (KU55933) for 45 minutes. During this incubation we opsonized $5x10^5$ *Staphylococcus aureus* for 15 minutes in double strength media. We used *S. aureus* as it has been isolated from acute and chronic infections of lungs from AT patients[139]. Neutrophils were then mixed with *S. aureus* at a multiplicity of infection (MOI) 0.2 for a period of four hours, taking aliquots every hour to measure the number of live bacteria.

We first tested the strain JE2 and found that after 4 hours of coincubation neutrophils treated with ATM inhibitor were less efficient at killing the pathogen (**Figure 4.1 A**) throughout the four-hour time course. Treatment with ATM inhibitor showed defects in bacteria killing, however no significant difference was seen at timepoints 1-3 hours. In addition, we decided to focus on the end point and saw a significantly decreased ability of neutrophils treated with ATM inhibitor to kill the strain JE2 when compared to the control neutrophils **(Figure 4.1 B**).

Following on from this we tested two other strains of *S. aureus*, SH1000 and Newman; the former is a well-established strain used in the labs that has not been completely characterised, while the latter is a more recent clinical isolate known to be resistant to methicillin. We found that throughout the 4 hours engagement both DMSO and ATM inhibitor treated cells were able to kill the pathogen, however there was not a significant difference in the killing of bacteria from ATM treated cells compared to the vehicle control. Neutrophils were less efficient at killing the strain Newman compared to JE2 and SH1000 strains, since more live bacteria were seen in the Newman strain throughout the 4 hours, as shown in (**Figure 4.1 A,C and E**). We decided to focus on the endpoint and found there was no significant difference between DMSO and ATM-inhibited neutrophils in their ability to kill the strain SH1000 (**Figure 4.1 D**) or Newman (**Figure 4.1 F**).

In summary, we found that KU55933 treated cells were less efficient in killing the pathogen *S. aureus* strain JE2, and therefore wondered if this deficiency was due to an impaired uptake of the pathogen or a degranulation defect. Since JE2 was the only strain to give us a significant difference we decided to keep studying the interaction between neutrophil and pathogen using this strain for further experiments.

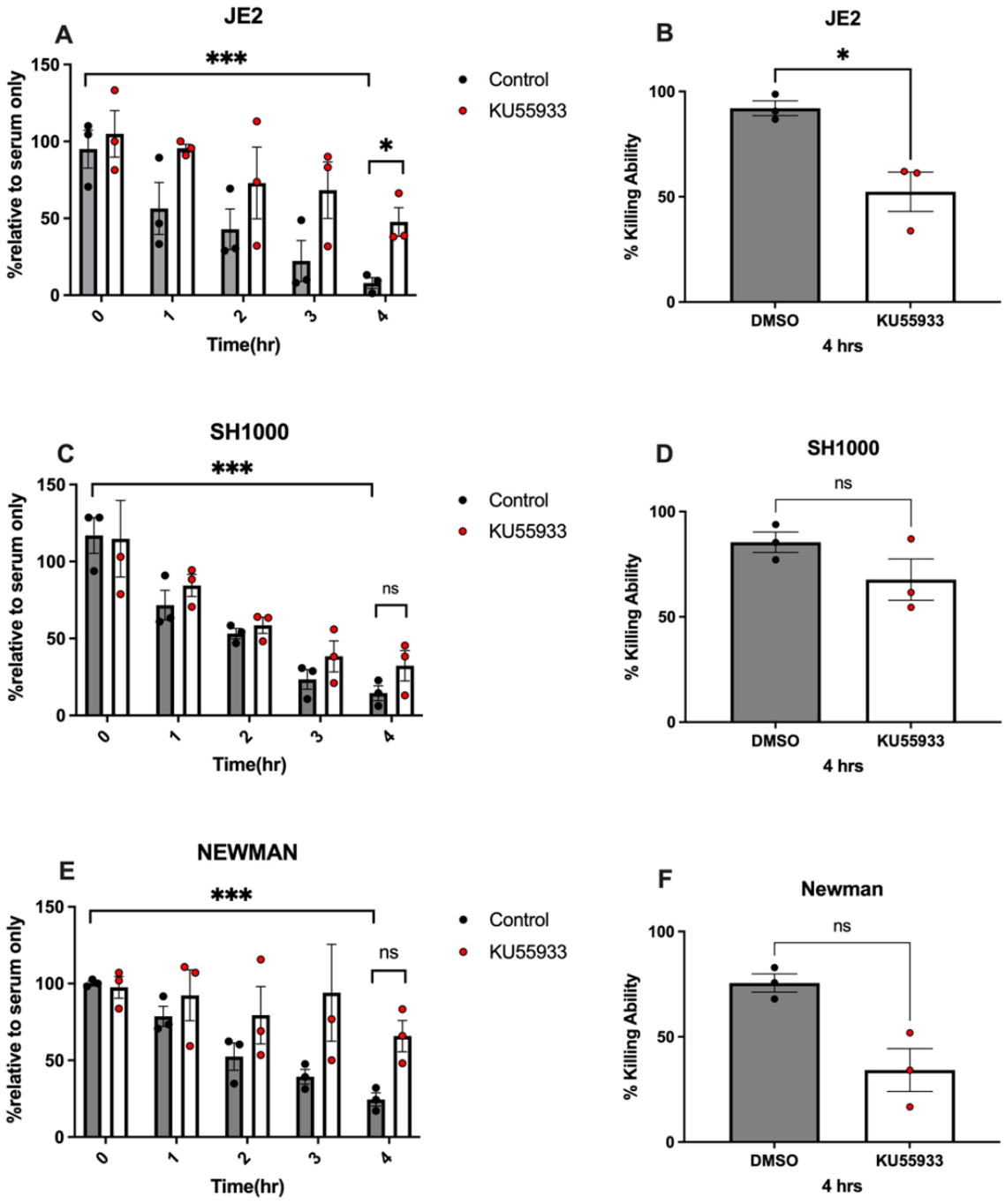

(legend on next page)

Figure 4.1: Neutrophils treated with an ATM inhibitor (KU55933) are impaired in killing *S. aureus* (A,C,E) Neutrophils from 3 healthy donors were pre-treated for 45 minutes with 10μM ATM inhibitor (KU55933) or vehicle control (DMSO). Neutrophils were then incubated with *S. aureus* (MOI 0.2) in medium containing 5% pooled human serum and 50μl aliquots were taken every hour, serially diluted, and plated in duplicate in Tryptic Soy Agar (TSA). Percentage of live bacteria was obtained by comparing bacterial counts against bacteria grown in media without neutrophils (serum only). (A) *S. aureus* strain JE2. (C) *S. aureus strain* SH1000. (E) *S. aureus* strain Newman. (B,D,F) Percentage of neutrophil killing ability at time point 4 hours, corresponding to strain shown on the left was obtained by comparing the percentage of dead bacteria at 4 hours with the starting time point (0 hours). Data is expressed as mean ± SEM. Log2 transformation was done and then two-way ANOVA was performed (A,C,E):**p< 0.003, ****p<0.0001. Paired two-tailed t-test was performed at time point 4 hours: *p <0.05 (n=3 healthy donors).

4.3 Inhibition of ATM with small molecule KU55933 does not affect neutrophil degranulation and engagement with S. aureus

We decided to address the question of whether neutrophils treated with ATM inhibitor were taking up fewer bacteria and showing an impaired degranulation. To answer this question, we used a flow cytometry approach where we fluorescently labelled opsonised heat-killed *S. aureus*, and co-incubated with neutrophils for one hour. As soon as neutrophils engage or phagocytose *S. aureus* they become positive for the fluorescent tag and we were able to measure the mean fluorescent intensity (MFI) of these cells over time. Secondly, we used fluorescently tagged antibodies against CD11b (ITGAM), CD66b (CEACAM8) and CD62L (L-selectin). The receptor CD11b is found on the plasma membrane, secretory vesicles, and tertiary granules, CD66b is found on the plasma membrane and, contrary to CD11b, in the secondary granules, while the receptor CD62L is found on the plasma membrane of the neutrophil. When the neutrophil starts engaging with *S. aureus*, it starts degranulating in a timely manner: first, tertiary granules, then secondary and finally primary granules[39,57]. Similarly, shedding of receptors starts happening after neutrophils start releasing their antimicrobial peptides[39]. Using the fluorescently tagged antibodies we can follow the degranulation pattern and shedding of neutrophils when engaging and phagocytosing *S. aureus* JE2 over a one-hour time course (**Figure 4.2 F**).

We incubated neutrophils of three healthy donors in media with either vehicle control or 10μM ATM inhibitor (KU55933) for 45 minutes. We then added the fluorescently

labelled heat-killed *S. aureus* at MOI 100 for one hour, taking aliquots at time points 0, 10, 30, 45 and 60 minutes.

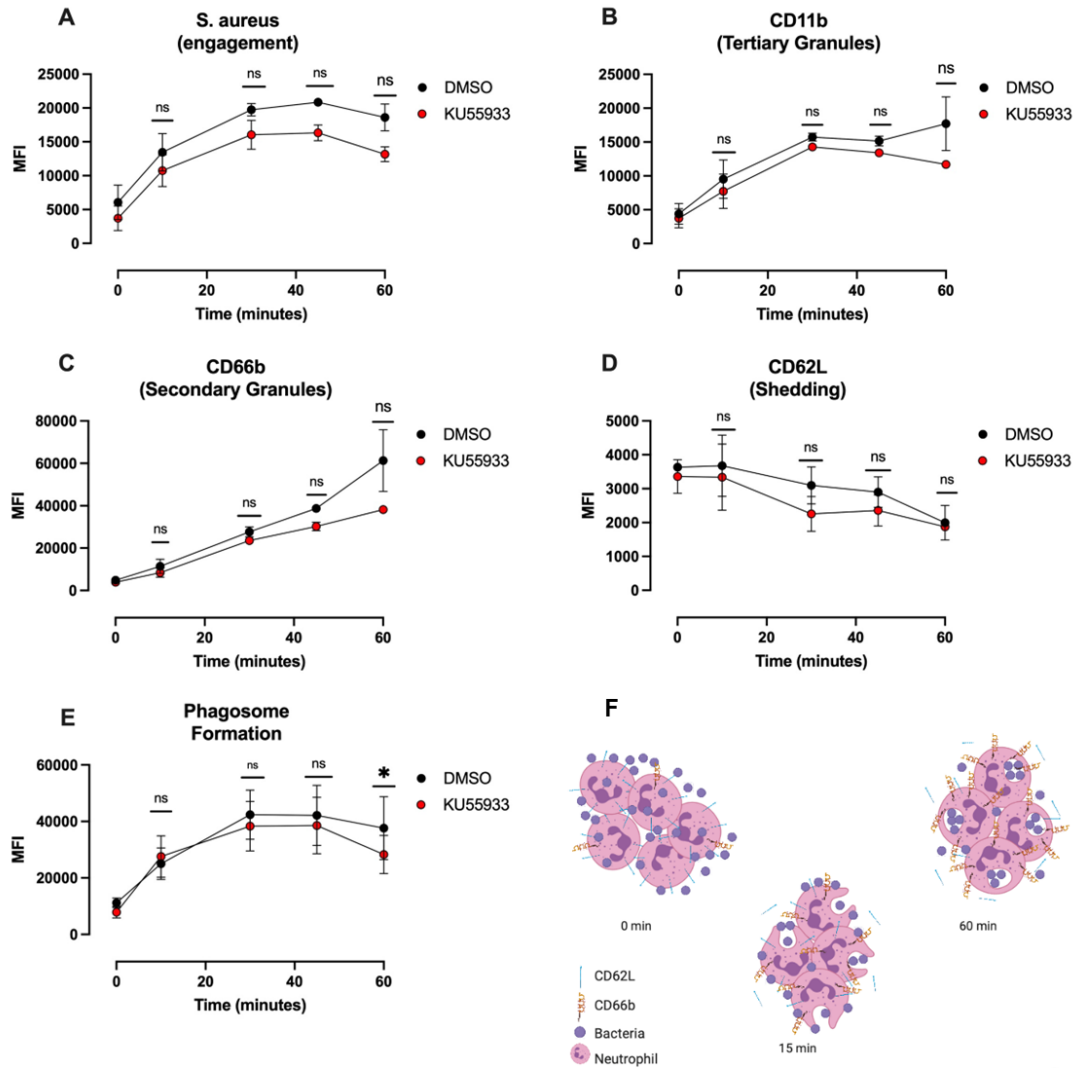

Figure 4.2: Neutrophils treated with an ATM inhibitor did not show impaired engagement with *S. aureus* and degranulation. Flow cytometry data showing engagement of neutrophils pre-incubated with vehicle (DMSO) or 10μM of the ATM inhibitor (KU55933) with cell trace violet-labelled *S. aureus* strain JE2. (A) Engulfment of labelled bacteria leads to increase in neutrophil fluorescence. (B) Degranulation of tertiary granules measured by flow cytometry using an antibody against the integrin receptor CD11b. (C) Degranulation of secondary granules measured by flow cytometry using an antibody against CEACAM8 (CD66b). (D) Shedding of L-selectin measured by flow cytometry using an antibody against CD62L.(E) Phagosome formation leads to increase neutrophil fluorescence measured by pHrodo dye labelled bacteria. Data is expressed as mean fluorescence intensity (MFI) ± SEM, Two-way ANOVA with Bonferroni correction was used to analyse between time points. *p<0.05, **p<0.003 (n=3 healthy donors).

We observed that neutrophils started gaining fluorescence after phagocytosing the fluorescently tagged bacteria, however this intensity decreased between 45 minutes and one-hour timepoint; this could be due to degradation of the fluorophore in the neutrophil phagosome. We found that after one hour of engagement there was a similar uptake of the bacteria, with no significance difference between conditions (**Figure 4.2 A**).

We next quantified CD11b which is a marker of degranulation of tertiary granules[39]. There was no difference in the starting expression of CD11b between the conditions, and both increased the membrane expression of CD11b over time. The highest expression was reached at 30 minutes, with a statistically significant difference between vehicle and inhibitor treated neutrophils. After 30 minutes, the fluorescence intensity started decreasing over the following timepoints (**Figure 4.2 B**). This could be explained by the fact that CD11b is one of the first receptors to be externalised by neutrophils in response to a stimulus. It has been shown that neutrophils also shed their receptors once they are no longer needed; a clear example is the L- selectin CD62L that starts with a high expression and as soon as the neutrophil is stimulated the expression decreases drastically[68].

We then analysed the expression of CD66b which is a marker of secondary granules. As shown in (**Figure 4.2 C**) both conditions start at similar levels of fluorescent intensity, which increases over time. Neutrophils treated with ATM inhibitor have a decreased degranulation trend from 30 minutes onwards, however no statistically significant difference was seen between conditions. We also observed that this receptor takes longer to increase its expression, showing that secondary granules are more difficult to mobilise than tertiary granules. Later, we analysed the shedding of CD62L. As shown in (**Figure 4.2 D**) both conditions start at a similar level of fluorescent intensity, and it decreases over time with a significant difference at 30 and 45 minutes between conditions. We observe that expression of this receptor does not decrease drastically over time, this was unexpected and could happen if neutrophils were pre-activated and had already began shedding before the experiment started.

Finally, we labelled opsonised heat-killed *S. aureus* JE2 with pHrodo dye, this dye becomes fluorescent with changes in pH. Once the bacteria enter the neutrophil phagosome, the acidic environment cause an increase in the neutrophil fluorescence

that we measured in (**Figure 4.2 E**), We found that at 30 and 45 minutes neutrophils treated with ATM inhibitor showed a trend to have less phagosome formation when compared to neutrophils treated with vehicle control.

In summary, we found that there is no difference in the ability of neutrophils treated with DMSO or ATM inhibitor to engage with bacteria, Similarly, ATM inhibition did not affect the degranulating capacity of tertiary and secondary granules in neutrophils as well as shedding, as seen in the similar levels of expression of the receptors CD11b, CD66b and CD62L between conditions. Even though, we could see a slight trend towards decrease phagosome formation of ATM inhibited neutrophils, this could not explain the deficiency in bacteria killing.

We then decided to analyse if treatment with the ATM inhibitor disrupted the migration capacity of neutrophils against a chemotactic stimulus.

4.4 ATM inhibition increases migration in vitro, while loss of ATM does not affect migration in vivo

It is known that neutrophils will migrate to a site of infection following a chemotactic gradient[76]. Therefore, we decided to analyse the migration ability of neutrophils treated with ATM inhibitor using the chemotactic peptide N-formyl-L-methionyl-L-leucyl-L-phenylalanine (fMLP); this bacterial peptide is known to bind G protein receptors and direct neutrophils to sites of infection[29]. We incubated neutrophils from 5 healthy donors in either DMSO or ATM inhibitor at 10μM for 45 minutes in a 5 μm pore transwell. The transwell was then placed on top of medium containing 100nM fMLP in a 24 well plate and left for two hours to allow the neutrophils to migrate through the transwell. We found that inhibition of ATM increased the migration ability of neutrophils towards the media containing fMLP (**Figure 4.3 A**).

To test if ATM regulates neutrophil migration in vivo, we used an infection model with the rodent malaria parasite *Plasmodium chabaudi* (*P. chabaudi*). We obtained histological sections of lungs and livers from infected and uninfected $ATM^{-/-}$ and controls, (courtesy of Prof. Miguel Soares, Instituto Gulbenkian de Ciência), and analysed day 8 post infection (dpi), known to be the peak of the parasitaemia. In this infection model, Plasmodium-parasitised erythrocytes sequester in liver and lung, and this is accompanied by chemotaxis of neutrophils into these organs[144].

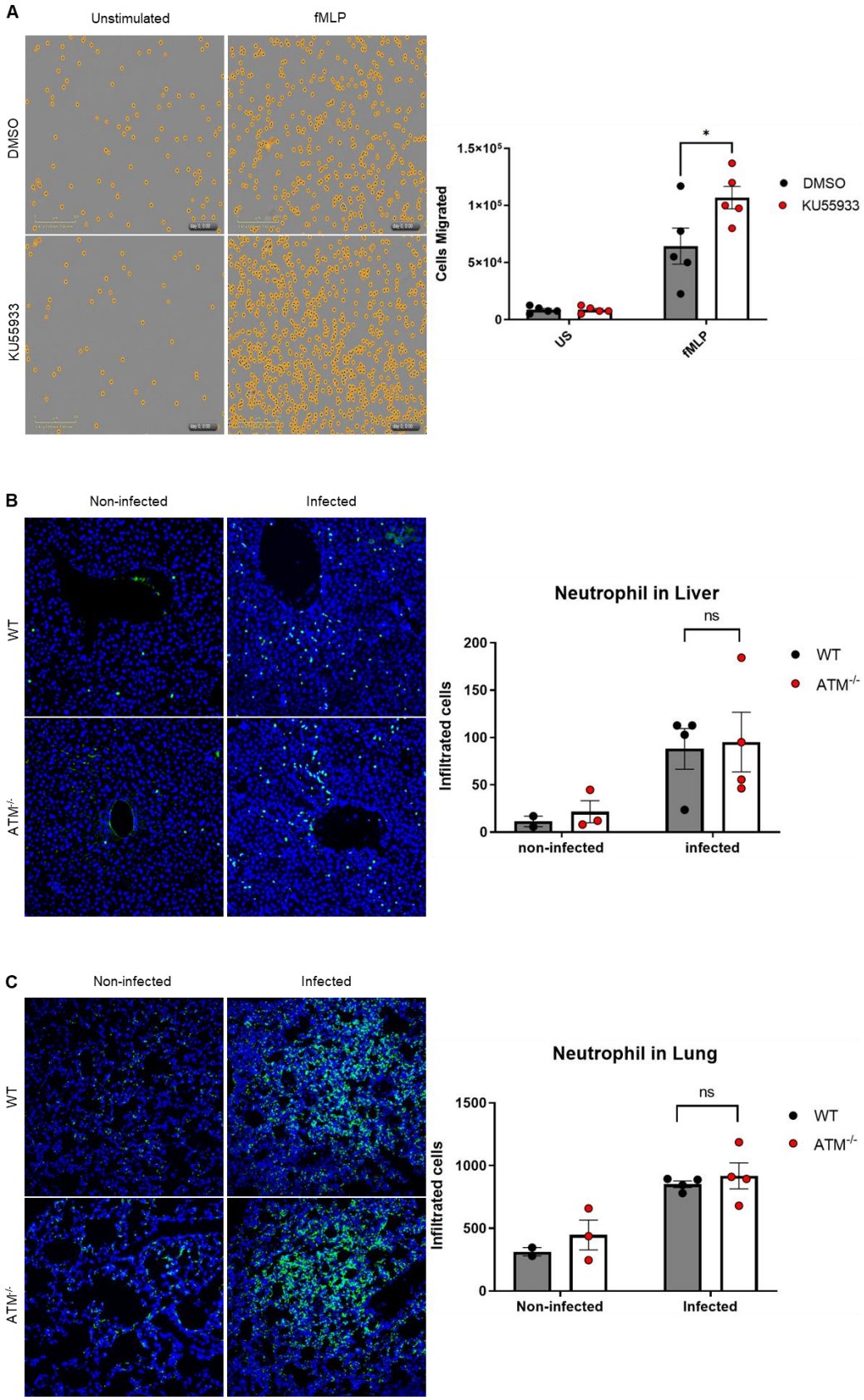

(legend on next page)

Figure 4.3: Neutrophil migration in response to a chemotactic gradient. (A) Neutrophils pre-treated with 10uM ATM inhibitor (KU55933) for 45 minutes showed an increased migration towards fMLP (300nM) compared to DMSO pre-treated cells (n= 5 healthy donors) (B) Immunofluorescence analysis of neutrophils in histological sections showed similar trafficking to the liver in WT and $ATM^{-/-}$ mice at day 8 post infection with the parasite *Plasmodium chabaudi* (n=2 WT and 3 $ATM^{-/-}$) uninfected and (n= 4) for infected. (C) Immunofluorescence analysis of neutrophils in histological sections showed similar trafficking to the lung in WT and $ATM^{-/-}$ mice at day 8 post infection with the parasite *Plasmodium chabaudi* (n=2 WT and 3 $ATM^{-/-}$) uninfected and (n= 4) for infected. Histological sections were imaged at 20x magnification using a widefield microscope (Leica), 10 fields of view were acquired for each mouse and neutrophils were counted using FIJI software for each field of view, an average of neutrophils per field of view per mice was plotted as infiltrated cells. Data is expressed as mean ± SEM. Statistical significance was calculated by two-tailed t-test: *p<0.02.

To analyse the tissue sections, we stained for neutrophils using the antibody against the neutrophil protein calgranulin (S1008A) followed by staining of the cell nuclei with 4',6-diamidino-2-phenylindole (DAPI). Using a widefield microscope we then captured ten different fields of view for each section. First, we looked at infiltration levels of neutrophils into the liver, one of the main affected organs during *P. chabaudi* malaria. We could see an increase in infiltrated cells between the non-infected and the infected sections, however, we did not see any difference in the number of infiltrated cells between wild type and knockout mice in the infected tissues (**Figure 4.3 B**). We then analysed the infiltrated cells in the lung of the mice and saw a similar result, namely an increased number of neutrophils in the lungs of infected mice, but no difference in the number of infiltrated cells between WT and $ATM^{-/-}$ mice (**Figure 4.3 C**).

In summary, we saw increased migration of neutrophils treated with ATM inhibitor towards the bacterial chemotactic peptide fMLP after 30 minutes of exposure. In an in vivo model with a eukaryotic pathogen, however, we did not see the same result, as the $ATM^{-/-}$ mice showed the same migration capacity as WT mice in the infected tissues. There is a possibility that migration capacity is dysregulated early on in infection and later becomes compensated after a long-term exposure. It is also possible that the chemotactic defect is specific for bacterial PAMPs and sensing of *Plasmodium* is not affected. Additional experiments are needed to characterise the role of ATM in neutrophil migration. We then decided to test the respiratory burst of

neutrophils against *S. aureus* and test if there was a defect that could explain the defect in killing.

4.5 ATM inhibition decreases neutrophil respiratory burst against receptor binding stimuli

Neutrophils release microbicidal ROS during their respiratory burst and this is crucial for neutrophil killing of *S. aureus*[81]. We used a luminol based assay to analyse the respiratory burst to various stimuli.

To begin with, we analysed the production of ROS by ATM-inhibited neutrophils using the mitogen phorbol 12-myristate 13-acetate (PMA); this stimulus crosses the cell membrane and directly activates Protein kinase C (PKC), stimulates the assembly of NOX2 on membranes and triggers the respiratory burst[35]. We used this stimulus as a positive control of ROS production and could not see any difference in ROS production over 4 hours between DMSO and inhibitor-treated neutrophils, as seen in the kinetic curve and the area under the curve measurement (**Figure 4.4 A and B**). This indicates that ATM is not required for NOX2 assembly and activity.

Next, we wanted to test signalling pathways upstream of PKC and NOX2 and thus we used the lectin Concanavalin A (ConA), which binds promiscuously to many receptors to trigger a respiratory burst[88]. Surprisingly, we saw that treating neutrophils with ATM inhibitor prevented them generating a respiratory burst against ConA. (**Figure 4.4 C and D**). We then used heat-killed *S. aureus* JE2 strain at an MOI 20 to see if another stimulus that requires receptor binding would show a similar inhibition of the respiratory burst as ConA. We found that ATM inhibition does not abolish the respiratory burst of neutrophils against *S. aureus*, however it considerably decreases it. (**Figure 4.4 E and F**). Following this, we decided to try *C. albicans,* a fungus known to bind the receptor dectin-1. We found that inhibiting ATM in neutrophils significantly decreased ROS production against *C. albicans* (MOI 5), as seen in (Fig 4G and H). This result was similar to the one we obtained against *S. aureus.*

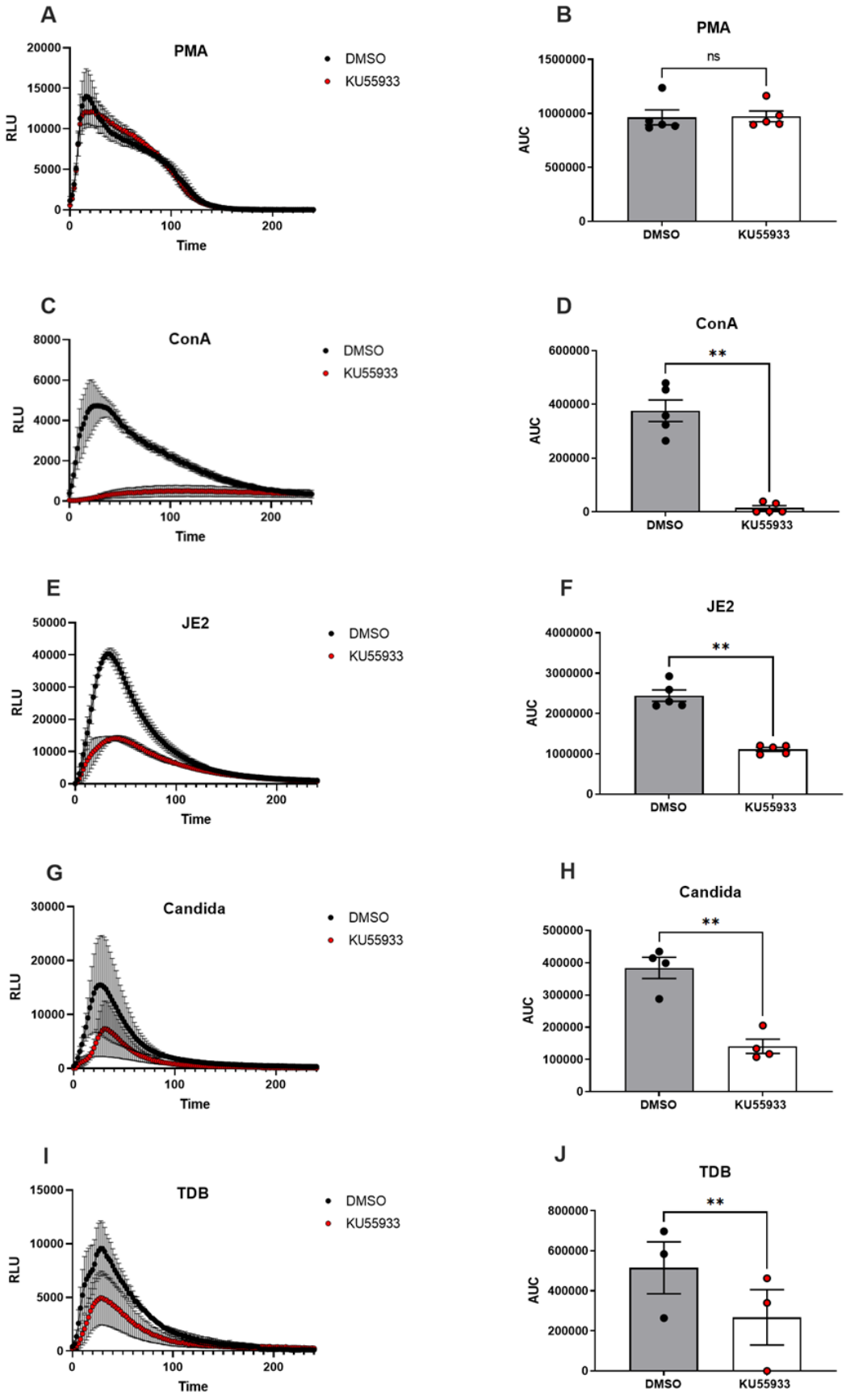

(legend on next page)

Figure 4.4: Respiratory burst against different stimuli by DMSO and ATMi treated neutrophils. Primary neutrophils were pre-treated with either vehicle control (DMSO) or 10 uM ATMi (KU55933). (A, C, E, G, I) Time course analysis of ROS production measured by luminol assay, in response to 100nM PMA (n=5) (A), 50ug/ml ConA (n=5) (C), *S, aureus* MOI 20 (n=5) (E), *C. albicans* MOI 5 (n=4) (G), and 50ug/ml TDB (n=3) (I). Data is expressed as mean relative light units (RLU) ± SEM. (B, D, F, H, J) Area under the curve (AUC) analysis corresponding to plots shown on the left. Data is expressed as mean ± SEM. Statistical significance was calculated by two-tailed t-test: **p<0.002.

Finally, we used the stimulus trehalose-6,6-dibehenate (TDB), a synthetic analogue of *Mycobacterium tuberculosis* cord factor, which binds the C-type lectin receptor mincle. We saw a similar result using this stimulus compared to *S. aureus* and *Candida*, as treating neutrophils with ATM inhibitor decreased the production of ROS (**Figure 4.4 I and J**).

To summarise, we found that treatment of primary neutrophils with ATM inhibitor led to impaired production of ROS against the pathogens *S. aureus* and *C. albicans* as well as the stimuli TDB. Moreover, ROS production was abolished against the chemical stimuli ConA. On the other hand, PMA ROS burst was not affected by the inhibition of ATM. It has been shown that ROS is needed to release neutrophil extracellular traps (NETs)[88], which are required by neutrophils to prevent pathogen dissemination. Therefore we went on to test NET production in ATM inhibited neutrophils.

4.6 ATM inhibition leads to impaired NET release against Concanavalin A

Neutrophils release neutrophil extracellular traps (NETs) when stimulated with the mitogen PMA and the lectin ConA[88]. Using a fluorescence microscopy approach, we went on to quantify NET production of primary neutrophils treated with ATM inhibitor.

We stimulated primary neutrophils treated with either DMSO or ATM inhibitor (KU55933) with PMA or ConA for four hours. ATM inhibited cells did not show defective NET production after stimulation with PMA, however, inhibition of ATM abolished NET production against the stimuli ConA (**Figure 4.5 A and B**).

In summary, we found that ATM inhibition did not affect NET release against PMA; on the other hand, the chemical stimuli ConA failed to induce NET production in these cells. As seen before, ATM inhibition did not impair ROS production against PMA but

completely abolished ConA ROS. This could explain the failure of ATM inhibited neutrophils to release NETs as it has been shown that NETs can be ROS-dependent[88].

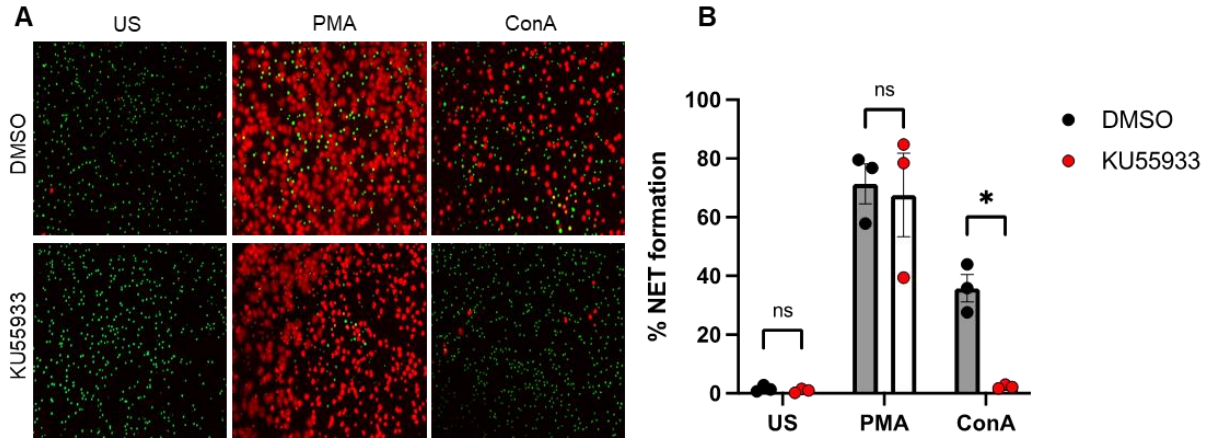

Figure 4.5: Neutrophil extracellular trap release against different stimuli by DMSO and ATMi treated neutrophils. Primary neutrophils were pre-treated with either vehicle control (DMSO) or 10uM ATM inhibitor (KU55933). Live cells were stained with the intracellular DNA dye SYTO green, while NETs were visualised with the extracellular dye SYTOX orange. (A) Representative images of neutrophils stimulated with 50nM PMA n=3 (mid panel) and 50ug/ml ConA n=3 (right panel).(B) Quantification of NET formation was calculated as number of NETs (Red) divided by live (green) plus NETs (red) .Cells were imaged at 10x magnification using a fluorescent microscope EVOS (ThermoFisher), 4 fields of view were acquired for each donor and NETs were counted using FIJI software for each field of view, an average of neutrophils per field of view per donor was plotted as percentage of NET formation. Data is expressed as mean ± SEM. Statistical significance was calculated by two-tailed t-test: *p<0.05. US: unstimulated.

4.7 Generation of a stable PLB-985 ATM knockout cell line

A limitation of using inhibitors is their off target effects. To address this, we decided to use the promyelocytic leukaemia cell line PLB-985, which can be differentiated into neutrophil-like cells after 6 days of treatment with the chemical compound N,N-Dimethylformamide (DMF). We used CRISPR/Cas9 technology to knockout *ATM* in this cell line and test if the depletion of the gene produced similar results to the ones observed in primary neutrophils treated with ATM inhibitor.

To generate a stable knockout cell line, we decided to target two different exonic regions using two different guide RNA (gRNAs), delivered into PLB cells with lentiviral constructs.

We successfully transduced cells with two gRNA constructs. To obtain a clonal cell line with a defined deletion we performed single cell cloning. Using the free software outknocker[136], we analysed our single cell clones from the first gRNA construct and we obtained one knockout cell line as seen in position B5 in (**Figure 4.6 A**). One allele had a 4-nucleotide deletion while the other one had a single nucleotide insertion, with both of these mutations expected to lead to a loss of ATM expression in the clone. We used western blot to confirm that our single clone had a complete knockout as demonstrated by three different antibodies against ATM (**Figure 4.6 B**).

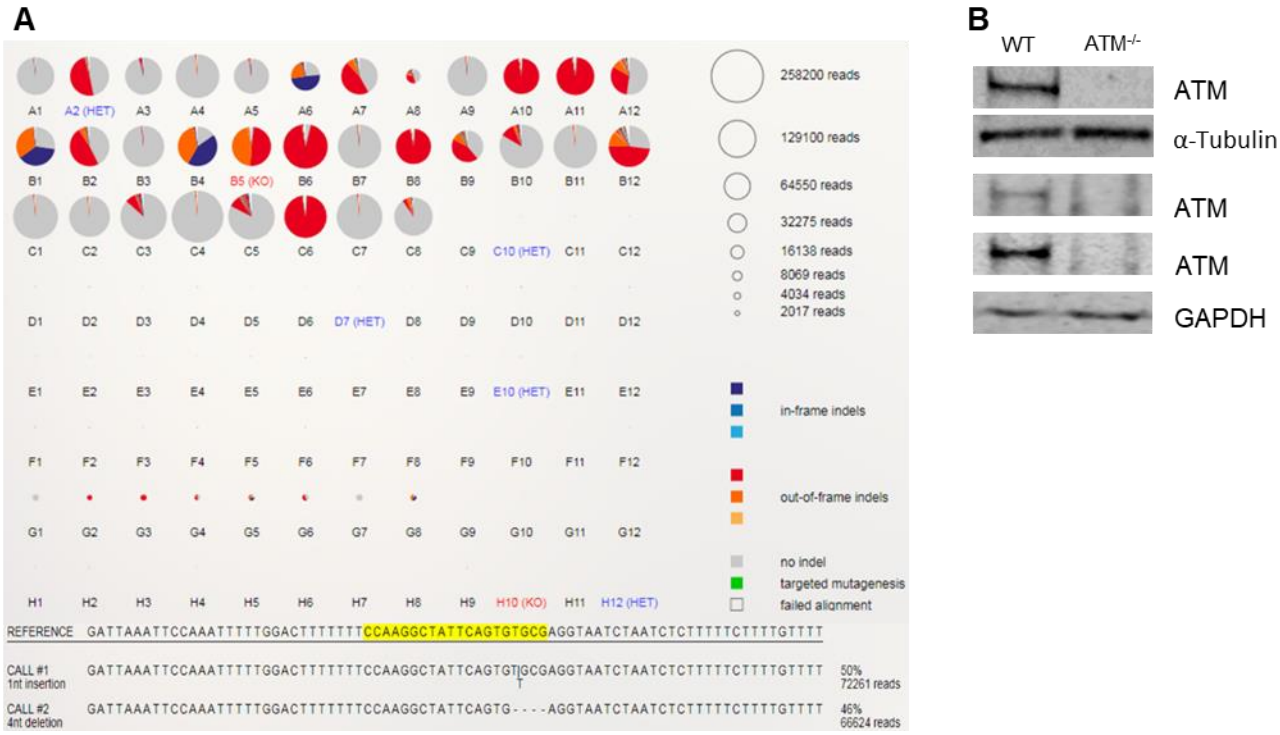

Figure 4.6: Generation of PLB-985 ATM knockout cell line. (A) Illustration of single cell clone analysis using the software Outknocker[136] to identify ATM$^{-/-}$ cells. DNA sequence at the bottom of the illustration compares the targeted locus in WT and CRISPR/Cas9 targeted cells. (B) Representative western blot to confirm *ATM* knockout. Three different antibodies against ATM were used and α-tubulin and GAPDH were used as loading controls.

We were able to generate a single ATM$^{-/-}$ clonal cell line from gRNA construct 1 and confirm the absence of the protein by western blot. Unfortunately, we did not obtain

any KO clones with gRNA2. We then decided to test the antimicrobial capacity of our ATM$^{-/-}$ PLB compared to PLB generated with a scramble gRNA as controls.

4.8 Loss of ATM impair antimicrobial activity of neutrophil-like cells

The next step was to test whether PLBs differentiated to a neutrophil-like cell lacking *ATM* would be able to kill the pathogen *S. aureus.*

We differentiated the PLBs for 6 days and then co-incubated with *S. aureus* at an MOI 0.2, taking aliquots every hour for four hours. Firstly, we could see that both wild type and ATM$^{-/-}$ differentiated PLBs (dPLBs) were able to progressively kill the pathogen over the four hours. Moreover, we could see that there was a significant decrease in the killing ability of the ATM$^{-/-}$ cells compared to the WT at 4 hours (**Figure 4.7 A and B**).

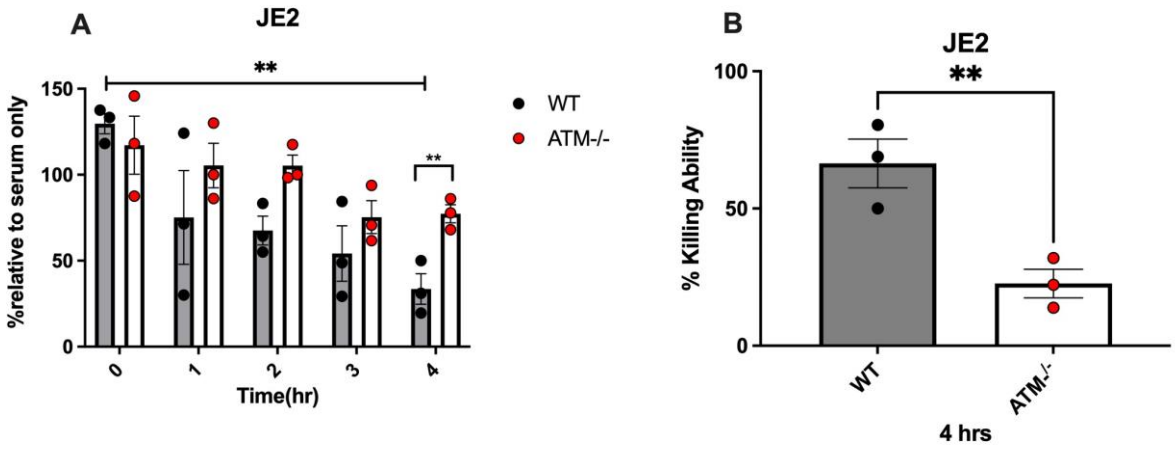

Figure 4.7: Impaired killing of *S. aureus* in ATM$^{-/-}$ PLB cells over 4 hours compared to wild type (WT) (A) Percentage of live JE2 bacteria over 4 hours of engagement with differentiated PLBs, Percentage of live bacteria was obtained by normalising bacteria engaged with PLBs with bacteria grown in media with serum only and without PLBs, over 4 hours. (B) Percentage of PLB killing ability at time point 4 hours of engagement with *S. aureus* strain JE2 (MOI 0.2), obtained by comparing the percentage of dead bacteria at 4 hours with the starting time point 0 hours. Data is expressed as mean± SEM. Statistical significance overtime was calculated by two-way ANOVA after Log2 transformation of the data (A): **p 0.003. Two-tailed t-test was performed at time point 4 hours: **p< 0.003 (n=3).

In summary, we saw that PLBs lacking ATM were less efficient at killing S. aureus, similar to what we had observed previously with pharmacological inhibition of ATM in primary neutrophils.

4.9 ATM knockout neutrophil-like cells do not show impaired engagement and degranulation

We then went on to test if there was any difference in the uptake of the pathogen or degranulation capacity. To test the engagement ability of dPLBs we used the same flow cytometry approach as with the primary neutrophils. We co-incubated differentiated PLBs with fluorescently tagged *S. aureus JE2* at MOI 100 for one hour and analysed different time points to see if the uptake or degranulation was affected.

We could not see a difference in the uptake of bacteria between WT and ATM$^{-/-}$ cells (**Figure 4.8 A**). As opposed to primary neutrophils, PLBs do not express CD66b, therefore we just analysed the expression of CD11b. S. aureus did not induce upregulation of CD11b, leading us to conclude that PLBs are not a good model for degranulation. We did not see a statistical difference in the degranulation of CD11b (**Figure 4.8 B**), although there was a trend.

In summary, we did not see any difference in the uptake ability between our WT and ATM$^{-/-}$ differentiated PLBs. We decided to see if the production of ROS was impaired in the ATM$^{-/-}$ compared to the WT, as the inhibited primary neutrophils had suggested earlier.

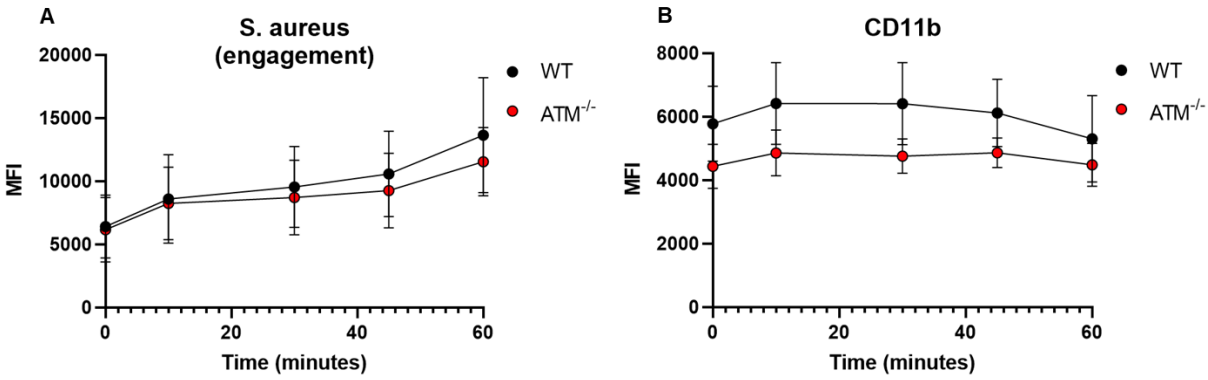

Figure 4.8: Engagement and degranulation of WT and ATM$^{-/-}$ PLB against *S. aureus*. (A) Flow cytometry data showing engagement of WT and ATM$^{-/-}$ PLBs with cell trace violet-labelled *S. aureus* strain JE2. Engulfment of labelled bacteria leads to increase in PLB fluorescence. (B) Degranulation was measured by flow cytometry using an antibody against the integrin receptor CD11b. Data is expressed as MFI mean ± SEM, Two-way ANOVA with Bonferroni correction was carried out and no statistical difference was found (n=3).

4.10 Loss of ATM only affects ROS production against lectin Concanavalin A

The neutrophil-like cell line PLB is known to produce a respiratory burst against fMLP and PMA[145]. We therefore wanted to know if the lack of *ATM* would influence the levels of ROS released by these cells. We could not see any difference in the production of ROS using the PKC agonist PMA in the kinetic curve, and also no significant difference was observed using area under the curve analysis between wild type and $ATM^{-/-}$cells (**Figure 4.9 A and B**). We then went on to test the lectin ConA. Compared to WT cells we found that $ATM^{-/-}$ cells were unable to produce a respiratory burst against ConA (**Figure 4.9 C**). This was further confirmed by analysing the area under the curve (**Figure 4.9 D**). We also tested the respiratory burst against *S. aureus* JE2 at MOI 20. We were able to see a small decrease in the production of ROS by $ATM^{-/-}$ cells in the kinetic curve, however the AUC analysis did not show a significant difference between WT and $ATM^{-/-}$ (**Figure 4.9 E and F**). We then tested the respiratory burst against *C. albicans* at MOI 5. We were not able to see a difference in the production of ROS and this was further confirmed after analysis of the AUC (**Figure 4.9 G and H**).

Finally, we tested the Mycobacterium tuberculosis-derived mincle agonist TDB and could see similar or slightly increased activity of $ATM^{-/-}$ cells in the respiratory burst kinetic curve. After analysing the area under the curve, however, we could not see any significant difference between conditions (**Figure 4.9 I and J**).

In summary, we found some similarities between the ATM knockout PLBs and the neutrophils treated with ATM inhibitor. We could not see a difference in PMA, but we saw a slight decreased response trend to *S. aureus* JE2 and an impaired respiratory burst against ConA. On the other hand, we saw a completely different result against TDB; whilst ATM-inhibited neutrophils have an impaired respiratory burst, $ATM^{-/-}$ PLBs did not seem to have any problem producing a respiratory burst against this stimulus.

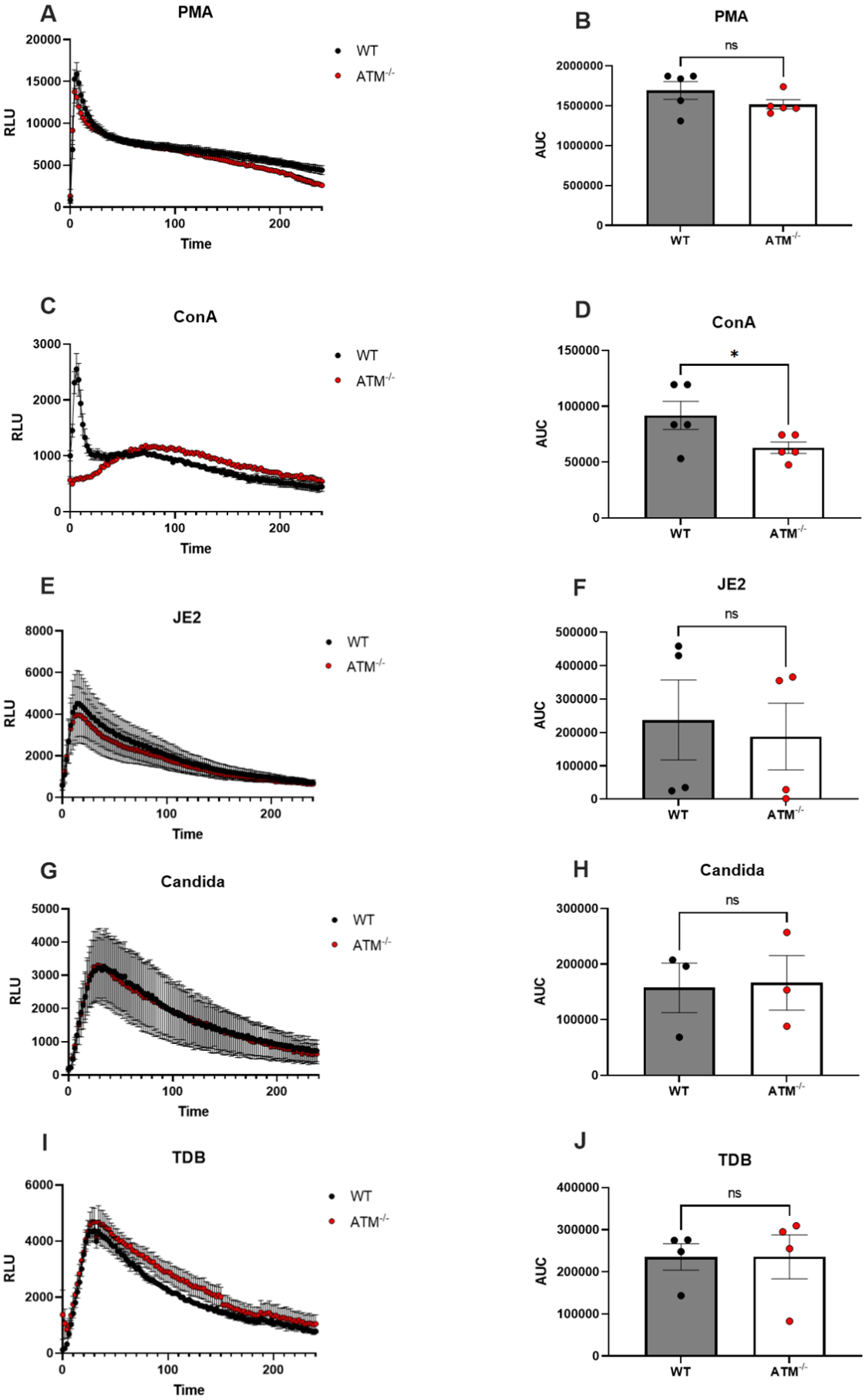

(legend on next page)

Figure 4.9: Respiratory burst (ROS) against different stimuli by WT and ATM$^{-/-}$ PLB cells. (A, C, E, G, I) Time course analysis of ROS production, measured by luminol assay, in response to 100 nM PMA (n=5) (A), 50ug/ml ConA (n=5) (C), S. aureus MOI 20 (n=4) (E), C. albicans MOI 5 (n=3) (G), 50ug/ml TDB (n=4) (I) (B, D, F, H, J) Area under the curve (AUC) analysis corresponding to plots shown on the left. Data is expressed as mean relative light units (RLU) ± SEM. (B,D,F,H) Data is expressed as mean ± SEM. Statistical significance was calculated by two-tailed t-test: *p<0.03.

4.11 Loss of ATM impairs NET-like release in neutrophil-like cells

PLBs differentiated into neutrophil-like cells, are able to release NET-like structures when stimulated with the mitogen PMA[45]. As we found that loss of ATM impaired ROS production against the chemical stimuli ConA, we wanted to see if ATM$^{-/-}$ neutrophil-like cells were able to release NET-like structures when challenged with this stimulus.

We found that ATM$^{-/-}$ neutrophil-like cells released significantly more NET-like structures when stimulated with PMA (**Figure 4.10 A and B**). However, we saw a decreased trend in the release of NET-like structures when stimulated with ConA, this was not statistically significant (**Figure 4.10 A and B**).

In summary, we demonstrated that neutrophil-like cells can release NET-like structures against the stimuli PMA and ConA. ATM$^{-/-}$ cells produced more NET-like structures against ConA, while ConA stimulated ones had similar levels to spontaneous NET release in the unstimulated cells.

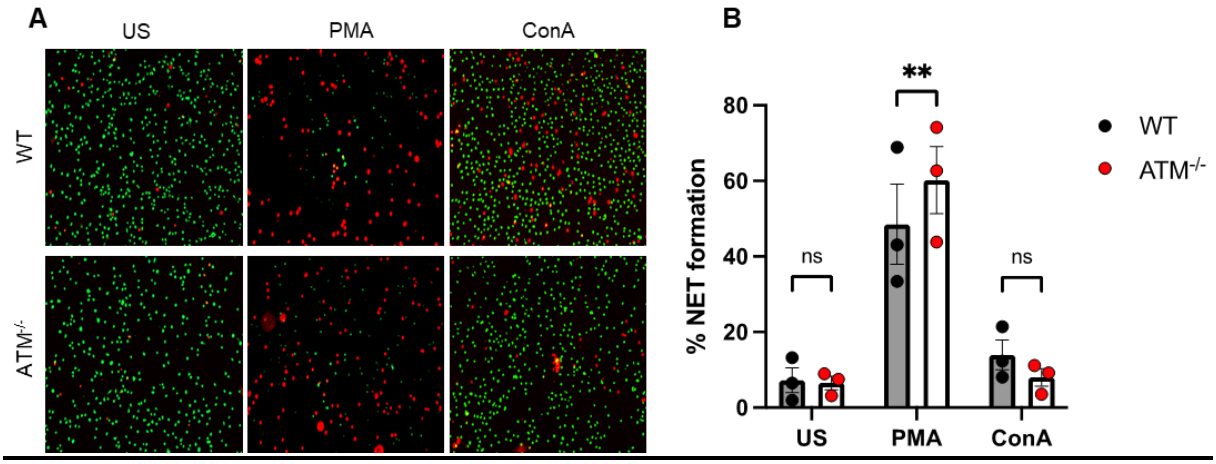

(legend on next page)

Figure 4.10: Neutrophil extracellular trap-like release against different stimuli in wild type and ATM knockout PLBs. PLBs were differentiated for 6 day to a neutrophil-like cell. Live cells were stained with the intracellular DNA dye SYTO green, while NETs were visualised with the extracellular dye SYTOX orange. (A) Representative images of neutrophil-like cells stimulated with 50nM PMA (n=3) (mid panel) and 50ug/ml ConA (n=3) (right panel).(B) Quantification of NET-like formation was calculated as number of NETs (Red) divided by live (green) plus NETs (red) .Cells were imaged at 10x magnification using a fluorescent microscope EVOS (ThermoFisher), 4 fields of view were acquired for each differentiation and NETs were counted using FIJI software for each field of view, an average of cells per field of view per differentiation was plotted as percentage of NET-like formation. Data is expressed as mean ± SEM. Statistical significance was calculated by two-tailed t-test: **p<0.003.

4.12 Loss of ATM does not affect chemokine secretion

Neutrophils treated with ATM inhibitor (KU55933) and from A-T patients are known to have increased release of the chemokine interleukin-8 (IL-8)[82]. We asked if our $ATM^{-/-}$ neutrophil-like cell was able to reproduce this finding. We stimulated the cells with bacterial peptide lipopolysaccharides (LPS) and the cytokine tumour necrosis factor α (TNF- α). We could not see a significant difference in the secretion of IL-8 between the $ATM^{-/-}$ and wild type differentiated cells (**Figure 4.11**). However, we could see that differentiated cells release IL-8 without any stimulation compared to undifferentiated cells. This could be explained by PLBs undergoing spontaneous apoptosis after differentiation and causing the remaining cells to release IL-8 upon recognition of DAMPs. In summary, we could not recapitulate previous findings of increased IL-8 secretion in cells treated with the pharmacological inhibitor of ATM and A-T neutrophils in our neutrophil-like *ATM* knockout system.

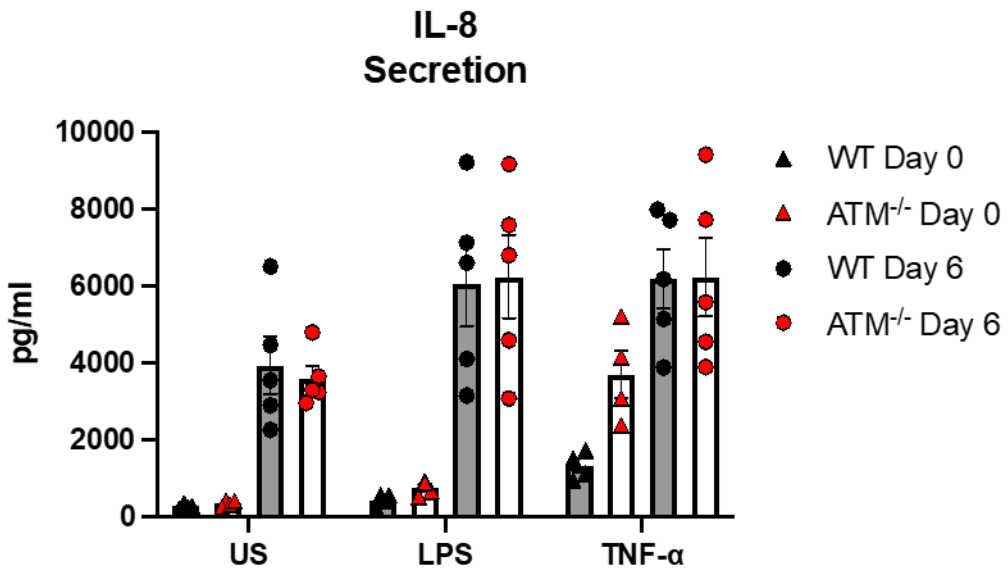

Figure 4.11: Loss of ATM does not affect Il-8 production. Neutrophil-like Il-8 production (n=5) in response to LPS and TNF-α. PLB cells were differentiated for 6 days and later stimulated with 100ng/ml LPS, 20ng/ml TNF-α for 18 hours. Cytokine concentration was measured by ELISA. Data is expressed as mean ± SEM. No statistical significance was found using a paired two-tailed t-test.

4.13 Generation of ATM inducible knockdown in PLB cell line

Stable, full knockout of an important gene can lead to genetic adaptation by other pathways that compensate for the loss of the protein and restore normal physiological function. During an acute inhibition, such as with pharmacological inhibitors, the cell might not have enough time to compensate, and therefore this may lead to more drastic phenotypes. To address this, we decided to generate an inducible ATM small hairpin RNA (shRNA) knockdown cell line of PLBs. This approach allowed us to significantly reduce ATM levels before or during differentiation, and then test the cells before they had a chance to engage genetic compensation.

We generated a plasmid with a doxycycline inducible shRNA against ATM and luciferase, which was used as a control. We transfected the plasmid into our PLBs using a 2nd generation lentiviral vector that included a puromycin resistance gene. We selected the cells that survived a puromycin selection process, without single cell cloning (in batch format). Once we had made our ATM inducible shRNA cell line we first tested if the induction of the plasmid was able to decrease the levels of ATM in our PLBs. We observed that treatment of the cells with 50ng/ml of doxycycline for

three days gave us a knockdown of approximately 70% as shown in (**Figure 4.12 A and B**).

We then decided to treat the cells with doxycycline from day one of differentiation and top up the media with doxycycline at day 4, in order to maintain the levels of ATM as low as possible to allow comparison with the CRISPR knockout. We first measured the respiratory burst of our shRNA cell line against the same stimuli as used previously.

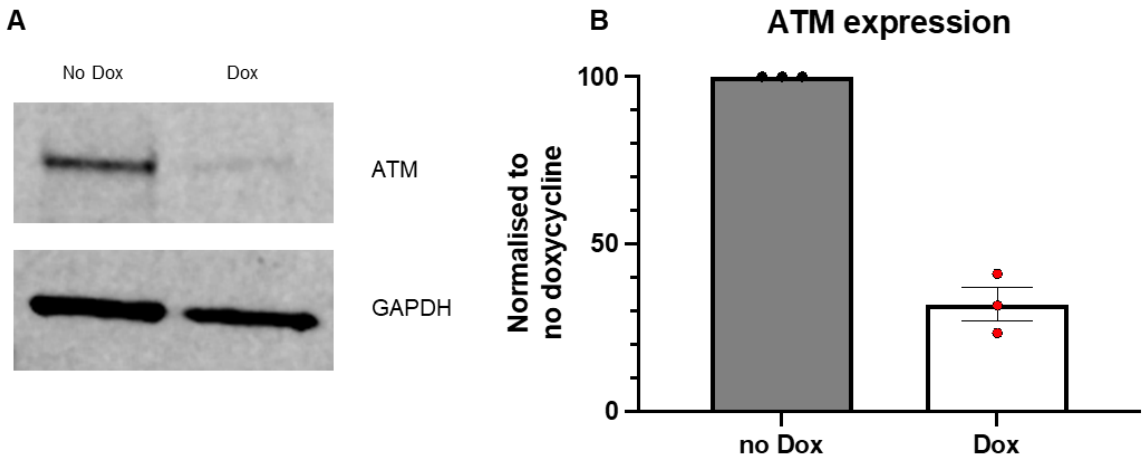

Figure 4.12: Generation of inducible PLB-985 ATM knockdown cell line. (A) Representative western blot to confirm knockdown of ATM. GAPDH was used as loading control. (B) Quantification of ATM expression after induction of shRNA using 50ng/ml doxycycline. Protein levels were first normalised using GAPDH. Percentage expression of ATM was obtained by comparing the levels of doxycycline treated cells against control (untreated) (n=3).

We could not see any differences in ROS production with PMA between the luciferase control shRNA and the ATM shRNA, as seen in the kinetic curve and the area under the curve analysis (**Figure 4.13 A and B**). We also tested *S. aureus* JE2 at MOI 20 and the mincle agonist TDB. In both cases, we observed that ATM knockdown cells had a decreased respiratory burst in the kinetic analysis, which was further confirmed by a significant reduction of the AUC (**Figure 4.13 C-D and G-H**). Finally, we saw that there was a slight increase in ROS production of ATM shRNA cells against *C. albicans*. This was not statistically significant after analysing by AUC (**Figure 4.13 E and F**).

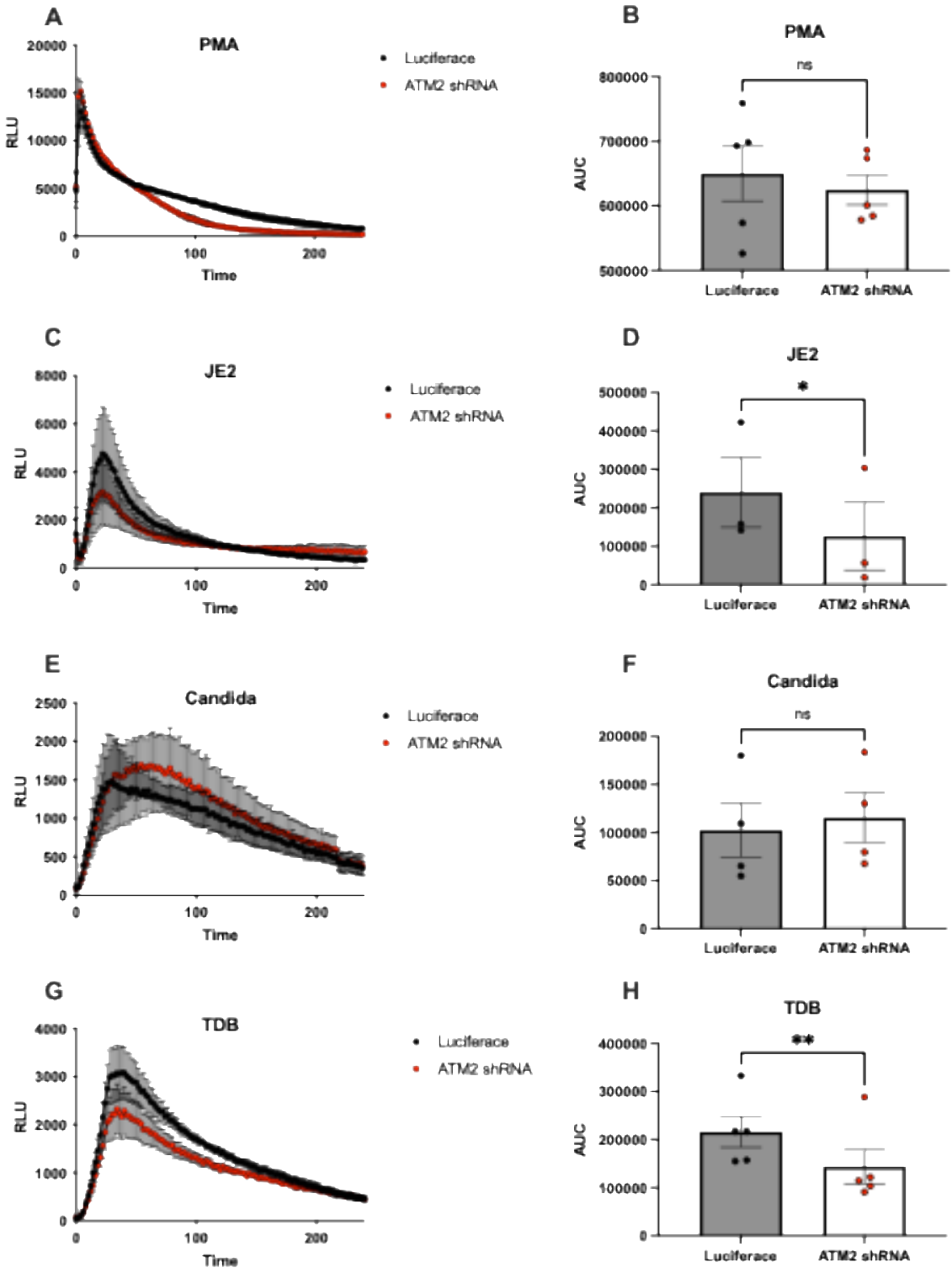

Figure 4.13: Respiratory burst (ROS) against different stimuli by control (luciferase) and ATM shRNA PLB cells. (A, C, E, G) Time course analysis of ROS production, measured by luminol assay, in response to 100 nM PMA (n=5) (A), S. aureus MOI 20 (n=3) (C), C. albicans MOI 5 (n=4) (E), 50ug/ml TDB (n=5) (G) (B, D, F, H) Area under the curve (AUC) analysis corresponding to plots shown on the left. Data is expressed as mean relative light units (RLU) ± SEM. (B,D,F,H) Data is expressed as mean ± SEM. Statistical significance was calculated by two-tailed t-test: *p<0.03. and **p<0.003.

In summary, we found that shRNA-mediated knockdown of ATM in PLBs at the beginning of the differentiation had similarities with the primary neutrophils treated with ATM inhibitor, as seen in the decreased respiratory burst against *S. aureus* and the mincle agonist TDB. On the other hand, we could see that ROS production after PMA stimulation is not affected in three different models.

4.14 Generation of ATM knockout neutrophil from CD34+ hematopoietic stem cells

We know PLBs have some limitations as i) they do not express as many receptors as primary neutrophils[145] and ii) at day 6 of differentiation they are not as terminally differentiated as primary neutrophils[135]. To overcome this limitation, we decided to perform a preliminary experiment using hematopoietic stem cells and differentiating them into neutrophils, in collaboration with Prof. Ash Toye's lab (School of Biochemistry, University of Bristol).

We isolated CD34+ hematopoietic stem cells (HSCs) from multiple apheresis cones of a three different donors by negative immunomagnetic selection. They were then expanded for three days before we attempted to knockout ATM using CRISPR/Cas9 ribonucleoprotein (RNP) delivered with nucleofection technology, which introduces into the cells two different gRNAs and the enzyme Cas9. The cells were left to recover for three days before starting the differentiation process which lasts for 15-17 days. In terminally differentiated neutrophils we tested for the degree of ATM knockdown (without single cell cloning) and obtained 90% knockdown of ATM in our batch of cells (**Figure 4.14 A and B**).

We next tested the ability of these neutrophils to kill bacteria, produce a respiratory burst, phagocytose and degranulate.

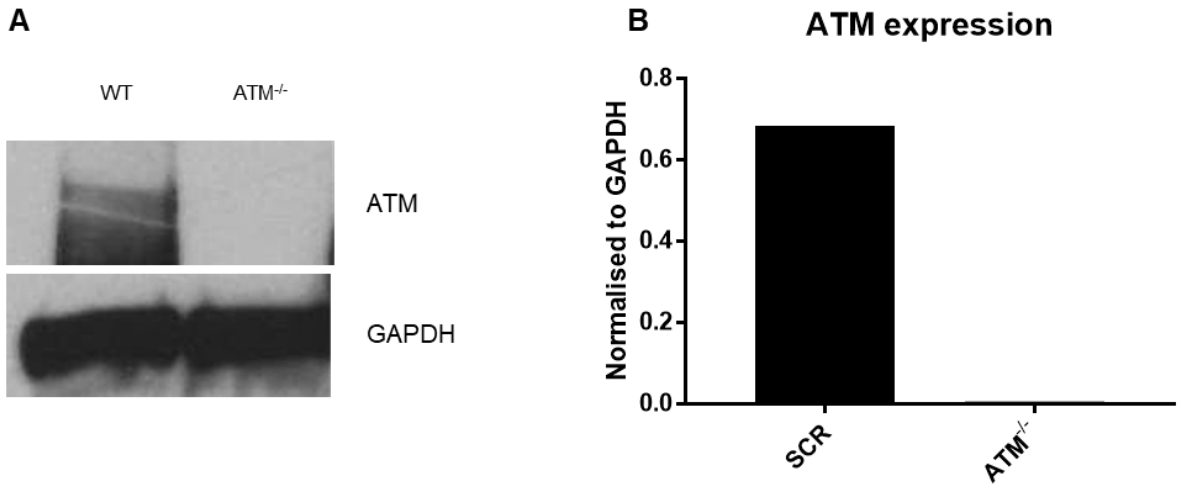

Figure 4.14: Generation of ATM knockdown neutrophil differentiated from hematopoietic stem cells. (A) Representative western blot to confirm knockdown of ATM. GAPDH was used as loading control. (B) Quantification of ATM expression. Protein levels were normalised using GAPDH (n=3).

After we confirm our CD34+ differentiated neutrophils had an ATM knockdown, we tested the ability of these cells to kill *S. aureus* strain JE2. We could see that across the 4 hours both the WT and the ATM knockdown were able to kill the pathogen, however, at the 4-hour timepoint we could see that ATM knockdown cells showed a trend for less efficiency at killing the pathogen when compared to the WT (**Figure 4.15 A and B**). These was similar to our results with primary neutrophils treated with an ATM inhibitor and to our ATM$^{-/-}$ dPLB.

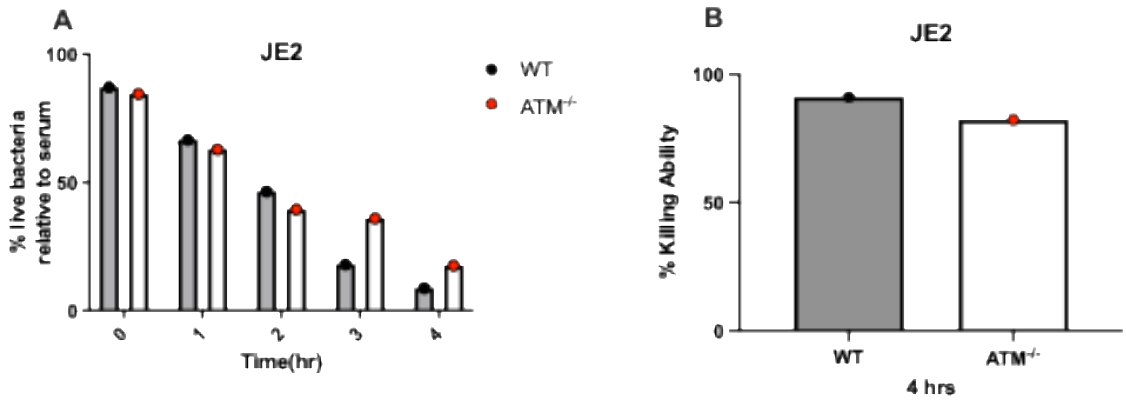

(legend on next page)

Figure 4.15: Impaired killing of *S. aureus* in ATM knockdown neutrophil differentiated from hematopoietic stem cells over 4 hours compared to wild type (WT). (A) Percentage of live JE2 bacteria over 4 hours of engagement with differentiated neutrophils. Percentage of live bacteria was obtained by normalising bacteria engaged with neutrophils with the control (bacteria grown in media without neutrophils) over 4 hours. (B) Percentage of neutrophil killing ability at time point 4 hours of engagement with *S. aureus* strain JE2. Percentage of neutrophil killing ability at time point 4 hours, corresponding to strain shown on the left was obtained by comparing the percentage of dead bacteria at 4 hours with the starting time point 0 hours. Neutrophils were differentiated for 17 days and incubated with *S. aureus* (MOI 0.2), 50 µl aliquots were taken every hour and further serial diluted and plated in duplicate in TSA (n=1).

We then went on to test their ability to phagocytose the pathogen, using the same fluorescently tagged bacteria we have used before. We co-incubated neutrophils and bacteria for 1 hour, taking aliquots at time points 0, 10, 30, 45 and 60 minutes. There was a trend into increased ability of ATM knockdown cells to uptake bacteria between conditions and similarly we saw a trend to increased degranulation of secondary granules in ATM knockdown compared to wild type. On the contrary, ATM knockdown cells had a trend to decreased degranulation of tertiary granules and lower phagosome formation compared to wild type, as seen in (**Figure 4.16 A-D**).

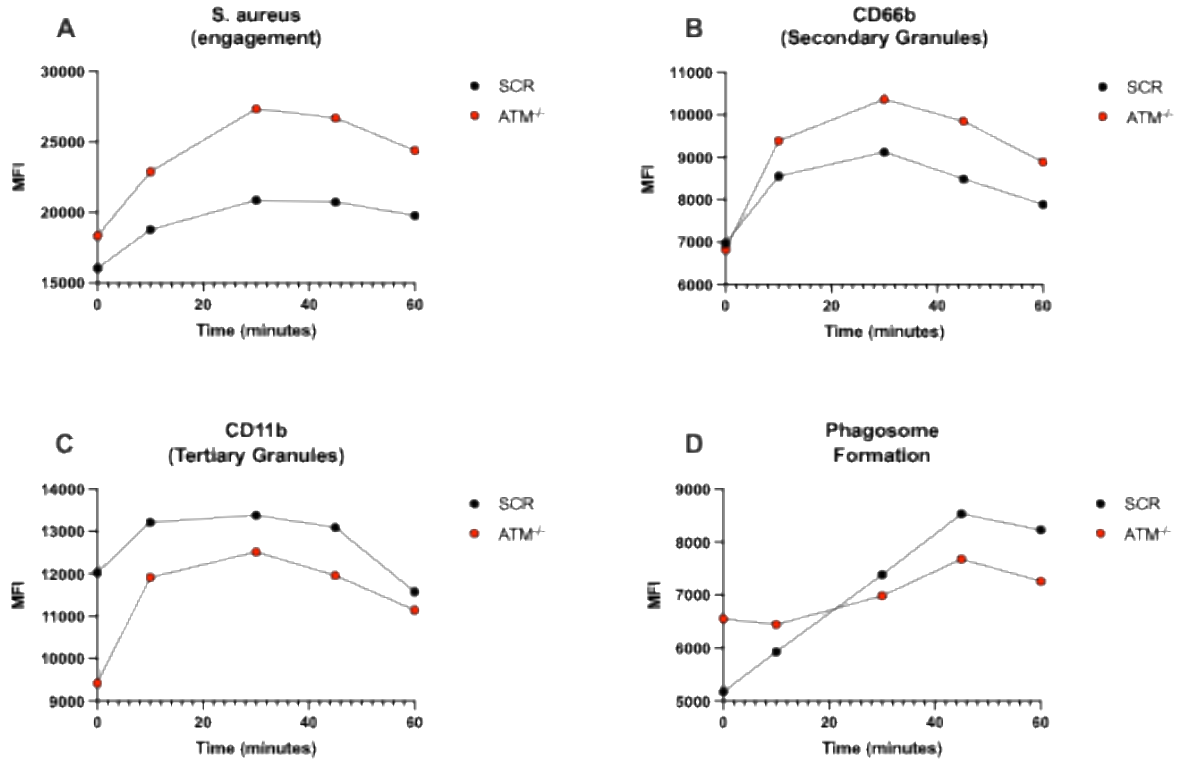

(legend on next page)

Figure 4.16: ATM knockdown neutrophils differentiated from hematopoietic stem cells showed increased engagement with *S. aureus* and degranulation of secondary granules. (A) Flow cytometry data showing engagement of neutrophils with cell trace violet-labelled S. aureus strain JE2. Engulfment of labelled bacteria leads to increase in neutrophil fluorescence. (B) Degranulation of secondary granules measured by flow cytometry using an antibody against CEACAM8 (CD66b) (C) Degranulation of tertiary granules measured by flow cytometry using an antibody against the integrin receptor CD11b. (D) Phagosome formation increases fluorescence as bacteria labelled with pHrodo dye enter the phagosome (n=1).

We went on to analyse the ability of these neutrophils to produce a respiratory burst against different stimuli. Firstly, we tested the mitogen PMA and saw that ATM knockdown cells showed reduced ROS production compared to wild type. This was different to the other three systems where PMA respiratory burst was not affected by pharmacological inhibition of ATM, complete knockout of ATM and transient knockdown of ATM (**Figure 4.17 A**). We then saw that ATM knockdown cells showed reduced ability to produce a respiratory burst against the lectin ConA, this was similar to the previous three systems tested (**Figure 4.17 B**). Finally, we tested the pathogens *S. aureus* and *C. albicans* and saw a decreased ROS production in both, with *Candida* ROS being more impaired in ATM knockdown cells. This result was similar to the one obtained with pharmacological inhibition of ATM in primary neutrophils and was contrasting to our complete knockout of *ATM* in the neutrophil-like cells where we could not see a significant difference. However, since this was only done with one donor, it will need further complementary experiments to see if the patterns seen remain the same.

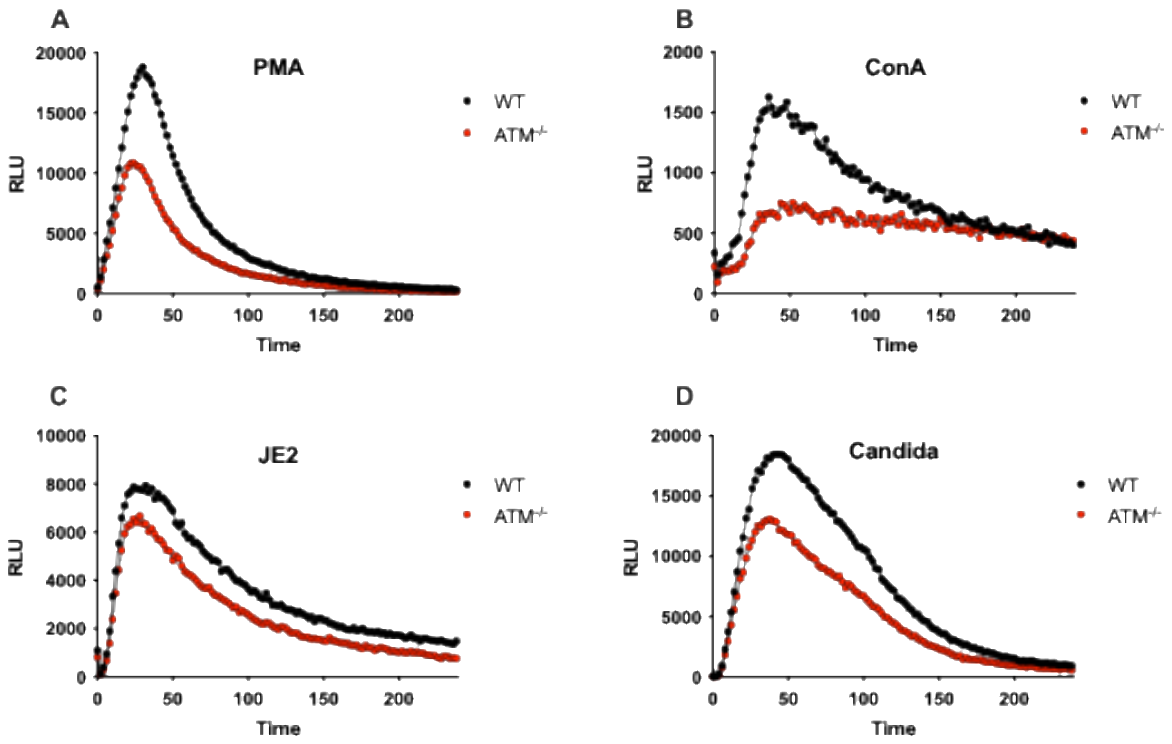

Figure 4.17: Respiratory burst (ROS) against different stimuli by wild type or ATM knockdown HSC differentiated neutrophils. (A, B, C, D) Time course analysis of ROS production, measured by luminol assay, in response to 100 nM PMA (A), 50ug/ml ConA (C), S. aureus MOI 20 (E), C. albicans MOI 5; (n=1).

In summary, ATM knockdown in differentiated neutrophils from hematopoietic stem cells showed a decrease antimicrobial capacity, comparable with the previous models of pharmacological inhibition and CRISPR/CAS9 knockout of ATM in primary neutrophils and the PLB cell line. We found a difference in bacteria engagement and degranulation that is the opposite to what we have seen in previous models, however, phagosome formation showed a similar decreased trend. Finally, respiratory burst production showed similar impairment with receptor binding stimuli, with PMA respiratory burst only impaired in this system. Since this was only done with one donor we will need further experiments to see if all trends remain the same and results can be compared to the previous systems.

4.15 Neutrophils from A-T patients do not show a defect in ROS production

We know the use of inhibitors might have off-target effects in the cells, similarly our models of PLB CRISPR knockout and shRNA knockdown could be missing some key

aspects of receptor mediated signalling compared to primary neutrophils. Similarly, neutrophils obtained from CD34+ differentiated cells, do not achieve a full maturity phenotype as compared to primary neutrophils. Therefore, we decided to test ROS production in A-T neutrophils since we had seen some contrasting results between models against the pathogen *S. aureus* and the lectin ConA.

In collaboration with Charité University Hospital, Berlin, Germany, we obtained neutrophils from A-T patients. Our collaborators in Berlin carried out the ROS assay with the stimuli PMA, ConA and *S. aureus*. These stimuli had shown different kinetics in our systems. Here we show PMA respiratory burst was similar between the A-T patient neutrophil compared to healthy donor neutrophil (**Figure 4.18 A-C**). Then we found A-T neutrophils were able to produce a respiratory burst against ConA similar to a healthy donor neutrophil, this was of our surprise, since we could not get a respiratory burst against this stimulus in neutrophils treated with ATM inhibitor and in our $ATM^{-/-}$ dPLB, while CD34+ differentiated neutrophils showed a decrease production of ROS. Furthermore, A-T neutrophils also had a similar ROS production against *S. aureus* compared to healthy donor neutrophils. This was also different to our previous experiments. We have showed neutrophils treated with ATM inhibitor had a significant decrease in ROS production against this stimulus, similarly our one repeat in CD34+ differentiated neutrophils had a decrease in ROS production in ATM knockdown cells compared to scramble ones. On the other hand, our $ATM^{-/-}$ dPLB had a similar ROS production against this stimulus compared to WT dPLB.

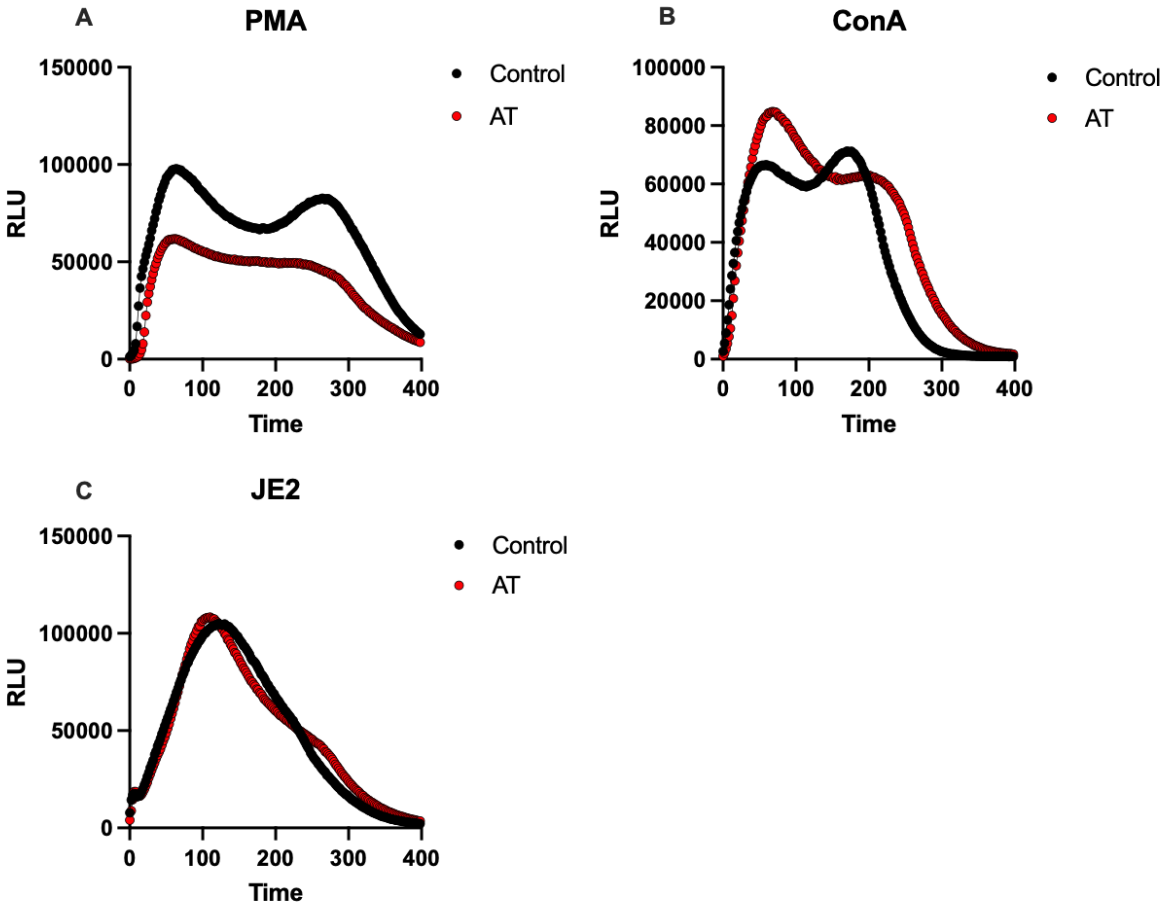

Figure 4.18: Respiratory burst (ROS) against different stimuli by healthy and A-T neutrophils. (A, B, C) Representative time course analysis of ROS production, measured by luminol assay, in response to 100 nM PMA (A), 50ug/ml ConA (C), S. aureus MOI 20 (n=3).

These results opened the question, whether A-T neutrophils had been able to compensate for the lack of *ATM*. Similarly, our knockout ATM PLB could have undergone genetic compensation for the lack of ATM. While an acute inhibition or decreased expression of ATM does not give the cell the opportunity to compensate and therefore, we see a different response to receptor binding stimuli. This will need further investigation into downstream signalling leading to NOX2 activation.

Since our ATM$^{-/-}$ dPLB had some interesting results in their antimicrobial activity. We decided to use it as a developmental model to study the development of neutrophils and see if defects in their development are involved in causing the defects in antimicrobial capacity we see in differentiated PLB.

4.16 Chapter Overview

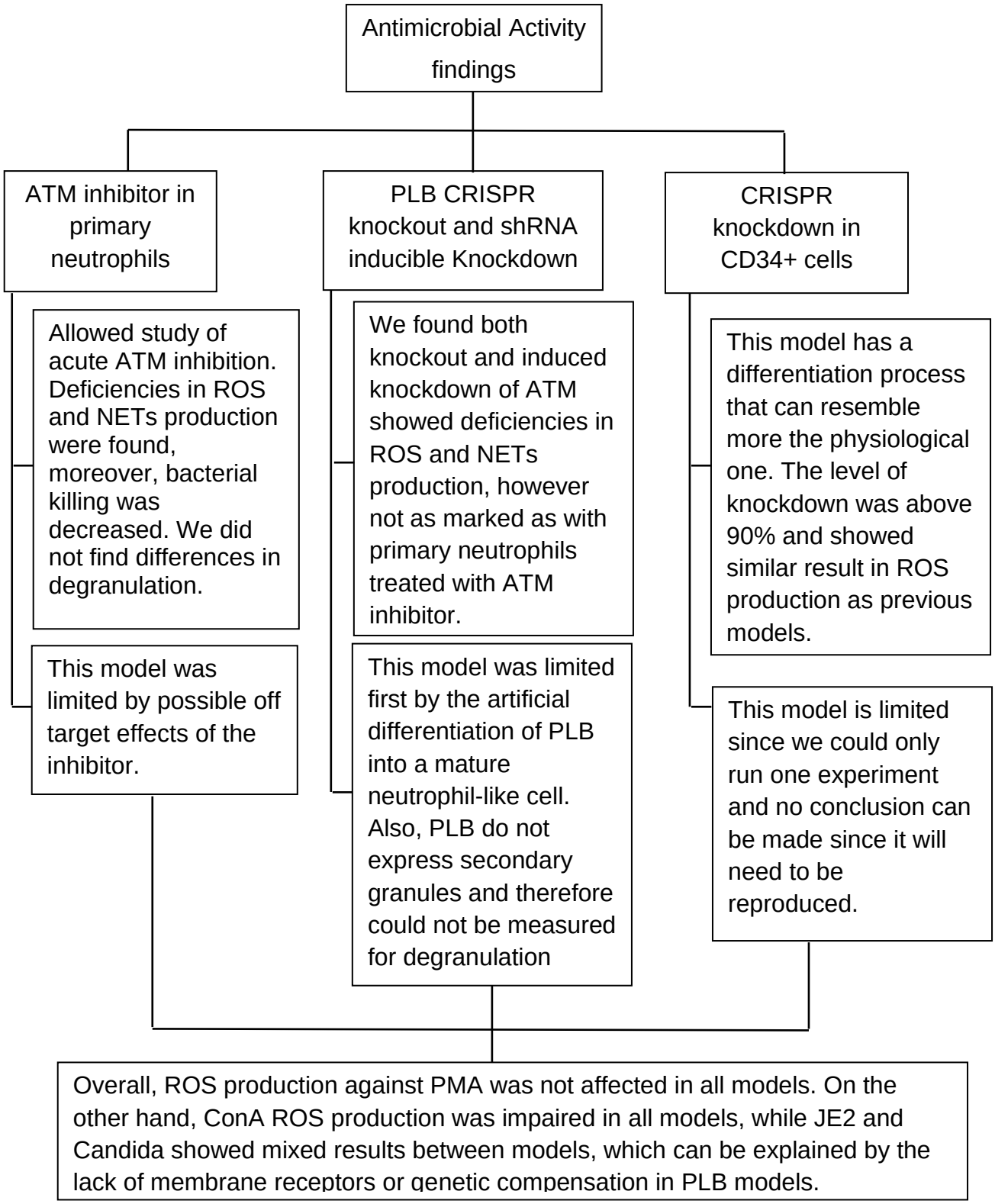

CHAPTER 5: The role of ATM in neutrophil development

5.1 Introduction

We showed in the previous chapter ATM$^{-/-}$ dPLB and A-T neutrophils have a different respiratory burst against the pathogen S. aureus compared to neutrophils treated with ATM inhibitor or shRNA knockdown. This made us question if something is happening in cells lacking ATM during their development, that is helping them to compensate for the lack of this protein through other mechanism and making them have a normal respiratory burst against *S. aureus*. Therefore, we hypothesise ATM is involved in neutrophil development.

We decided to use the promyelocytic leukaemia cell line (PLB) to study the role of ATM in neutrophil development. Previously, this cell line has been used to study neutrophil biology and functionality[135,145–148]. It can be genetically modified and can be differentiated to a mature neutrophil-like cell using different reagents including N,N-Dimethyl formamide (DMF)[135,145,147–149]. Neutrophil-like dPLB cells express some of the membrane receptors found in a mature neutrophil, for example integrin-α receptor (CD11b)[135,145] and the formyl peptide receptor (FPR1)[135,145]. These can have different levels of expression depending on the reagent used for differentiation[135,145]. FCγ receptor IIA (CD32A)[147] was also found in the membrane of PLBs differentiated with the previous reagents mentioned, while Pivot-Pajot and colleagues could not see expression of FCγ receptor IIIA (CD16b)[147]. A previous study done by Selmeczy and colleagues[150], showed expression of this receptor after differentiation with DMF, complement receptor type 1 (CD35) was also found in the membrane of neutrophil-like cells[145].

Similarly, expression of some granule proteins were found in these neutrophil-like cells[147], however they fail to express specific (secondary) granules compared to a mature neutrophil[135]. Gene expression analysis performed by Rincon and colleagues[135] found similarities in expression of genes related to primary and tertiary granules, secretory vesicles as well as genes involved in respiratory burst, while no correlation was found for genes encoding secondary granule proteins[135]. This was also shown in another study where Pivot-Pajot and colleagues[147] analysed granule

gene expression in undifferentiated and differentiated PLB by qPCR[147]. Quiescent mature neutrophils have low transcription and short lifespan[7], making it difficult to do genetic manipulation on these cells. Therefore, use of PLB to understand neutrophil behaviour in a genetic disease has been a good model as shown in by Zhen and colleagues[149] who developed a X-CGD PLB and found the phenotype can be rescued by expression of transgenic gp91^{phox} [149].

Previously, development of T cells has been shown to be impaired in AT patients, showing an immature phenotype and lack of antigen receptor variety[151]. However, there is little evidence on how mutations in ATM can affect the development of neutrophils in these patients, this chapter aims to understand the effects of loss of ATM in the development of neutrophils.

5.2 Loss of ATM leads to increased expression of integrin-α (CD11b) on neutrophil membrane

Terminally mature neutrophils have a characteristic lobulated nucleus and express a variety of receptors on their plasma membrane, including integrin-α receptor (CD11b) which is known to increase its expression during neutrophil development[56] and therefore serves as a maturity marker. We differentiated our PLB cell line with DMF over 6 days to obtain a neutrophil-like cell and made cytospins to analyse nuclear shape and cytoplasm staining. After differentiation we could only see partial lobulation and condensation of the nucleus compared to undifferentiated cells. Neutrophils are known to have a light pink cytoplasmic staining, since their granules do not react to the haematoxylin and eosin staining, while early progenitors show a blue staining of their cytoplasm. We found a change in cytoplasmic staining from a light blue cytoplasm at Day 0 to a light pink at Day 6 with haematoxylin and eosin[9] (**Figure 5.1 A**). This allowed us to see both our WT and ATM$^{-/-}$ PLB were differentiating into a neutrophil-like cell.

To further assess if our neutrophil-like cell line was successfully differentiating, we measured the expression of CD11b at different stages of differentiation (Day 0, Day 4 and Day 6). We analysed the expression of CD11b by flow cytometry and found that its expression in the cell membrane was increasing during differentiation (**Figure 5.1 B**).

ATM$^{-/-}$ differentiated PLBs (dPLB) showed an increased expression of CD11b in their membrane in 6 different differentiations compared to WT dPLB (**Figure 5.1 C**), we then tested a second ATM$^{-/-}$ clone and showed a similar pattern of increased CD11b expression in 3 different differentiations compared to WT dPLB (**Figure 5.1 D**).

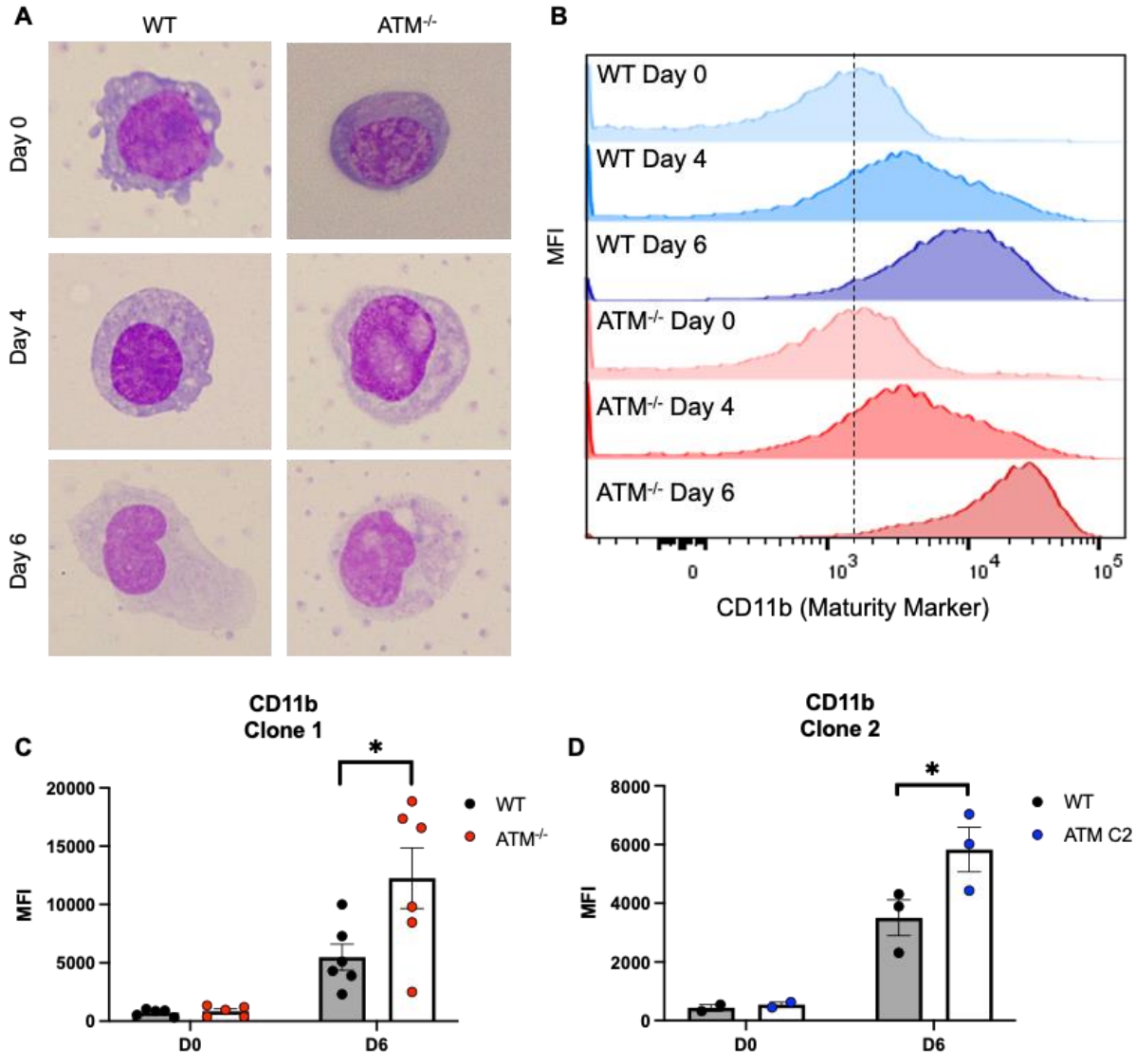

(legend on next page)

Figure 5.1: WT and ATM$^{-/-}$ PLB differentiation into a neutrophil-like cell. Loss of ATM causes increased expression of CD11b receptor. PLB-985 cell line was differentiated over six days in RPMI media supplemented with DMF. (A) Cytospins were made with 1x10^4 cells and stained with eosin and haematoxylin dyes. Representative images of WT (left column) and ATM$^{-/-}$ (right column) at Day 0, 4 and 6 of differentiation. Changes in cytoplasmic colour can be seen from Day 0 to Day 6. Nuclear shape is also changed from Day 0 to 4 and Day 6. (B) Representative histograms of CD11b (maturity marker) expression at Day 0, 4 and 6 of differentiation. (C) Quantification of B in all pooled experiments from clone 1 ATM$^{-/-}$ neutrophil-like cells show an increase expression of the maturity marker CD11b at Day 6 of differentiation compared to WT (n=6). Paired two-tailed student's t-test analysis, *p<0.05. (D) Quantification of B in all pooled experiments from clone 2 ATM$^{-/-}$ neutrophil-like cells show an increase expression of the maturity marker CD11b at Day 6 of differentiation compared to WT (n=3). Paired two-tailed student's t-test analysis, *p<0.05. Data is expressed as mean fluorescence intensity (MFI) ± SEM.

We questioned if this phenotype was also happening in neutrophils of AT patients. We obtained neutrophils from 4 A-T patients and 3 healthy controls from a collaboration with Charité University Hospital, Berlin Germany. We analysed 8 different membrane receptors and found that CD11b was significantly increased in neutrophils from AT patients compared to healthy controls (**Figure 5.2 B**). These results showed development of neutrophils is affected by the loss of ATM. We then went on to analyse mitochondrial capacity during development, since it is known that neutrophils change from oxidative phosphorylation (OXPHOS) to glycolysis to fulfil their energy requirements, and ATM has been shown to be involved in mitochondrial stability (mitophagy)[38].

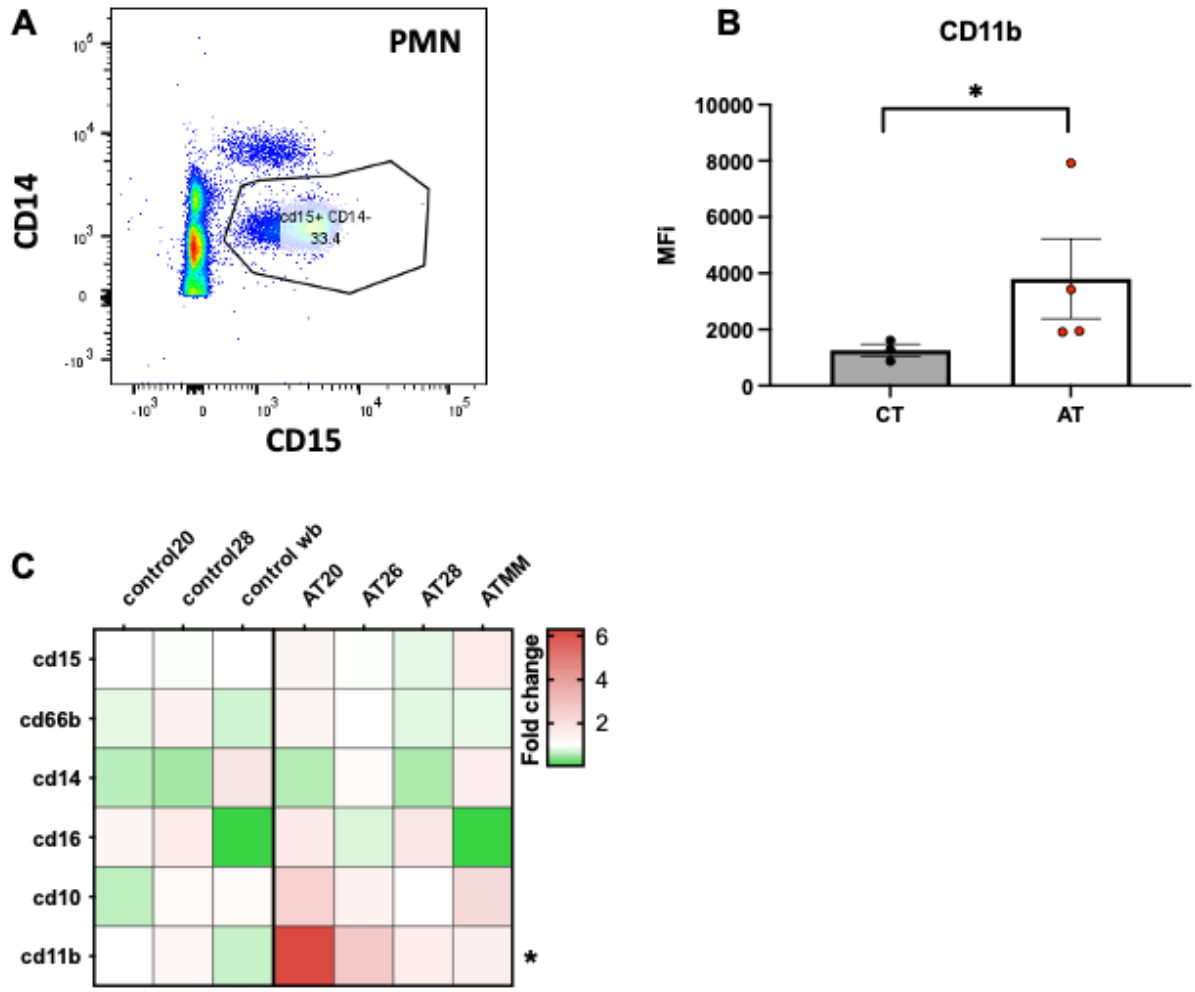

Figure 5.2: Neutrophils from A-T patients show increased CD11b. Whole blood from healthy and A-T donors was stained with an 8-colour panel, CD14 was used to gate out monocytes, while IL5-R was used to gate out eosinophils. (A) Gating strategy to isolate neutrophils from whole blood. After gating for single cells using Forward Scatter Area (FSC-A) against FSC height (FSC-H), we gated neutrophil population as CD14- CD15+. (B) Quantification of A in all pooled A-T patients (n=4) and healthy donors (n=3); A-T neutrophils show an increase in expression of the receptor CD11b compared to healthy donors' neutrophils. Unpaired two-tailed student t-test *p<0.05 (C) Heatmap showing the different MFI for each individual donor and patient for six of the markers. Two-way ANOVA *p<0.05 (n=3 healthy donors) and (n=4 A-T patients). Data is expressed as mean fluorescence intensity (MFI) ± SEM.

5.3 Loss of ATM does not affect neutrophil mitochondrial capacity but increases glycolytic capacity

Development of neutrophils is marked by a shift from OXPHOS to glycolysis to fulfil the energy requirement of the cell[38]. Neutrophils are also known to decrease mitochondrial mass during their development[44], defining a shift in metabolic pathways.

We decided to analyse these changes in metabolism in our ATM$^{-/-}$ PLB cell line (clone 1) using the Seahorse extracellular flux analyser. This technique allows us to distinguish between reliance on glycolysis versus mitochondrial oxidation, using reagents that interfere with either pathway. Glycolysis is measured by measurements of the extracellular acidification rate (ECAR) caused by release of lactate through glycolysis. While OXPHOS is detected by measurement of oxygen consumption rate (OCR) caused by oxygen being used by mitochondria to fuel the electron transport chain.

We analysed mitochondrial respiration and glycolytic capacity of wild type and ATM$^{-/-}$ undifferentiated PLB and dPLB using the mitochondrial stress test. This test first injects the drug Oligomycin which blocks the complex V of the electron transport chain, then there is the injection of the mitochondrial membrane uncoupler carbonyl cyanide 4-(trifluoromethoxy)phenylhydrazone (FCCP) which cause the mitochondria to work at its full capacity. Finally, a combined injection of Rotenone an inhibitor of Complex I and Antimycin A an inhibitor of complex 3 completely shuts down mitochondrial activity. We first focused on the basal reads of oxygen consumption rate (OCR) and extracellular acidification rate (ECAR), which allows to analyse which pathway is being used by the cell under normal conditions and prior to the first injection of the drugs. We could see that undifferentiated PLB cells rely more on mitochondrial activity to generate energy, while dPLB rely more on glycolytic activity (**Figure 5.3 A-D**). This result confirmed that our PLBs were differentiating into a neutrophil-like cell line, as it showed a shift from oxidative phosphorylation (OXPHOS) to glycolysis to generate energy, something that has previously been shown for primary neutrophils[38,44]. We could not see a difference in mitochondrial capacity between WT and ATM$^{-/-}$ cells in either undifferentiated PLB and dPLB. On the other hand, we found a significant increase in glycolytic capacity of ATM$^{-/-}$ dPLB compared to WT, the same effect was not seen in the undifferentiated ones (**Figure 5.3 D**). Therefore, we decided to further test the difference in glycolytic capacity seen in our dPLB.

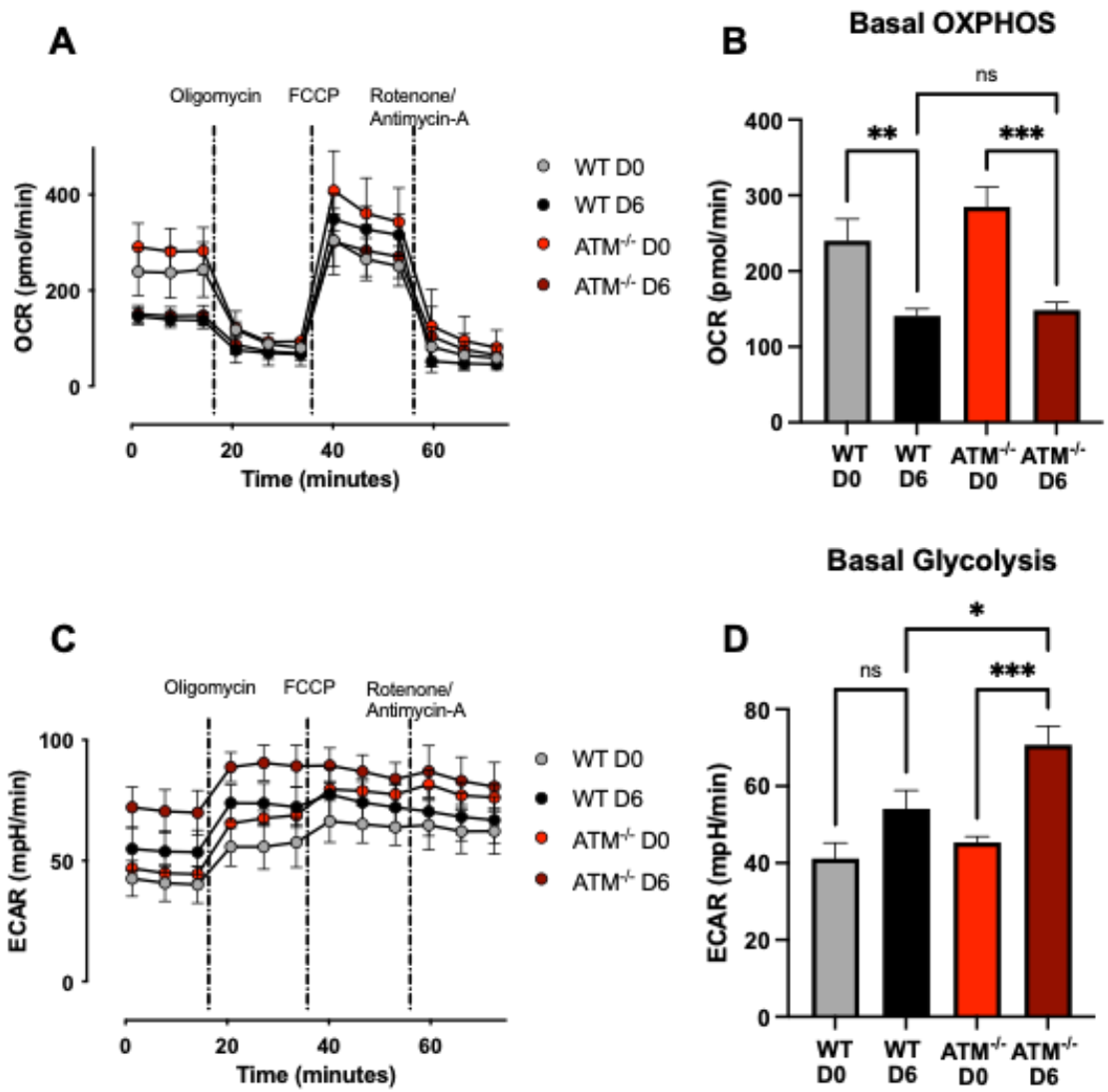

Figure 5.3: ATM loss does not affect mitochondrial capacity but does enhance glycolysis in differentiated neutrophil-like cells. PLB undifferentiated (D0) and differentiated (D6) cells were tested using the extracellular flux analyser Seahorse (Agilent Technologies). Oxygen consumption rate (OCR) measurement shows mitochondrial capacity while extracellular acidification rate (ECAR) corresponds to glycolytic capacity. (A) Kinetic measurement of OCR in $ATM^{-/-}$ and WT PLB undifferentiated and differentiated. Mitochondrial stress test was carried out without inhibitor (basal reads), after injection of the complex V inhibitor (Oligomycin; 2.5µM), after mitochondrial membrane uncoupler (FCCP; 0.5µM) injection and finally after injection with complex I and III inhibitors (Rotenone and Antimycin-A; 0.5µM). (B) Bar graph showing basal oxygen consumption (C) Kinetic measurement of ECAR in $ATM^{-/-}$ and WT PLB at day 0 and 6. (D) Basal measurement shows day 6 PLB are more glycolytic compared to day 0, and $ATM^{-/-}$ day 6 are significantly more glycolytic than WT PLB Day 6 of differentiation (n=6). Data is expressed as mean ± SEM, two-way ANOVA with multiple comparison test *p<0.05, **p<0.003, ***p<0.0003.

To test if ATM$^{-/-}$ dPLB were in fact more glycolytic than WT dPLB, we analysed their glycolytic function using the glycolysis stress test. This test relies on starving the cell from glucose prior to the test and then inject glucose to measure the glycolytic and maximal glycolytic function of the cells; by injecting glucose and a mitochondrial membrane inhibitor, this forces the cell to only rely on glycolysis, moreover we use 2-deoxy-d-glucose (2-DG) to inhibit glycolysis. Firstly, we analysed glycolysis in ATM$^{-/-}$ and WT undifferentiated and dPLB. ECAR measurements after glucose injection showed both WT and ATM$^{-/-}$ undifferentiated PLB had a similar glycolysis activity. There was a trend of increased glycolysis between undifferentiated and differentiated WT PLB, while there was a significant increase in ATM$^{-/-}$ dPLB compared to undifferentiated ones (**Figure 5.4 A and B**). We could see there was a trend of increased glycolysis in ATM$^{-/-}$ dPLB compared to WT dPLB, however, we could not see a significant difference (**Figure 5.4 B**).

Then we analysed the glycolytic capacity which refers to the maximal glycolysis a cell can perform after inhibition of mitochondrial metabolism using the complex V inhibitor oligomycin. We could see an increase in glycolytic capacity of both WT and ATM$^{-/-}$ dPLB compared to undifferentiated ones, however this increase was not significant (**Figure 5.4 C**). Also, similar levels of glycolytic capacity were seen across conditions, opposite to basal glycolysis where we could see an increased trend in ATM$^{-/-}$ dPLB compared to WT.

In summary, we were able to confirm our WT and ATM$^{-/-}$ PLB were undergoing metabolic changes typical of neutrophil differentiation as they shift from OXPHOS to glycolytic metabolism. Furthermore, we saw that at basal levels ATM$^{-/-}$ dPLB had a trend to be more glycolytic compared to WT dPLB, this result together with the increased expression of CD11b marker raised the question of whether loss of *ATM* could cause a hyper maturation phenotype in neutrophils. To address this question, we decided to analyse nuclear shape and size of PLB during differentiation, since a hallmark of neutrophil development is their ability to compact their chromatin to form the characteristic lobulated nucleus[7,44].

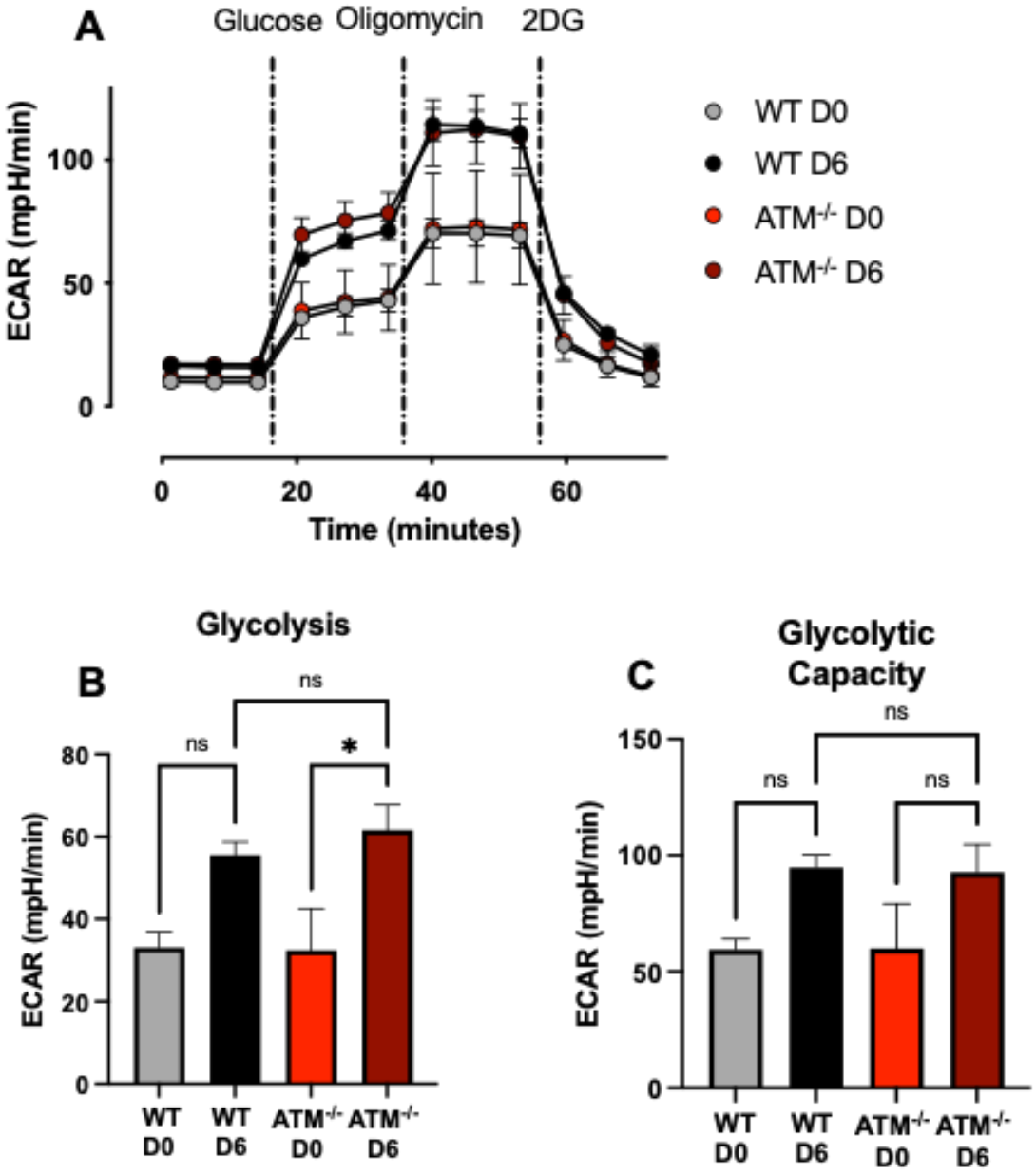

Figure 5.4: PLB differentiation increases glycolytic capacity in both WT and ATM$^{-/-}$ dPLB. PLB undifferentiated (D0) and differentiated (D6) cells were tested using a glycolysis stress test using the extracellular flux analyser Seahorse (Agilent Technologies). Extracellular acidification rate (ECAR) corresponds to glycolysis. (A) Kinetic measurement of ECAR in ATM$^{-/-}$ and WT PLB at day 0 and 6. Glycolysis stress test was carried out with media without glucose (basal reads), after injection of glucose 10mM, then injection of Oligomycin 2.5µM and finally injection of 2-Deoxy-D-Glucose (2-DG) 50mM. (B) Measurement after glucose injection shows day 6 PLB are more glycolytic compared to day 0, and ATM$^{-/-}$ day 6 show an increase glycolytic trend compared to WT PLB Day 6 of differentiation (n=4). (C) Measurement after oligomycin injection shows day 6 PLB have an increased glycolytic capacity trend compared to day 0 (n=4). Two-way ANOVA with multiple comparison test *p<0.05. Data is expressed as mean ± SEM,

5.4 ATM is potentially involved in neutrophil nuclear compaction during differentiation

Neutrophil differentiation from hematopoietic stem cell to a mature neutrophil is characterised by the compaction and multilobulation of the nuclei[7]. We decided to test if loss of ATM was involved in the compaction and shape of the nuclei in our PLB model using transmission electron microscopy (TEM) imaging to analyse nuclear shape and size during three different days of differentiation (Day 0, 4 and 6) (**Figure 5.5 A**).

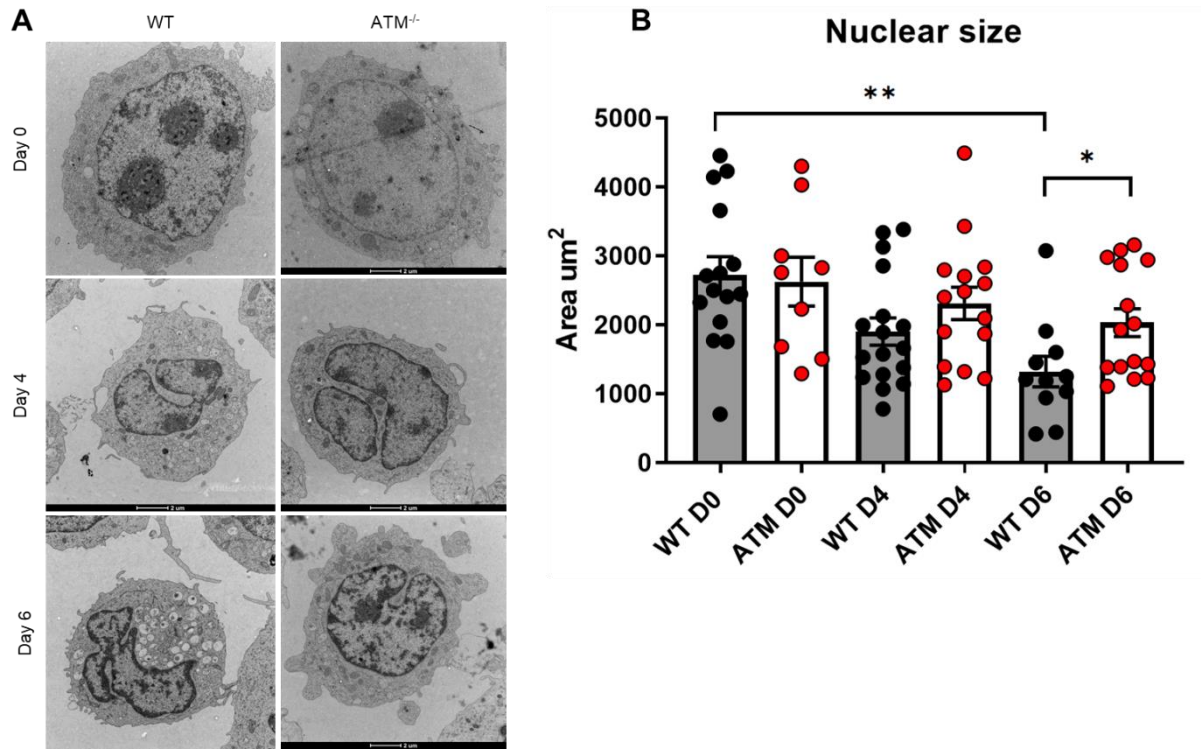

Figure 5.5: Loss of ATM potentially causes impaired nuclear compaction in differentiated neutrophil-like cells. (A) Representative transmission electron microscopy (TEM) images of WT and ATM$^{-/-}$ PLB at Day 0, 4 and 6 of a single differentiation experiment. (B) Analysis of nuclear size throughout differentiation show less nuclear compaction in ATM$^{-/-}$ cells at Day 6 compared to WT. (n=1 differentiation), 10-15 individual cells were imaged for each condition and day. Data is expressed as area (μm^2) ±SEM. Two-way ANOVA analysis for interaction across days of differentiation **p<0.003. Unpaired t-test was performed at Day 6 *p<0.05.

We analysed cells from a single differentiation and quantified at least 10 cells for each day of differentiation. We found that ATM loss at day 0 of differentiation did not show any difference in nuclear shape or ratio of nucleus to cytoplasm when compared to

wild type. We could see a trend of smaller nuclei of WT cells at day 4 compared to day 0, but there was no difference at day 4 between conditions. We detected a significant decrease in nuclear size between day 6 and day 0 in WT PLB (**Figure 5.5 B**), however no significant difference in nuclear size was seen in ATM$^{-/-}$ cells between day 0 and 6. At day 6 we saw a significant difference in nuclear size: WT PLB showed a smaller nuclear area compared to ATM$^{-/-}$ PLB. This result showed a defect in nuclear compaction in ATM defective cells. ATM has been linked with nuclear compaction during DNA repair after double strand breaks[152] , and our result suggests a role for ATM in nuclear compaction during neutrophil development.

We wanted to know if the difference in nuclear size seen in the PLB will be similar in neutrophils from A-T patients. We were able to obtain neutrophils from two healthy donors and three A-T patients at Charite University Hospital, Berlin Germany. The isolated neutrophils were stained with DAPI, a DNA-specific dye. Images were acquired and nuclear shape was analysed by confocal microscopy (performed by Christian Goosman, Max Planck Institute for Infection Biology, Berlin) (**Figure 5.6 A**). We analysed DAPI mean fluorescence intensity and volume of the nuclei to see if there was a difference in size and compaction between healthy donors and patients. We found A-T neutrophils had decreased nuclei fluorescence intensity compared to healthy donor neutrophils, while this was not significant, it could mean their nuclei are less compact since brighter nuclei staining is likely related to a higher compaction state (**Figure 5.6 B**). On the other hand, we did not see any difference in the volume of the neutrophil nuclei between healthy donors and A-T patients (**Figure 5.6 C**).

In summary, we found loss of *ATM* in PLB has an effect on nuclear compaction, as seen in the increased nuclear size of ATM$^{-/-}$ PLB at Day 6 compared to WT. However, because of time constraints, TEM was performed on a single differentiation and must be repeated. On the other hand, we could not see the same effect on the neutrophils from A-T patients compared to healthy donors, where the size was similar between conditions. Moreover, we found a decompaction trend in the nuclei of A-T neutrophils. These differences could be caused by methodological differences; while both transmission electron and confocal microscopy allow to analyse the cell slice by slice, the resolution and state of the cell is different. While cells prepared for TEM are in suspension, cells prepared for confocal microscopy are attached to a coverslip and

the shape of the nuclei can change depending on attachment efficiency and how spread out the cell is. To further understand if loss of ATM had effects on chromatin, we decided to analyse expression of different genes by qPCR at different days of PLB differentiation.

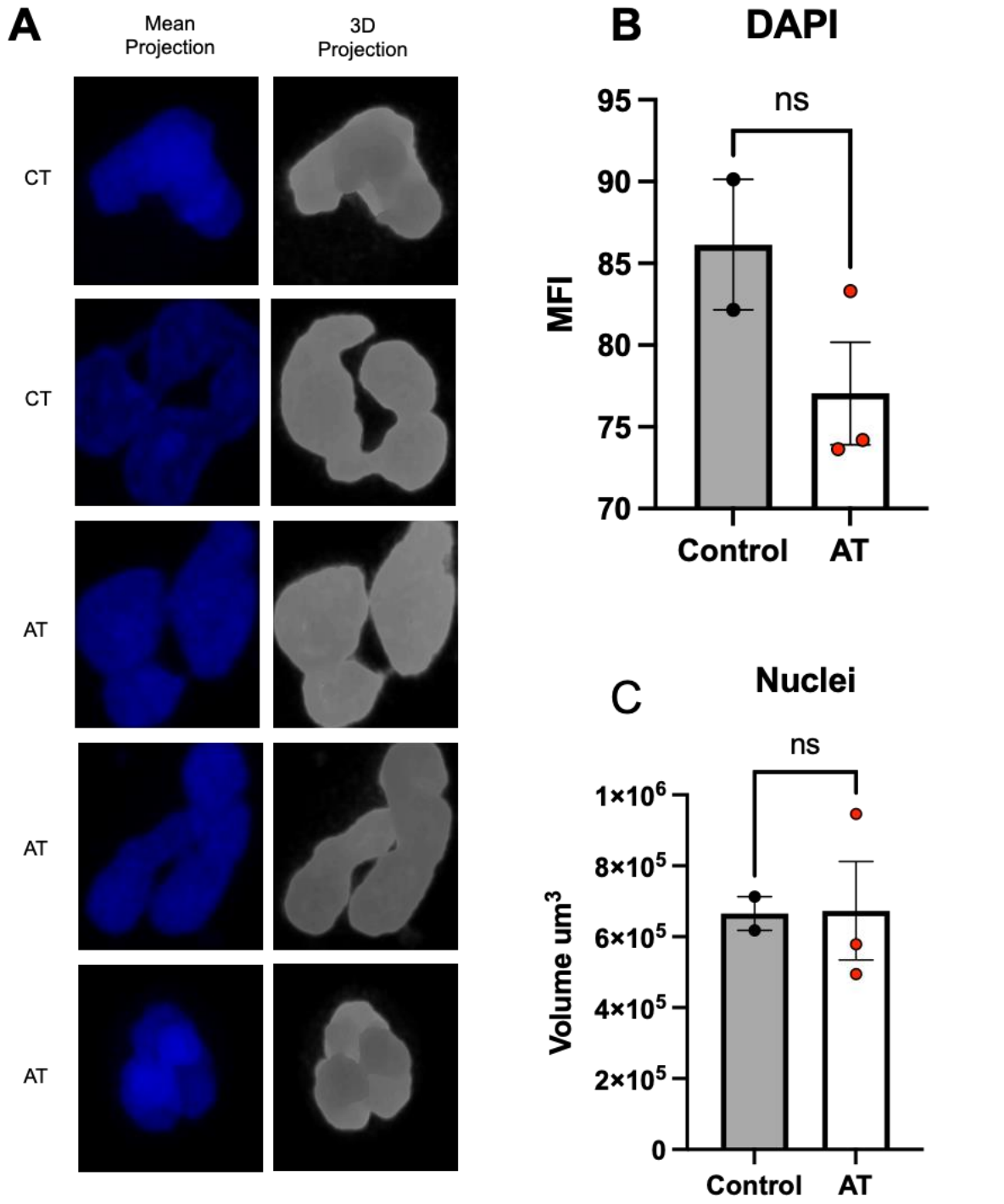

(legend on next page)

Figure 5.6: A-T patients' neutrophils potentially have less chromatin compaction. Confocal images were acquired in a SP8 confocal microscope by Christian Goosman at Max Planck, Berlin. (A) Representative images of healthy donor (n=2) and A-T (n=3) neutrophils stained with DAPI. (B) DAPI mean fluorescence intensity (MFI). Ten individual cells were analysed, and MFI values were averaged for each healthy donor n=2 and A-T patients n=3. (C) Nuclear volume (μm^3). Ten cells per individual donor and 20 stacks per cell were analysed to obtain the volume of the nuclei. Images were analysed using MIA plugin on ImageJ and workflow was made my Dr Dominic Alibhai (Wolfson imaging facility, Bristol). Unpaired student's t-test was performed, and no significant differences were found. Data is expressed as ±SEM.

5.5 ATM loss alters gene expression

ATM is known to be involved in chromatin decompaction and the rearrangement of the nuclear landscape in response to DNA damage[152] . Since neutrophils can turn off the transcription of genes no longer needed and turn on the transcription of other genes when they differentiate[38], we wondered if ATM modulates this mechanism.

We used 3 different differentiation days (0,4 and 6) in both WT and $ATM^{-/-}$ PLB (clone 1) and analysed by qPCR genes that are expressed in early, mid and late stages of neutrophil development. Firstly, we quantified the expression of myeloperoxidase (MPO) and cathepsin G (CSTG) throughout the differentiation process. We found both genes were highly expressed at Day 0 in both WT and $ATM^{-/-}$ and decreased their expression throughout the next differentiation days (**Figure 5.7 A and B**). This result agrees with the literature were genes of azurophilic granules are expressed in early stages of development (promyeloblast) and decrease their expression with advancing differentiation[7,56]. Noteworthy, we found that *MPO* had a significant increase expression in $ATM^{-/-}$ Day 0 PLB compared to WT, although this effect may be driven by outliers. A similar trend was observed with *CSTG*, however this was not significant.

Then we went on to analyse the expression of genes that are upregulated in later stages of neutrophil development such as peptidyl arginase deaminase 4 (PAD4), arginase (ARG1), leucine rich repeat kinase 2 (LRRK2) and aquaporin 9 (AQP9), *ARG1* is known to be stored in the gelatinase (tertiary) granules, which appear during the metamyelocyte stage of neutrophil development[64,66]. We found *ARG1* to be gradually upregulated from Day 0 to Day 6, having the higher expression at Day 6 of differentiation in both WT and $ATM^{-/-}$. $ATM^{-/-}$ PLB at Day 6 had a significantly

increased expression of *ARG1* compared to WT (**Figure 5.7 C**). *LRRK2* is found in the cytoplasm of neutrophils and is involved in vesicular trafficking[153]. *LRRK2* expression increased from Day 0 to Day 6 in WT PLB, on the contrary, ATM$^{-/-}$ PLB did not increased the expression of *LRRK2* during differentiation and showed a significantly decreased expression at Day 6 compared to WT (**Figure 5.7 D**).

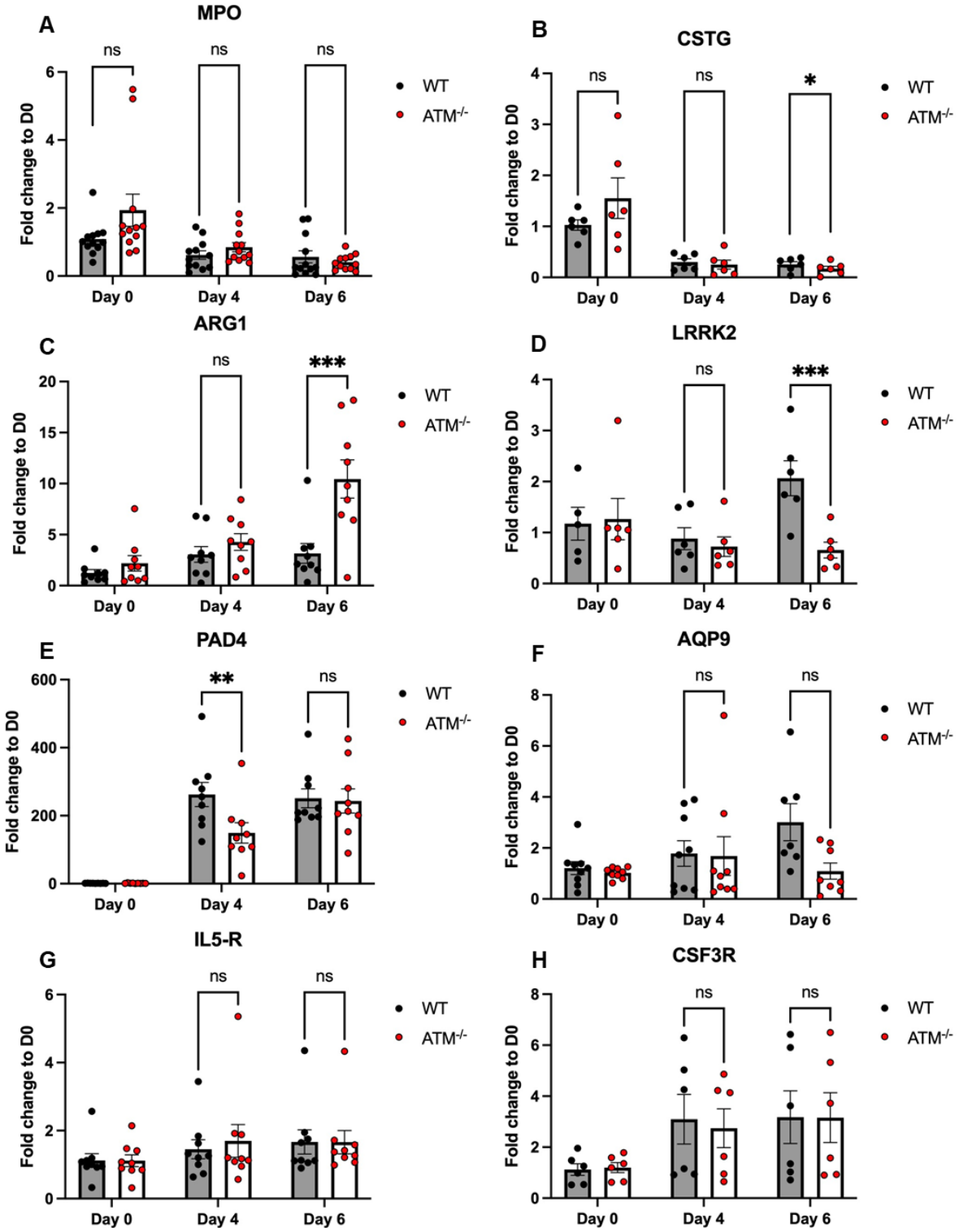

(legend on next page)

Figure 5.7: Loss of ATM alters gene expression. Quantitative Real-time PCR (qRT-PCR) analysis of gene expression in PLB cells. Transcript abundance of genes expressed in early stages of differentiation; MPO and CSTG are proteins of azurophilic granules transcribed during the promyelocyte stage (A and B), genes expressed in late stages of development; PAD4, ARG1, LRRK2 and AQP9 increase transcription during metamyelocyte stage (C-F), and lineage defining genes: IL5-R is expressed in eosinophils while CSF3R is predominantly expressed in neutrophils (H and I). Data is expressed as fold change compared to Day 0 ± SEM. Two-way ANOVA with multiple comparison was used to analyse significant differences after Log2 transformation of the data. **p<0.003, ***p<0.0003 (n=6-12)

AQP9 is found on the plasma membrane of neutrophils[154]. We found *AQP9* increased its expression in WT PLB from Day 0 to Day 6, while ATM$^{-/-}$ cells did not change their expression levels during differentiation; at Day 6 we can see a trend for decreased expression in ATM$^{-/-}$ PLB compared to WT (**Figure 5.7 D**); however this was not significant.

PAD4 is expressed after the myelocyte stage and is found in the cytoplasm of neutrophils[7]. *PAD4* expression increases from Day 0 to Day 4 and remains similar at Day 6 in WT PLB, this pattern was similar in ATM$^{-/-}$ PLB, however ATM$^{-/-}$ had a significant decrease expression at Day 4 (**Figure 5.7 E**), compared to WT and by day 6 they showed a similar level of expression compared to WT PLB. We also used granulocyte colony stimulating factor receptor (CSF3R) to corroborate our PLB were differentiating into a neutrophil-like cell. We could see an increase in *CSF3R* expression from Day 0 to Day 6 in both WT and ATM$^{-/-}$ PLB, there was no difference in gene expression between WT and ATM$^{-/-}$ throughout the three different differentiation days.

Finally, we decided to analyse if loss of *ATM* could affect lineage commitment. We decided to test for a gene marking eosinophil fate, we used interleukin 5 receptor (IL5-R) as a marker of eosinophil differentiation. Which has been previously shown to be increased in PLB defective in histone 1 variants[45]. *IL5-R* expression was not affected during differentiation in either WT and ATM$^{-/-}$ PLB.

In summary, we found loss of *ATM* dysregulates gene expression during PLB differentiation, with gene-specific transcriptional changes, with upregulation of some genes and downregulation of others. We wanted to assay expression changes in a

more unbiased manner. Therefore, we decided to analyse protein abundance in differentiated PLBs by using mass spectrometry to see if we could find similar results.

5.6 ATM loss decreases expression of C-type lectin receptors

In a preliminary experiment, we analysed by tandem mass spectrometry (TMT) day 6 differentiated cells from two independent differentiations. A third differentiation was excluded because of failure to detect upregulation of differentiation markers and failure to cluster with their counterparts during principal component analysis (PCA). We detected a total of 3180 proteins (**Figure 5.8**), using a cut off of ($p<0.05$) we found 120 proteins with significantly altered expression, furthermore, we only found 1 protein that passed a 1 Log two-fold change difference threshold. We were unable to replicate findings of increased expression of CD11b previously found by flow cytometry, indicating our mass spectrometry experiment was not sensitive enough, likely due to small sample size. Furthermore, this experiment lacked analysis of undifferentiated cells. Since some controls were missing, and we were only able to analyse two independent differentiations, we decided to use this data as preliminary data. Due to the sub optimally low number of replicates, we failed to detect differentially expressed proteins, with the exception of a single one. Interestingly the membrane receptor CLEC5A (**Figure 5.8**) demonstrated a significant decrease in $ATM^{-/-}$ dPLB compared to WT. CLEC5A is a C-type lectin important in pathogen recognition, including detection of *S. aureus*, potentially explaining deficient killing of this microbe (**Figure 4.1 A**).

To confirm reduced expression of *CLEC5A* we analysed transcript abundance in $ATM^{-/-}$ dPLB compared to WT. We analysed by qPCR between six and twelve independent differentiations at Day 0, 4 and 6. We found the expression of CLEC5A increased from day 0 to day 6 in both $ATM^{-/-}$ and WT PLBs and no difference was seen between conditions at day 0 and 4. However, by day 6 we could see a significant decrease in the expression of CLEC5A in $ATM^{-/-}$ cells compared to WT (**Figure 5.9 A**), confirming our proteomic result. We then went on to analyse other C-type lectin receptors known to be expressed in neutrophils and PLBs to see if their expression was also altered by loss of *ATM.*

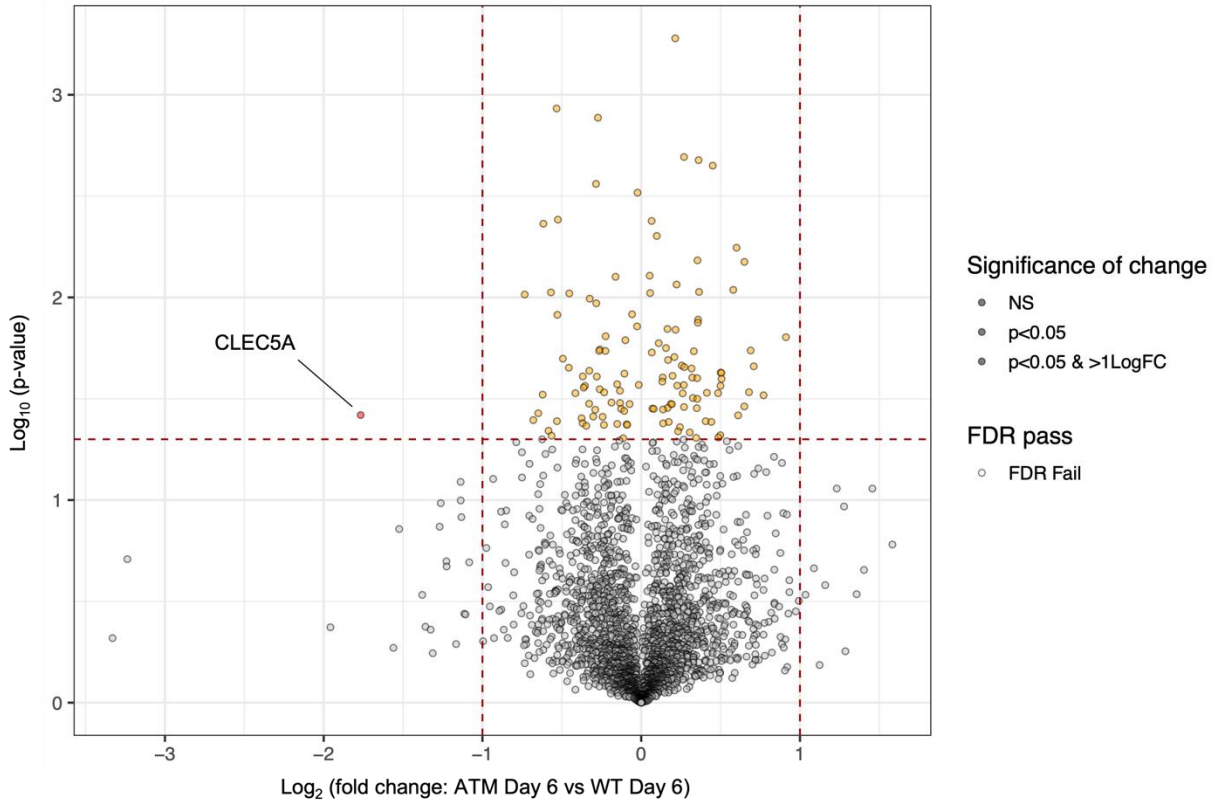

Figure 5.8: Loss of ATM affects CLEC5A expression in neutrophil-like cells. Tandem mass spectrometry analysis of ATM$^{-/-}$ and WT dPLB. Volcano plot showing protein abundance between ATM$^{-/-}$ and WT dPLB, displayed as log_{10} p-value and log_2 fold change p<0.05 (n=2).

We found that CLEC4E (Mincle), CLEC6A (Dectin-2) and CLEC7A (Dectin-1) follow a trend of increasing expression from day 0 to day 6 with no significant difference at day 0 or 4 between conditions, except from Clec6A where we can see a significant decrease in ATM$^{-/-}$ cells compared to WT at day 4. Moreover, at day 6 we could see a significant decrease in gene expression for the three CLECs in ATM$^{-/-}$ compared to WT (**Figure 5.9 B-D**). On the other hand, we saw CLEC12A (inhibitory receptor) showed a trend to decrease its expression from day 0 to 6; we found a significant decrease in ATM$^{-/-}$ cells compared to WT at day 4 and 6 of differentiation. These results confirm that expression of C-type lectin receptors is impaired in ATM$^{-/-}$ cells, as seen before in the relative expression of CLEC5A protein by mass spectrometry.

Finally, we analysed by flow cytometry the expression of CLEC5A in undifferentiated PLB and dPLB. We found expression of CLEC5A increased after differentiation in both

ATM$^{-/-}$ and WT as seen in the histogram (**Figure 5.10 A**). As seen before in our mass spectrometry data and gene expression, we could see a decreased expression of CLEC5A receptor in the ATM$^{-/-}$ dPLB clone 1 compared to WT (**Figure 5.10 B**). However, this was not the case in ATM$^{-/-}$ dPLB clone 2 (**Figure 5.10 C)**.

In summary, we found that CLEC5A receptor was decreased in one clone of ATM$^{-/-}$ dPLB by three different methods, although this was not confirmed in a second clone. Regulation of CLEC proteins by ATM thus needs further investigation and is ongoing. Nevertheless, there is evidence to indicate that ATM regulates gene expression in neutrophils and so we decided to see if these alterations were caused by defects in the chromatin landscape or nuclear structure.

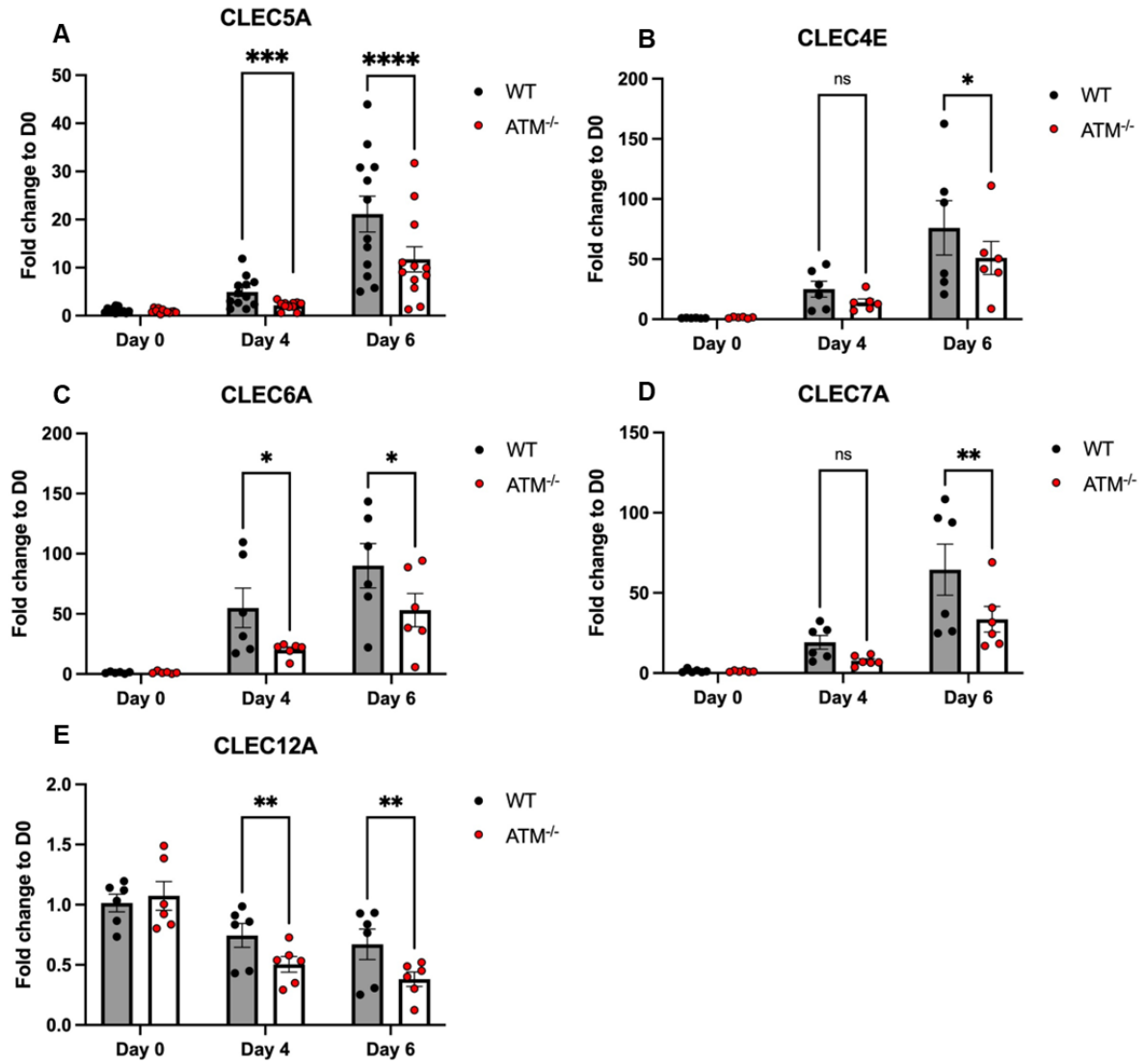

(legend on next page)

Figure 5.9: Loss of ATM decreases the expression of C-type lectin receptors. (A-E) Relative gene expression of indicated genes in ATM$^{-/-}$ and WT PLB at Day 0, 4 and 6 post start of differentiation (n=6-12). Statistical analysis was performed by two-way ANOVA with multiple comparison test after Log2 transformation of the data. *p<0.05, **p<0.003, ****p<0.0001. Data is expressed as ± SEM.

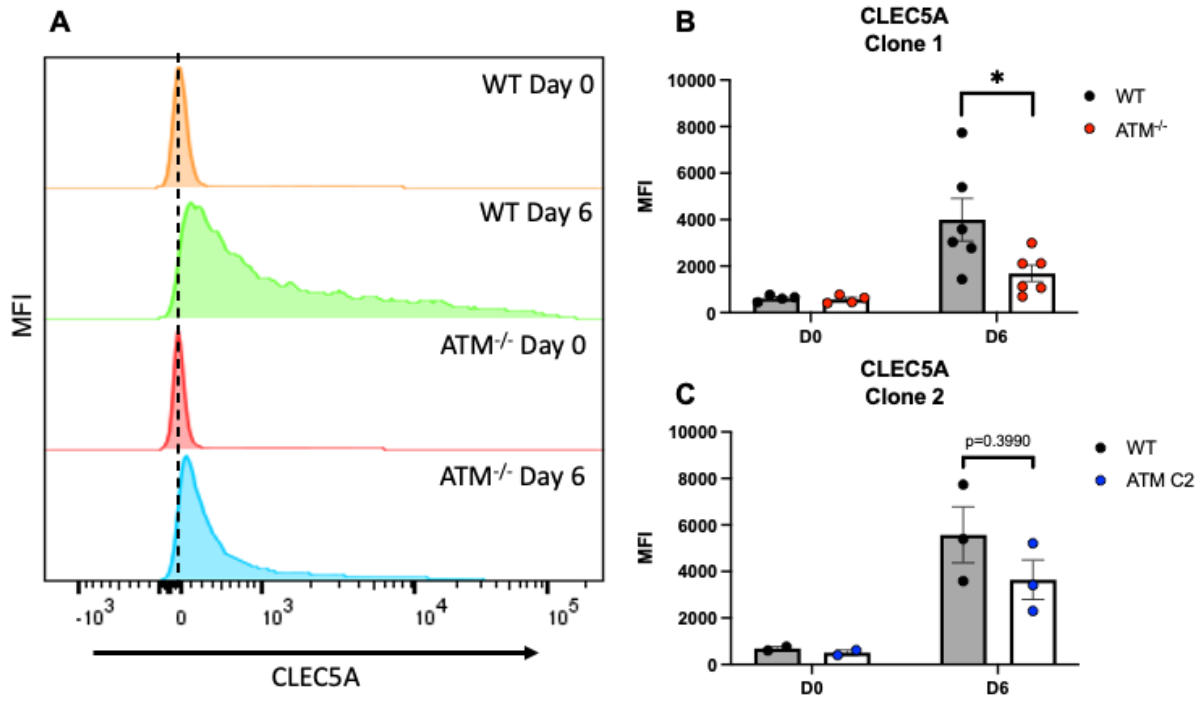

Figure 5.10: Loss of ATM decreases the expression of CLEC5A in dPLB. (A) Representative histograms of CLEC5A expression at Day 0 and 6 of differentiation. (B) Quantification of A in all pooled experiments from clone 1 (n=6) and (C) clone 2 (n=3): ATM$^{-/-}$ neutrophil-like cells show a decrease expression of the C-type lectin receptor CLEC5A Day 6 of differentiation compared to WT, Paired two-tailed t-test analysis, *p<0.05. Data is expressed as ± SEM.

5.7 ATM loss affects heterochromatin marks but not nuclear lamina composition

It has been shown ATM can regulate heterochromatin and euchromatin transitions during DDR[155]. For instance, it regulates chromatin compaction states at the ends of DNA breaks by phosphorylating KRAB-associated protein 1 (KAP-1)[112]. For instance it has been shown in lymphoblasts lacking ATM an aberrant distribution of highly condensed chromatin areas throughout the nucleus in comparison to WT lymphoblast where they are found in the periphery of the nuclei[152]. Therefore, we decided to analyse the expression of two different epigenetic marks related to constitutive (H3K9me3) and facultative (H3K27me3) heterochromatin[156]. Constitutive chromatin

has been shown to be enriched with H3K9me3 and present with hypoacetylation and can be found in satellite regions and repeated sequences[156]. While facultative heterochromatin has been shown to be enriched with H3K27me3 and contrary to constitutive heterochromatin, it is found in areas of active genes[156]; therefore, it can be reverted to an open conformation when genes need expressing and can be repressed when the gene is no longer needed. We also looked at nuclear lamina components, as it has been shown that the nuclear lamina composition changes over neutrophil differentiation[157] . We could not detect a difference in the expression of Lamin A/C and B1 between WT and $ATM^{-/-}$ dPLB clone 1, however we could see a trend for increased expression in Lamin A/C from day 0 to day 6 in both conditions (**Figure 5.11 A-C**). We then analysed the expression of the two different heterochromatin marks. We could not see a difference in the constitutive mark (H3K9me3) between conditions and over the course of differentiation. On the other hand, we found a significant decreased expression of the facultative mark (H3K27me3) in $ATM^{-/-}$ PLB clone 1 compared to WT on the three different days of differentiation (**Figure 5.11 A and D-E**). This result could potentially explain the alteration in gene expression, as this repressive mark is known to appear in genes that are silenced[156].

In summary, we found the facultative repressive mark was significantly decreased in $ATM^{-/-}$ cells, while the constitutive repressive mark and the nuclear lamina variants had no significant difference compared to WT cells. However, it remains unclear if this is a clonal effect and this result needs to be validated with additional ATM knockout clones.

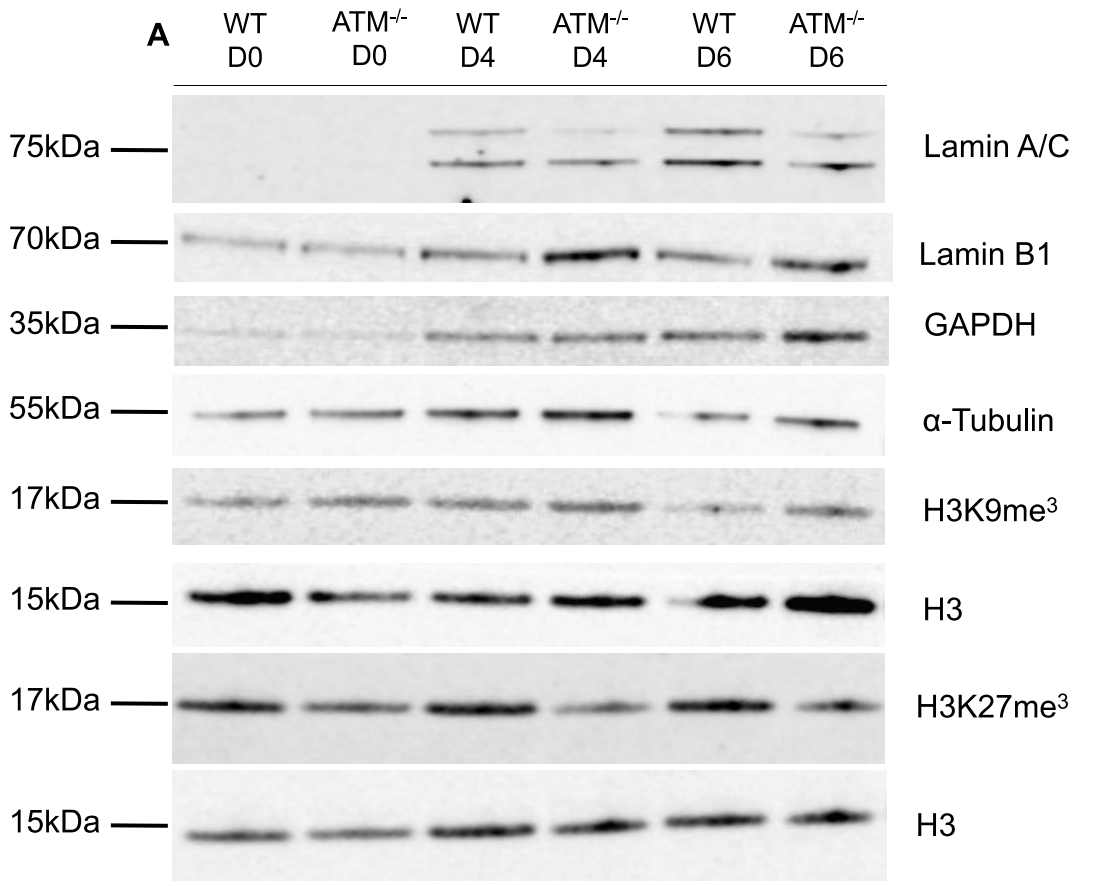

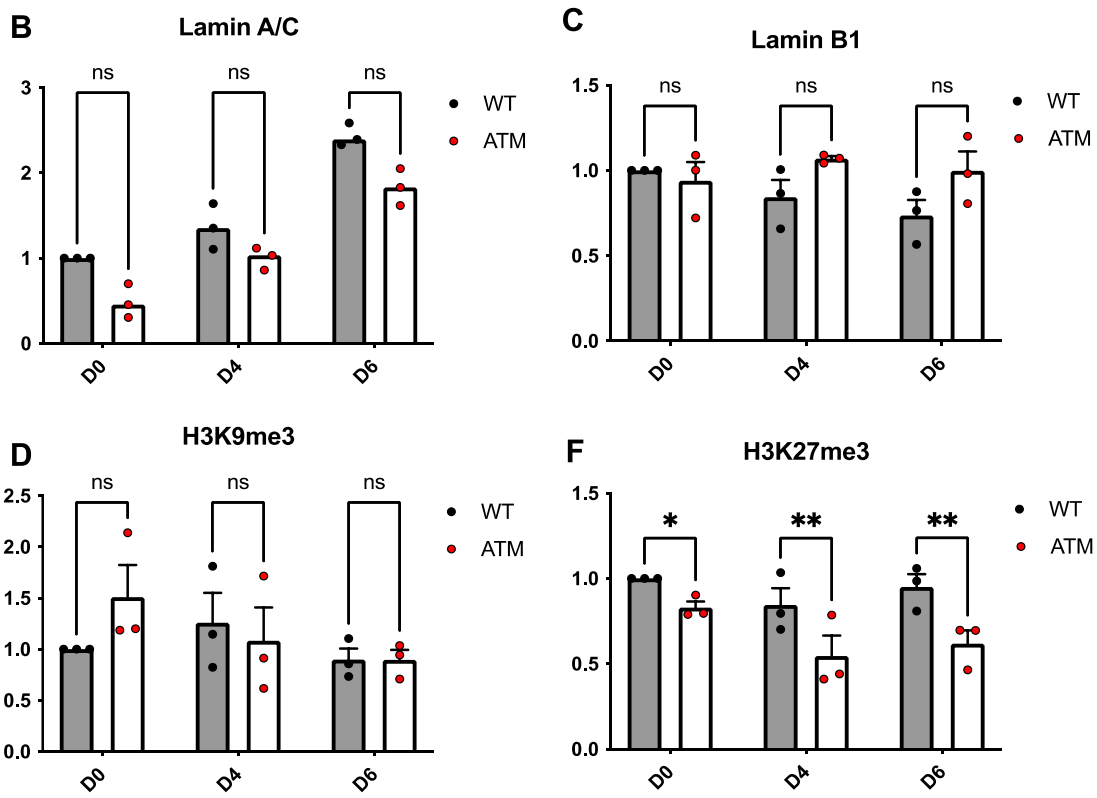

(legend on next page)

Figure 5.11: Loss of ATM does not significantly affect nuclear lamina expression and constitutive heterochromatin but does decrease facultative heterochromatin. (A) Representative western blots for indicated protein, samples were normalised to loading control α-Tubulin or Histone H3. (B-E) Quantification of western blots during $ATM^{-/-}$ and WT PLB differentiation (n=3). Data is expressed as mean ± SEM, paired t-test was performed in samples from each day of differentiation *p<0.05, **p<0.003.

In conclusion, we found in this chapter loss of *ATM* dysregulates neutrophil development. Firstly, we found both $ATM^{-/-}$ dPLB and A-T neutrophils have an increased expression of the maturity marker CD11b compared to WT dPLB and healthy donors respectively. In addition, glycolytic capacity was increased in $ATM^{-/-}$ dPLB compared to WT dPLB; altogether, this could demonstrate a hyper mature neutrophil phenotype. Moreover, dysregulation in gene expression showed there was an increase in granule gene expression (eg MPO, CSTG and ARG1), while genes involved in maturation such as (PAD4, LRRK2 and AQP9) had a downregulated expression pattern compared to WT PLB.

The expression of C-type lectin receptors genes was also downregulated in $ATM^{-/-}$ PLB compared to WT, while expression of CLEC5A in dPLB membrane was also decreased compared to WT dPLB, although this awaits confirmation in additional clones. These changes in expression of genes and membrane receptors can potentially be explained by the changes in nuclear shape and chromatin compaction seen in both $ATM^{-/-}$ dPLB and neutrophils from A-T patients. Our preliminary Western blot data indicates that H3K27me3 repressive chromatin mark is downregulated. It is possible that there are few changes in the amount of repressive marks, however their particular distribution could be affecting the expression of the previously mentioned genes. Further experiments are needed to understand which pathways are enhanced and which ones are downregulated. RNAseq analysis of healthy donors and A-T patients will be the ideal experiment to follow up and identify in a non-biased way the pathways that are dysregulated. To directly probe chromatin compaction level in A-T neutrophils, ChIP-seq or ATAC-seq can be taken to understand which chromatin marks are increased or decreased.

5.8 Chapter Overview

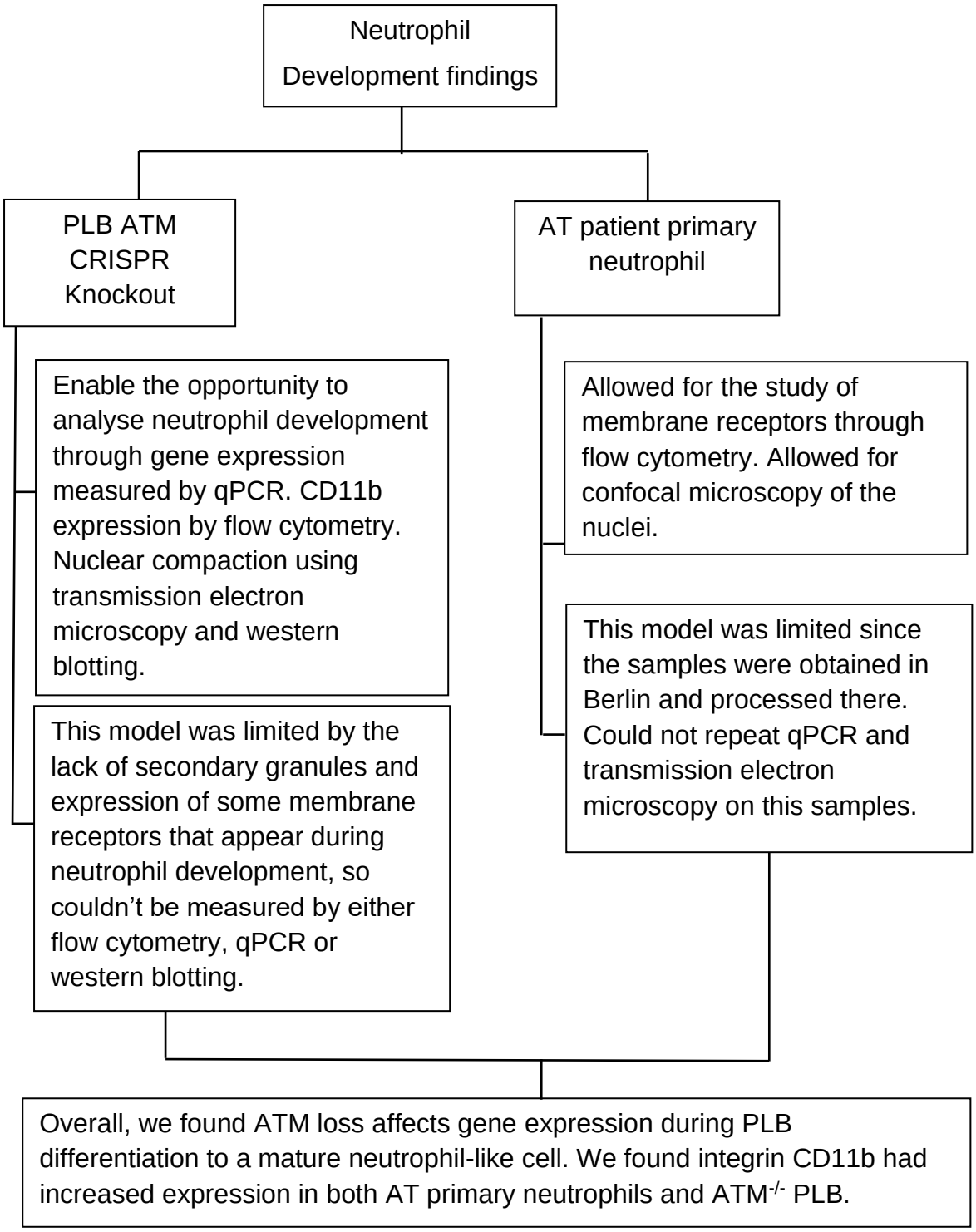

CHAPTER 6: Discussion

This work aimed to understand the role of *ATM* in the activity and development of neutrophils. Immunodeficiencies in A-T patients had been focused on immunoglobulins deficiencies and adaptive immunity[98,151,158]. Previous studies in B and T-cells from A-T models have shown defects in class switch recombination (CSR)[151,158] and variable diversity joining (V(D)J)[159,160], affecting the development, variety of receptors and immunoglobulins[102]. However, neutrophil activity and development in A-T have not been fully described. It has been shown that neutrophils in A-T disease have a longer lifespan and increased pro-inflammatory phenotype, characterised by increased IL-8 secretion[82]. Another study in a mouse model in the context of lung injury and sepsis-induced by bleomycin, showed loss of *ATM* caused increased myeloperoxidase and higher neutrophil counts in bronchoalveolar lavage samples[161]. Additionally, it has been shown that A-T neutrophils are more susceptible to undergo spontaneous Netosis in comparison to healthy donors[162]. This project aimed to address some of these questions using as an experimental model the promyelocytic leukaemia cell line PLB-985, where we were able to knockout *ATM*.

6.1 Loss of *ATM* does not affect cell lineage commitment to neutrophil-like cell but affects phenotype

Firstly, we demonstrated PLB differentiation into a neutrophil-like cell was not affected by the loss of *ATM.* A study made by Sollberger and colleagues shows deficiency of histone 1 variants (H1.2 and H1.4) drives PLB differentiation into an eosinophil-like cell, as seen by the increased expression of *IL5R* and *GATA-1*[45]. We found loss of *ATM* did not affect eosinophil lineage commitment as expression of IL5R measured by qPCR was not increased and had a similar expression to wildtype PLB before, during and after differentiation. Additionally, we showed similar expression of *G-CSF Receptor* (CSF3R) compared to wild type and saw an increased expression in both WT and ATM$^{-/-}$ dPLB compared to undifferentiated cells.

ATM$^{-/-}$ dPLB had increased expression of the maturity marker CD11b after differentiation with DMF, compared to undifferentiated ATM$^{-/-}$ cells. Different groups[145,147,148,163] differentiate WT PLB with all-trans retinoic acid, DMSO or DMF,

and showed by flow cytometry analysis increased CD11b expression in WT dPLB after differentiation. We further showed ATM$^{-/-}$ dPLB have significantly higher levels of CD11b surface expression compared to WT. Similarly, we found neutrophils from A-T patients had increased CD11b expression compared to healthy donor neutrophils. This can be related with a hyper-mature neutrophil phenotype, however we do not see hyper-lobulation in either ATM$^{-/-}$ dPLB or A-T neutrophils.

A study done by Pivot-Pajot and colleagues[147] showed WT dPLB phagocytic capacity by confocal microscopy and flow cytometry using fluorescently labelled zymosan particles. In this project we showed ATM$^{-/-}$ dPLB had the ability to phagocytose S. aureus. Moreover, S. aureus killing was decreased in ATM$^{-/-}$ compared to WT dPLB, this will be further discussed in **section 6.3**. WT dPLB have been shown to have a respiratory burst against TNF-α, fMLP and PMA[148,163], as well as being able to release NET-like structures[164,165]. Similarly, ATM$^{-/-}$ dPLB were able to produce ROS and NET-like structures against the soluble PKC agonist PMA but failed to do so in response to the lectin ConA.

In this section, we have shown loss of ATM does not affect neutrophil lineage fate in PLB differentiation, however, there are differences in the phenotype compared to WT. For instance, increased expression in the membrane receptor CD11b and defects in antimicrobial capacity and respiratory burst that will be covered in the next sections.

6.2 Inhibition or loss of ATM impairs oxidative burst in response to ConA but not PMA

Neutrophils are known to carry out different activities to fight pathogens; they can phagocytose, undergo a respiratory burst, release NETs, degranulate their antimicrobial peptides and migrate towards a chemotactic gradient[7,8,68]. Previous studies have shown that both neutrophils and dPLB are able to mount a respiratory burst against the soluble stimuli PMA[46,163,166], as well as release NETs[87,164]. In this study, we found respiratory burst against PMA was not affected by pharmacological inhibition, CRISPR knockout, or shRNA knockdown of *ATM*. Similarly, NET production in response to PMA was similar to vehicle in ATM-inhibitor treated neutrophils and in ATM$^{-/-}$ and wild type dPLB. PMA is known to activate PKC directly and, in turn, induce the respiratory burst by NADPH oxidase complex activation[82]. In order to analyse

membrane signalling, we decided to use the lectin ConA as stimulus since it requires binding to membrane receptors and signaling via spleen tyrosine kinase (SYK) to induce ROS production[167]. We found that both pharmacological inhibition and loss of *ATM* abolish the respiratory burst in primary neutrophils and dPLB compared to the vehicle and wildtype controls. ConA-induced NET formation in primary neutrophils treated with ATM inhibitor and in $ATM^{-/-}$ dPLB was also blocked, which is to be expected, since the respiratory burst is required for ConA NETs, as seen in a previous study where CGD neutrophils failed to release NETs against ConA[88]. There is the possibility that PMA bypasses any need for ATM to be involved in transducing downstream signalling. It has been shown ATM is required for TLR3 downstream signalling activation of NF-κB in HEK293T cells[168]; however, in neutrophils from A-T patients, NF-κB activity is enhanced[82].

We observed differences between the chemical inhibition of ATM and the genetic loss of ATM in PLB compared to neutrophils from A-T patients in ROS production. We showed PMA respiratory burst was not affected between the three conditions, however, ConA respiratory burst as mentioned before was blocked in $ATM^{-/-}$ dPLB and chemically inhibited primary neutrophils, while A-T primary neutrophils had a similar ConA respiratory burst compared to healthy controls. These differences could be off-target effects of the inhibitor blocking different signalling pathways. PLBs do not express as many receptors as a mature neutrophil, and it is possible other receptors are involved in primary neutrophils in transducing downstream signalling without the need for ATM. It will be interesting to also test A-T neutrophils NET production against ConA since we could not do this experiment during this project.

While we don't see the same phenotype in A-T patients compared to our CRISPR knockout PLB, it could be possible that our findings in PLBs is caused by a clone specific defect, therefore a good way to elucidate this will be testing multiple clones with the same stimuli. Another possibility is that A-T neutrophils are compensating for the loss of *ATM* through different receptors that don't require ATM downstream signalling. On the other hand, $ATM^{-/-}$ PLB might also be compensating for the loss of *ATM* (eg. with *S. aureus*) but fail to do so in response to ConA as they do not express as many membrane receptors and granules compared to a primary neutrophils[147,169]. It will be interesting to test this in neutrophils from $ATM^{-/-}$ mice and see if they show a

similar response to A-T neutrophils, since they will express more membrane receptors and granular proteins that might be important for the compensation mechanism.

The difference seen with the inhibitor could be caused by off-target effects involving other signalling pathways that are necessary for transducing the signal. KU55933 inhibitor is known to inhibit with less efficiency DNA-PK, ATR which are known to have similar targets to ATM as both of them are part of the DDR signalling[107,110]. It will be worth trying to block other receptors that are involved in the recognition of ConA and using inhibitors of other kinases involved in the signal transduction leading to ROS production to see if we can recapitulate the phenotype. Similarly, we could try a double knockout PLB cell line targeting ATM and ATR or DNA-PK. This could help us elucidate if our inhibitor is also affecting their function. Another cause for this phenotype could be a lack of compensation upon pharmacological inhibition, since it is an acute treatment, it does not give the cell enough time to compensate for the inhibition of ATM. Future research could explore if an ATM kinase dead PLB would also show a similar phenotype since it has been shown to be a more lethal phenotype in mice[100].

6.3 Pharmacological Inhibition and loss of ATM impairs neutrophil antimicrobial activity

Neutrophil antimicrobial capacity has been poorly studied in A-T patients; a study made by Datta and colleagues showed neutrophil antimicrobial capacity against *C. albicans* was not affected in A-T patients[170]. In contrast, we show inhibition of ATM in primary neutrophils impaired their ability to kill *S. aureus* compared to vehicle control. This was not related to their phagocytic capacity since phagosome formation was not affected in ATM inhibited neutrophils. We then tested respiratory burst, degranulation, and pathogen engagement. The former has been shown to be required for the killing of gram positive bacteria by neutrophils [23], while degranulation and pathogen engagement can tell us the degree of activation of the neutrophil.

We showed a significant decrease in respiratory burst against *S. aureus* as well as for *C. albicans* and the mincle agonist TDB in primary neutrophils treated with ATM inhibitor. Cytoplasmic ATM has been shown to promote the pentose phosphate pathway after being activated by ROS[128,171]. The pentose phosphate pathway (PPP)

is involved in the production of NADPH that is required to prevent oxidative damage[128], however in neutrophils NADPH production is required for a proper NOX2 activity[35,81]. It was recently shown by Britt and colleagues[172] that NADPH production by PPP is necessary for the production of superoxide by NOX2, and neutrophil respiratory burst was blocked by using an inhibitor of PPP. Inhibition of ATM could be affecting this pathway and, in turn, decreasing the amount of ROS released, impairing the antimicrobial capacity against *S. aureus*. Previous studies using metabolomics[172] have shown a shift from glucose metabolism to PPP after PMA activation, it will be interesting to see if this is also happening in neutrophils against *S. aureus* and see if this is decreased when treated with an ATM inhibitor. Similarly, we could use an inhibitor of PPP and see if this defect in antimicrobial activity against *S. aureus* can be recapitulated. This will help us explain the mechanism by which ATM is affecting the antimicrobial capacity of neutrophils.

The defect in bacterial killing was recapitulated in PLBs where *ATM* was knocked out using CRIPS/CAS9 technology. We find WT dPLB are not as effective as primary neutrophils in killing bacteria, as shown in previous studies[75,173].

Moreover, $ATM^{-/-}$ dPLB had less killing ability compared to wildtype dPLB, recapitulating the results shown with the inhibitor-treated primary neutrophils. Similarly, pathogen engagement was not affected in $ATM^{-/-}$ dPLB compared to wildtype. It will be important to repeat this experiment with a second clone or with our shRNA PLB model to exclude any effect of cell cloning. On the other hand, the respiratory burst was not affected in $ATM^{-/-}$ dPLB compared to wildtype when stimulated with *S. aureus*, *C. albicans* and TDB. This result could argue that small molecule KU55933 has off-target effects that could impair the production of ROS. To address this, we generated an inducible *ATM* knockdown PLB cell line where we show respiratory burst against *S. aureus* was decreased compared to luciferase control, similar to what we show with the inhibitor in primary neutrophils. This raised the question of whether an acute inhibition or downregulation of *ATM* does not allow the cell to compensate with other pathways, while a stable knockdown might allow genetic compensation from the cell. This could be explained by the lethal phenotype shown in mice embryos where loss of ATM kinase activity through targeted deletion of the active site is not viable, while a full knockdown of ATM allows embryos to develop properly[174].

This could show how having residual expression of ATM without kinase activity does not allow for a genetic compensation as seen in a full knockdown[174]. Moreover, it will be interesting to test the antimicrobial activity in neutrophils from atypical A-T patients, which have residual ATM activity compared to the classical A-T patients that in most cases do not express ATM. Even though atypical patients present symptoms at later age, the antimicrobial capacity of their immune cells has not been tested. Further experiments with our shRNA cell line would allow us to determine if residual expression of active ATM prevents the antimicrobial deficiency that we see in neutrophils treated with inhibitor or in our PLB knockout model. Similarly, a kinase dead ATM PLB cell line will allow to test the question whether the presence of the protein without kinase activity prevents compensation by other pathways, or potentially has a dominant negative effect.

The functional perturbations we see in our ATM$^{-/-}$ dPLB could be explained by the decrease in *LRRK2* and *CLEC5A* expression. The proteins encoded by these two genes have been implicated in various immune responses. Firstly, LRRK2 has been shown to be required to mount an immune response against *Salmonella* and *Listeria*[175,176]. siRNA knockdown of LRRK2 in mouse macrophages decreased their antimicrobial activity against *Salmonella typhimurium* [175]. Similarly, an *LRRK2* knockout mouse model showed decreased antimicrobial activity against the pathogen *Listeria monocytogenes,* as shown by the higher CFU counts in the liver and faecal samples of infected mice compared to wildtype controls[176]. On the other hand, LRRK2 knockout has been shown to be beneficial against *Mycobacterium tuberculosis* infection, as one study shows LRRK2 inhibits phagosome maturation and loss of it improves antimicrobial capacity, demonstrated by lower CFU counts in LRRK2 KO bone marrow-derived macrophages and human-induced pluripotent stem cell-derived macrophages challenged with *M. tuberculosis*[177].

Similarly, CLEC5A has been shown to be either protective against bacterial infections or detrimental in viral infections[22–24]. CLEC5A was shown to be involved in severe dengue disease by increasing the release of pro-inflammatory cytokines (e.g. TNF-α, IL-1β and IL-18) by monocytes and macrophages[24,178]. On the other hand, CLEC5A knockout in mice impaired their antimicrobial capacity against *L. monocytogenes* infection[23]. This study showed a decrease in killing ability from CLEC5A$^{-/-}$ mice

neutrophils, with no difference in phagocytosis against *L. monocytogenes* and *S. aureus*. However, they find a reduction in ROS production against *L. monocytogenes* and *S. aureus* but not to LPS[23]. This was similar to our results in ATM$^{-/-}$ dPLB and ATM inhibited primary neutrophils, where we found a defect in killing ability and no difference in phagocytosis; however, ROS production was only affected in the primary neutrophils treated with inhibitor but not in the ATM$^{-/-}$ dPLB. It is possible that the downregulation of LRRK2 and CLEC5A in ATM$^{-/-}$ dPLB is causing a decrease in killing ability. It will be necessary to repeat these findings in a second knockout clone to make sure it is not a clone effect and is truly due to loss of ATM phenotype. On the other hand, the result obtained with chemical inhibition of ATM argues the need for this kinase for downstream signalling after binding of the pathogen to CLEC5A receptor; further studies with a kinase-dead ATM PLB could be useful to address this question.

Furthermore, ATM has been shown to be necessary for proper inflammasome activity shown previously by Erttmann and colleagues[133]. They found loss of ATM increases ROS which further inhibit inflammasome activity and reduce production of the pro-inflammatory cytokine IL-1β. This will need to be further investigated in our ATM inhibited primary neutrophils and ATM$^{-/-}$ dPLB since we don't see decrease ROS production against PMA, but we see differences in ROS production against *S. aureus* between our models that could be affecting inflammasome activity.

In summary, our data suggests that ATM may be required for a proper antimicrobial activity against *S. aureus*. More work is needed to fully understand the role of ATM in the antimicrobial activity of neutrophils.

6.4 Systemic immune defects in AT

Previous studies have shown differences in immunoglobulin levels in A-T patients and defects in B and T-cell maturation could also be implied in the defect in antimicrobial capacity [97,101,106], It could be possible that low titre of antibodies affects opsonization ability in A-T patients. All the experiments in this project, were done by opsonising *S. aureus* and *C. albicans* with pooled serum from healthy donors; therefore, it will be interesting to know if the antimicrobial defect we see will replicate with nonopsonised pathogens. In addition, it will require further experiments to analyse antimicrobial ability in A-T neutrophils compared to healthy donors with opsonised and non-

opsonised pathogens and see if we can recapitulate the antimicrobial defect we have shown in this study. Similarly, opsonisation of the pathogen with homologous serum from A-T patients will be interesting for comparing the effectiveness of opsonisation compared to healthy serum.

In addition, we found CD11b; a receptor able to recognize opsonized pathogens[31] was increased in our ATM$^{-/-}$ dPLB and A-T neutrophils. Since we had opsonised *S. aureus* and *C. albicans* with pooled serum from healthy donors, it could explain why we cannot see a significant difference in the respiratory burst of our dPLB and A-T primary neutrophils compared to ATM inhibited neutrophils. It will be worth trying to opsonise this pathogens with pooled serum from A-T patients and see if we see the same results we have shown or since A-T patients have immunoglobulins deficiencies[101,106,139], this might affect the opsonisation process and we might have deficiencies in the respiratory burst from ATM$^{-/-}$ dPLB and A-T neutrophils.

The role of ATM in regulating CLR expression must be validated with another knockout clone, but if it holds true after testing with other clones, non-opsonised pathogens might be interesting to test in both dPLB and A-T neutrophil ROS assays.

It will be necessary to repeat some of these experiments with neutrophils from A-T patients as well as with a second ATM$^{-/-}$ clone of PLB to address any clone specific defect that could have happened in our first ATM$^{-/-}$ clone as well as to test ROS production when using A-T pooled serum to opsonise the pathogen and non-opsonised pathogens.

6.5 Nuclear compaction and gene expression is altered in ATM$^{-/-}$ PLB

Nuclear compaction has been shown in PLB differentiation[146,147] but is reduced compared to nuclear compaction seen in neutrophil differentiation[44]. The role of ATM in either proliferation or differentiation has been previously reviewed[106,179]. For instance, it has been shown ATM is required for B and T-cell differentiation[180] and to promote stemness in HSCs[106]. In this study we showed ATM$^{-/-}$ dPLB have less compact nuclei compared to WT dPLB. Loss of LBR or over-expression of lamin A/C cause a hypo-lobulated nuclei in HL-60 cells and mice neutrophils[52] but we could not find differences in nuclear lamina composition that would allow us to explain this nuclear compaction difference. It will also be worth analysing chromatin compaction

on our ATM$^{-/-}$ dPLB compared to WT using fluorescently tagged histone H2A with both green and red fluorescent proteins (GFP) and (RFP) using fluorescence-lifetime imaging microscopy (FLIM). It has been previously shown by Sherrard and colleagues [122] that cells lacking ATM demonstrate an increase in nuclear compaction in NIH3T3 cells, using this histone tagged system.

Proper neutrophil responses are dependent on finely tuned gene expression. In this study, we show ATM$^{-/-}$ dPLB has a dysregulation in gene expression; while some genes show a significant increase, others show a significant decrease during differentiation. Moreover, ATM has been shown to be involved in epigenetic changes by modulating the activity of different enzymes from the polycomb repressive complex 1 and 2, specifically SUV39H1 and EZH2,[123,181,182] and transcription factors[179]. Here we find expression of the C-type lectin receptors CLEC4E, CLEC5A, CLEC6A and CLEC7A was downregulated in ATM$^{-/-}$ dPLB compared to WT. ATM is known to modulate expression of various transcription factors[168,179], so it could be possible loss of ATM affects the transcription factors involved in the expression of these different C-type lectin receptors. For instance, it was previously shown that CLEC5A expression is regulated by the transcription factor PU.1[183]. Further experiments will allow to know the expression level of this transcription factor in our ATM$^{-/-}$ PLB model, as well as repeat the qPCR experiments in a second clone or with the shRNA PLB. Similarly, it will be necessary to analyse the expression of CLEC4E, CLEC5A, CLEC6A and CLEC7A in primary neutrophils from A-T patients compared to healthy controls and see if our findings hold true in the patients.

In addition to gene expression differences, we saw changes in nuclear compaction by electron microscopy and a significant decrease by western blot of the facultative repressive chromatin mark H3K27me3[156]. This chromatin mark has been shown to be involved in the repression of transcription and higher chromatin compaction[184,185]. These changes in expression of the repressive chromatin mark and nuclear compaction could explain the difference we see in gene expression of PLB lacking ATM. Similarly, changes in cytokine transcription have been shown in primary neutrophils from A-T patients, where they show a higher de-novo transcription of the pro-inflammatory chemokines IL-8 and Mip1α in A-T primary neutrophils and neutrophils treated with an ATM inhibitor when challenged with LPS[82]. A role for ATM

in the levels of H3K27me3 has been previously reviewed in[102], were they described an increase in the levels of H3K27me3 and shift in their location. Similarly, a study made by Li and colleagues[182] showed increased expression of H3K27me3 in the cerebellar cortex of A-T patients and $ATM^{-/-}$ mice[182]. Even though we see a decreased pattern in the expression of H3K27me3 in our $ATM^{-/-}$ PLB, it could be possible that the location of the repressive mark has shifted on the chromatin as mentioned earlier in[102] and this is causing the differences in gene expression we see in our model. Furthermore, it will be necessary to repeat these experiments with a second clone to rule out any clone specific phenotype. To better understand which genes are being affected and where the repressive chromatin mark is being localised, it will be necessary to perform chromatin immunoprecipitation sequencing (ChIP-seq), this will allow us to pinpoint promotors being affected by the loss of ATM and the changes in chromatin organisation. Another interesting approach to determine the level of chromatin compaction can be the use of assay for transposase-accessible chromatin sequencing (ATAC-seq), which will allow us to assess the genome chromatin accessibility and levels of different active and repressive histone marks.

6.6 Future perspectives

To further address these differences seen in the PLBs we are planning to carry out RNAseq in primary neutrophils from A-T patients, compared to age-match healthy donors; simple changes in RNA transcripts can answer the question of how transcriptionally active A-T neutrophils are compared to healthy donors. Moreover, we could focus on which transcripts are enriched and this will allow us to determine if A-T neutrophils are more prone to transcribe pro-inflammatory genes or if there are deficiencies in the transcription of genes necessary for a proper immune response.

In addition, we will carry out flow cytometry analysis to analyse the expression of the C-type lectin receptors in A-T neutrophils. If the decrease expression phenotype holds true, we will be able to confirm a role of ATM in the expression of this receptors and draw a mechanism for the antimicrobial deficiency seen in our model of chemical inhibition and genetic knockout of ATM in neutrophil and neutrophil-like cells.

The data we obtained from our inhibitor experiments also opens the question for a role in ATM in transducing downstream signalling after pathogen recognition for a proper

respiratory burst. Future studies could answer the question if ATM directly or indirectly regulates the activity of the NADPH complex. Immunoprecipitation assays could help identify the proteins interacting with ATM after recognition of ligands by membrane receptors. Similarly, phospho-proteomics of neutrophils treated with ATM inhibitor or A-T patients stimulated with *S. aureus* could show signalling pathways affected by deficiency of ATM.

A previous study by Evrard and colleagues[38] showed it is possible to isolate different stages of neutrophil differentiation from mice bone marrow and analyse their phenotypic signatures, it will be interesting to see if the changes in gene expression we showed will be better explain using this approach with $ATM^{-/-}$ mice compared to WT.

6.7 Limitations of the study

PLB cell line is a good model to study the role of ATM in the development of neutrophils. However, there are some limitations while using this model; it has been reported that dPLB does not achieve a state of complete neutrophil maturation[75,146], they do not express specific granules and lack or have a lower amount of some membrane receptors found in primary neutrophils[75,147,164,169]. These differences made comparisons to primary neutrophils more complicated since we could not run a more complex flow cytometry panel as the one, we managed to do on A-T neutrophils.

Due to COVID restrictions, we were not able to get access to A-T samples as easy as we would have wanted to, since our collaboration was with Charité University Hospital, Berlin, Germany. Similarly, we could not get more samples from $ATM^{-/-}$ mice, since we got these from our collaboration with Prof. Miguel Soares, Instituto Gulbenkian de Ciência.

Finally, a single CRISPR clone may introduce artefacts and therefore the need of a second clone will allow to confirm the results we have shown to be related to the loss of *ATM* and not to a clone specific defect. Also, off target effects caused by the inhibitor blocking other kinases involved in DDR might prevent cells for any compensation and a more dramatic effect on neutrophil antimicrobial activity. Therefore, using a mice model would be a possibility to overcome these limitations, since their neutrophils have a better resemblance to a mature human neutrophil, and it avoids the off-target effects

of inhibitors, allowing for both neutrophil development and antimicrobial activity analysis. However, it will be worth knowing the mice ATM mutation, since some ATM$^{-/-}$ mice models do not resemble the A-T phenotype as it has been previously shown[186].

CHAPTER 7: Conclusion

In this thesis, we demonstrated that knockout of ATM in the myeloid cell line PLB-985 causes a dysregulation in gene expression throughout their differentiation into neutrophil-like cells. We showed increased expression of genes related to granular proteins (MPO, ARG1, CSTG) as well as decrease expression of genes involved in the maturation of neutrophils (AQP9, PAD4, LRRK2) in our $ATM^{-/-}$ cells. We demonstrated an increase in CD11b expression on the surface of A-T neutrophils, which confirmed the increased expression of the same receptor on the surface of our $ATM^{-/-}$ dPLB.

We hypothesise ATM is involved in the arrangement of chromatin marks and therefore affecting gene expression. Obtaining new samples of A-T neutrophils will allow to further investigate changes in transcription between A-T patients and healthy donors through RNAseq or CHIP-seq.

We also demonstrated a deficiency in antimicrobial capacity that was accompanied by decreased ROS production but not mediated by altered phagocytic activity. The reduced oxidative burst against the lectin ConA with the ATM inhibitor and $ATM^{-/-}$ dPLB emphasizes the importance of investigating a role for ATM in the transduction of downstream signalling of C-type lectin receptors. We could not confirm this phenotype in A-T neutrophils, which had ROS production similar to healthy controls. Further experiments will help elucidate these differences.

In conclusion, we described a novel role for ATM in the development and antimicrobial activity of neutrophils. This could lead to a potential therapeutic target in immunodeficiency or inflammatory disease.

References

1. Abbas AK, Lichtman AH, Pillai S. *Cellular and Molecular Immunology E-Book*. 9th ed. Philadelphia, United States: Elsevier; 2017.
2. Paul WE. *Fundamental Immunology*. 7th ed. Philadelphia, United States: Wolters Kluwer Health/Lippincott Williams & Wilkins; 2013.
3. Delves PJ, Martin SJ, Burton DR, Roitt IM. *Roitt's Essential Immunology*. 13th ed. Chichester, West Sussex: John Wiley & Sons, Ltd; 2017.
4. Coico R, Sunshine G. *Immunology : A Short Course*. 7th ed. Chichester, West Sussex, UK: John Wiley & Sons, Incorporated; 2015.
5. Williams A, Hussell T, Lloyd C. *Immunology: Mucosal and Body Surface Defences*. 1st ed. Chichester, West Sussex: John Wiley & Sons; 2012.
6. Male DK. *Immunology*. 8th ed. United States: Elsevier/Saunders; 2013.
7. Lawrence SM, Corriden R, Nizet V. The Ontogeny of a Neutrophil: Mechanisms of Granulopoiesis and Homeostasis. *Microbiol Mol Biol Rev*. 2018;82(1):1-22. doi:10.1128/mmbr.00057-17
8. Rosales C. Neutrophil: A cell with many roles in inflammation or several cell types? *Front Physiol*. 2018;9(FEB):1-17. doi:10.3389/fphys.2018.00113
9. Wickramasinghe SN, Erber WN. *Normal Blood Cells*. 2nd ed. Churchill Livingstone: Elsevier Ltd; 2011. doi:10.1016/B978-0-7020-3147-2.00001-8
10. Kawasaki T, Kawai T. Toll-like receptor signaling pathways. *Front Immunol*. 2014;5(SEP):1-8. doi:10.3389/fimmu.2014.00461
11. Sameer AS, Nissar S. Toll-Like Receptors (TLRs): Structure, Functions, Signaling, and Role of Their Polymorphisms in Colorectal Cancer Susceptibility. *Biomed Res Int*. 2021;2021. doi:10.1155/2021/1157023
12. Deguine J, Barton GM. MyD88: A central player in innate immune signaling. *F1000Prime Rep*. 2014;6(November):1-7. doi:10.12703/P6-97
13. Tone K, Stappers MHT, Willment JA, Brown GD. C-type lectin receptors of the Dectin-1 cluster: Physiological roles and involvement in disease. *Eur J Immunol*. 2019;49(12):2127-2133. doi:10.1002/eji.201847536
14. Brown GD, Willment JA, Whitehead L. C-type lectins in immunity and homeostasis. *Nat Rev Immunol*. 2018;18(6):374-389. doi:10.1038/s41577-018-0004-8
15. Hardison SE, Brown GD. C-type lectin receptors orchestrate antifungal immunity. *Nat Immunol*. 2012;13(9):817-822. doi:10.1038/ni.2369
16. Drouin M, Saenz J, Chiffoleau E. C-Type Lectin-Like Receptors: Head or Tail in Cell Death Immunity. *Front Immunol*. 2020;11(February). doi:10.3389/fimmu.2020.00251
17. Lima-Junior DS, Mineo TWP, Calich VLG, Zamboni DS. Dectin-1 Activation during Leishmania amazonensis Phagocytosis Prompts Syk-Dependent Reactive Oxygen Species Production To Trigger Inflammasome Assembly and Restriction of Parasite Replication . *J Immunol*. 2017;199(6):2055-2068. doi:10.4049/jimmunol.1700258
18. Kimura Y, Inoue A, Hangai S, et al. The innate immune receptor Dectin-2 mediates the phagocytosis of cancer cells by Kupffer cells for the suppression of liver metastasis. *Proc Natl Acad Sci U S A*. 2016;113(49):14097-14102. doi:10.1073/pnas.1617903113
19. Kerscher B, Willment JA, Brown GD. The Dectin-2 family of C-type lectin-like

receptors: An update. *Int Immunol*. 2013;25(5):271-277. doi:10.1093/intimm/dxt006
20. Yoshikawa M, Yamada S, Sugamata M, Kanauchi O, Morita Y. Dectin-2 mediates phagocytosis of Lactobacillus paracasei KW3110 and IL-10 production by macrophages. *Sci Rep*. 2021;11(1):1-12. doi:10.1038/s41598-021-97087-9
21. Thompson A, da Fonseca DM, Walker L, et al. Dependence on Mincle and Dectin-2 Varies With Multiple Candida Species During Systemic Infection. *Front Microbiol*. 2021;12(February):1-13. doi:10.3389/fmicb.2021.633229
22. Hsieh S. *Advances in Experimental Medicine and Biology Lectin in Host Defense Against Microbial Infections*. (Hsieh S-L, ed.). Springer Nature Singapore; 2018. doi:10.1007/978-981-15-1580-4
23. Chen ST, Li FJ, Hsu TY, et al. CLEC5A is a critical receptor in innate immunity against Listeria infection. *Nat Commun*. 2017;8(1). doi:10.1038/s41467-017-00356-3
24. Wu MF, Chen ST, Yang AH, et al. CLEC5A is critical for dengue virus-induced inflammasome activation in human macrophages. *Blood*. 2013;121(1):95-106. doi:10.1182/blood-2012-05-430090
25. Kim YK, Shin JS, Nahm MH. NOD-like receptors in infection, immunity, and diseases. *Yonsei Med J*. 2016;57(1):5-14. doi:10.3349/ymj.2016.57.1.5
26. Saxena M, Yeretssian G. NOD-like receptors: Master regulators of inflammation and cancer. *Front Immunol*. 2014;5(JUL):1-16. doi:10.3389/fimmu.2014.00327
27. Loo YM, Gale M. Immune Signaling by RIG-I-like Receptors. *Immunity*. 2011;34(5):680-692. doi:10.1016/j.immuni.2011.05.003
28. Rehwinkel J, Gack MU. RIG-I-like receptors: their regulation and roles in RNA sensing. *Nat Rev Immunol*. 2020;20(9):537-551. doi:10.1038/s41577-020-0288-3
29. Borish LC, Steinke JW. 2. Cytokines and chemokines. *J Allergy Clin Immunol*. 2003;111(2 SUPPL. 2):460-475. doi:10.1067/mai.2003.108
30. Khanna-Gupta A, Berliner N. *Granulocytopoiesis and Monocytopoiesis*. Seventh Ed. Elsevier Inc.; 2018. doi:10.1016/B978-0-323-35762-3.00027-5
31. Kennedy AD, Deleo FR. Neutrophil apoptosis and the resolution of infection. *Immunol Res*. 2009;43(1-3):25-61. doi:10.1007/s12026-008-8049-6
32. Kruger P, Saffarzadeh M, Weber ANR, et al. Neutrophils: Between Host Defence, Immune Modulation, and Tissue Injury. *PLoS Pathog*. 2015;11(3):1-22. doi:10.1371/journal.ppat.1004651
33. Yin C, Heit B. Armed for destruction: formation, function and trafficking of neutrophil granules. *Cell Tissue Res*. 2018;371(3):455-471. doi:10.1007/s00441-017-2731-8
34. Dahlgren C, Karlsson A, Bylund J. Intracellular Neutrophil Oxidants: From Laboratory Curiosity to Clinical Reality. *J Immunol*. 2019;202(11):3127-3134. doi:10.4049/jimmunol.1900235
35. Nguyen GT, Green ER, Mecsas J. Neutrophils to the ROScue: Mechanisms of NADPH Oxidase Activation and Bacterial Resistance. *Front Cell Infect Microbiol*. 2017;7(August). doi:10.3389/fcimb.2017.00373
36. Hawley RG, Ramezani A, Hawley TS. Hematopoietic Stem Cells. *Methods Enzymol*. 2006;419(06):149-179. doi:10.1016/S0076-6879(06)19007-2
37. Bjerregaard MD, Jurlander J, Klausen P, Borregaard N, Cowland JB. The in vivo profile of transcription factors during neutrophil differentiation in human bone marrow. *Blood*. 2003;101(11):4322-4332. doi:10.1182/blood-2002-03-0835

38. Evrard M, Kwok IWH, Chong SZ, et al. Developmental Analysis of Bone Marrow Neutrophils Reveals Populations Specialized in Expansion, Trafficking, and Effector Functions. *Immunity*. 2018. doi:10.1016/j.immuni.2018.02.002
39. Ley K, Hoffman HM, Kubes P, et al. Neutrophils: New insights and open questions. *Sci Immunol*. 2018;3(30):eaat4579. doi:10.1126/sciimmunol.aat4579
40. Rosales C. Neutrophils at the crossroads of innate and adaptive immunity. *J Leukoc Biol*. 2020;108(1):377-396. doi:10.1002/JLB.4MIR0220-574RR
41. Doulatov S, Notta F, Eppert K, Nguyen LT, Ohashi PS, Dick JE. Revised map of the human progenitor hierarchy shows the origin of macrophages and dendritic cells in early lymphoid development. *Nat Immunol*. 2010;11(7):585-593. doi:10.1038/ni.1889
42. Paul F, Arkin Y, Giladi A, et al. Transcriptional Heterogeneity and Lineage Commitment in Myeloid Progenitors. *Cell*. 2015;163(7):1663-1677. doi:10.1016/j.cell.2015.11.013
43. Fingerhut L, Dolz G, de Buhr N. What is the evolutionary fingerprint in neutrophil granulocytes? *Int J Mol Sci*. 2020;21(12):1-37. doi:10.3390/ijms21124523
44. Ford Bainton D, Ullyot JL, Farquhar MG. The Development of Neutrophilic Polymorphonuclear Leukocytes in Human Bone Marrow. *J Exp Medice*. 1971;134:907-934.
45. Sollberger G, Streeck R, Apel F, Caffrey BE, Skoultchi AI, Zychlinsky A. Linker histone h1.2 and h1.4 affect the neutrophil lineage determination. *Elife*. 2020;9:1-24. doi:10.7554/eLife.52563
46. Sollberger G, Tilley DO, Zychlinsky A. Neutrophil Extracellular Traps: The Biology of Chromatin Externalization. *Dev Cell*. 2018;44(5):542-553. doi:10.1016/j.devcel.2018.01.019
47. Borregaard N, Theilgaard-Mönch K, Sørensen OE, Cowland JB. Regulation of human neutrophil granule protein expression. *Curr Opin Hematol*. 2001;8(1):23-27. doi:10.1097/00062752-200101000-00005
48. Yu C, Cantor AB, Yang H, et al. Targeted deletion of a high-affinity GATA-binding site in the GATA-1 promoter leads to selective loss of the eosinophil lineage in vivo. *J Exp Med*. 2002;195(11):1387-1395. doi:10.1084/jem.20020656
49. Hirai H, Zhang P, Dayaram T, et al. C/EBPβ is required for “emergency” granulopoiesis. *Nat Immunol*. 2006;7(7):732-739. doi:10.1038/ni1354
50. Zhu Y, Gong K, Denholtz M, et al. Comprehensive characterization of neutrophil genome topology. *Genes Dev*. 2017;31(2):141-153. doi:10.1101/gad.293910.116
51. Hoffmann K, Sperling K, Olins AL, Olins DE. The granulocyte nucleus and lamin B receptor: Avoiding the ovoid. *Chromosoma*. 2007;116(3):227-235. doi:10.1007/s00412-007-0094-8
52. Manley HR, Keightley MC. The Neutrophil Nucleus: An Important Influence on Neutrophil Migration and Function. *Front Immunol*. 2018;9(December):1-18. doi:10.3389/fimmu.2018.02867
53. Collard JF, Senecal JL, Raymond Y. Redistribution of nuclear lamin A is an early event associated with differentiation of human promyelocytic leukemia HL-60 cells. *J Cell Sci*. 1992;101(3):657-670. doi:10.1242/jcs.101.3.657
54. Li Y, Li M, Weigel B, Mall M, Werth VP, Liu M. Nuclear envelope rupture and NET formation is driven by PKCα-mediated lamin B disassembly. *EMBO Rep*. 2020;21(8):1-19. doi:10.15252/embr.201948779
55. Cohen T V., Klarmann KD, Sakchaisri K, et al. The lamin B receptor under

transcriptional control of C/EBPε is required for morphological but not functional maturation of neutrophils. *Hum Mol Genet*. 2008;17(19):2921-2933. doi:10.1093/hmg/ddn191
56. Borregaard N. Development of neutrophil granule diversity. *Ann N Y Acad Sci*. 1997;832:62-68. doi:10.1111/j.1749-6632.1997.tb46237.x
57. Borregaard N, Sehested M, Nielsen BS, Sengeløv H, Kjeldsen L. Biosynthesis of granule proteins in normal human bone marrow cells. Gelatinase is a marker of terminal neutrophil differentiation. *Blood*. 1995;85(3):812-817. doi:10.1182/blood.v85.3.812.bloodjournal853812
58. Gullberg U, Bengtsson N, Bülow E, Garwicz D, Lindmark A, Olsson I. Processing and targeting of granule proteins in human neutrophils. *J Immunol Methods*. 1999;232(1-2):201-210. doi:10.1016/S0022-1759(99)00177-5
59. Le Cabec V, Cowland JB, Calafat J, Borregaard N. Targeting of proteins to granule subsets is determined by timing and not by sorting: The specific granule protein NGAL is localized to azurophil granules when expressed in HL-60 cells. *Proc Natl Acad Sci U S A*. 1996;93(13):6454-6457. doi:10.1073/pnas.93.13.6454
60. Borregaard N, Kjeldsen L, Lollike K, Sengelov H. Granules and secretory vesicles of the human neutrophil. *Int J Pediatr Hematol*. 1996;3(5):307-319.
61. Strzepa A, Pritchard KA, Dittel BN. Myeloperoxidase: A new player in autoimmunity. *Cell Immunol*. 2017;317(January):1-8. doi:10.1016/j.cellimm.2017.05.002
62. N'Diaye E-N, Darzacq X, Astarie-Dequeker C, Daffe M, Calafat J, Maridonneau-Parini I. Fusion of Azurophil Granules with Phagosomes and Activation of Tyrosine Kinase Hck are Specifically Inhibited During Phagocytosis of Mycobacteria by Human Neutrophils. *J Immunol*. 1998;161:4983-4991.
63. Kjeldsen L, Bainton D, Sengelov H, Borregaard N. Structural and functional heterogeneity among peroxidase-negative granules in human neutrophils: identification of a distinct gelatinase- containing granule subset by combined immunocytochemistry and subcellular fractionation. *Blood*. 1993;82(10):3183-3191. doi:10.1182/blood.v82.10.3183.3183
64. Borregaard N, Cowland JB. Granules of the human neutrophilic polymorphonuclear leukocyte. *Blood*. 1997;89(10):3503-3521. doi:10.1182/blood.v89.10.3503
65. Othman A, Sekheri M, Filep JG. Roles of neutrophil granule proteins in orchestrating inflammation and immunity. *FEBS J*. 2021:1-22. doi:10.1111/febs.15803
66. Kjeldsen L, Sengelov H, Lollike K, Nielsen M, Borregaard N. Isolation and characterization of gelatinase granules from human neutrophils. *Blood*. 1994;83(6):1640-1649. doi:10.1182/blood.v83.6.1640.1640
67. Rawat K, Syeda S, Shrivastava A. Neutrophil-derived granule cargoes: paving the way for tumor growth and progression. *Cancer Metastasis Rev*. 2021;40(1):221-244. doi:10.1007/s10555-020-09951-1
68. Amulic B, Cazalet C, Hayes GL, Metzler KD, Zychlinsky A. Neutrophil Function: From Mechanisms to Disease. *Annu Rev Immunol*. 2012;30(1):459-489. doi:10.1146/annurev-immunol-020711-074942
69. Nauseef WM, Borregaard N. Neutrophils at work. *Nat Immunol*. 2014;15(7):602-611. doi:10.1038/ni.2921
70. Theyab A, Algahtani M, Alsharif KF, et al. New insight into the mechanism of granulocyte colony-stimulating factor (G-CSF) that induces the mobilization of

neutrophils. *Hematol (United Kingdom)*. 2021;26(1):628-636. doi:10.1080/16078454.2021.1965725
71. Rigby KM, DeLeo FR. Neutrophils in innate host defense against Staphylococcus aureus infections. *Semin Immunopathol*. 2012;34(2):237-259. doi:10.1007/s00281-011-0295-3
72. Scapini P, Lapinet-Vera JA, Gasperini S, Calzetti F, Bazzoni F, Cassatella MA. The neutrophil as a cellular source of chemokines. *Immunol Rev*. 2000;177(4):195-203. doi:10.1034/j.1600-065X.2000.17706.x
73. Lim K, Hyun YM, Lambert-Emo K, et al. Neutrophil trails guide influenzaspecific CD8+ T cells in the airways. *Science (80-)*. 2015;349(6252). doi:10.1126/science.aaa4352
74. Tecchio C, Micheletti A, Cassatella MA. Neutrophil-derived cytokines: Facts beyond expression. *Front Immunol*. 2014;5(OCT):1-7. doi:10.3389/fimmu.2014.00508
75. Blanter M, Gouwy M, Struyf S. Studying neutrophil function in vitro: Cell models and environmental factors. *J Inflamm Res*. 2021;14:141-162. doi:10.2147/JIR.S284941
76. Metzemaekers M, Gouwy M, Proost P. Neutrophil chemoattractant receptors in health and disease: double-edged swords. *Cell Mol Immunol*. 2020;17(5):433-450. doi:10.1038/s41423-020-0412-0
77. El-Benna J, Hurtado-Nedelec M, Marzaioli V, Marie JC, Gougerot-Pocidalo MA, Dang PMC. Priming of the neutrophil respiratory burst: role in host defense and inflammation. *Immunol Rev*. 2016;273(1):180-193. doi:10.1111/imr.12447
78. Fontayne A, Dang PMC, Gougerot-Pocidalo MA, El Benna J. Phosphorylation of p47phox sites by PKC α, βII, δ, and ζ: Effect on binding to p22phox and on NADPH oxidase activation. *Biochemistry*. 2002;41(24):7743-7750. doi:10.1021/bi011953s
79. Dang PMC, Raad H, Derkawi RA, et al. The NADPH oxidase cytosolic component p67phox is constitutively phosphorylated in human neutrophils: Regulation by a protein tyrosine kinase, MEK1/2 and phosphatases 1/2A. *Biochem Pharmacol*. 2011;82(9):1145-1152. doi:10.1016/j.bcp.2011.07.070
80. Cross AR, Segal AW. The NADPH oxidase of professional phagocytes - Prototype of the NOX electron transport chain systems. *Biochim Biophys Acta - Bioenerg*. 2004;1657(1):1-22. doi:10.1016/j.bbabio.2004.03.008
81. Winterbourn CC, Kettle AJ, Hampton MB. Reactive Oxygen Species and Neutrophil Function. *Annu Rev Biochem*. 2016;85(1):765-792. doi:10.1146/annurev-biochem-060815-014442
82. Harbort CJ, Soeiro-Pereira PV, Von Bernuth H, et al. Neutrophil oxidative burst activates ATM to regulate cytokine production and apoptosis. *Blood*. 2015;126(26):2842-2851. doi:10.1182/blood-2015-05-645424
83. Brinkmann V, Reichard U, Goosmann C, et al. Neutrophil Extracellular Traps Kill Bacteria. *Science (80-)*. 2004;303(5663):1532-1535. doi:10.1126/science.1092385
84. Thanabalasuriar A, Scott BNV, Peiseler M, et al. Neutrophil Extracellular Traps Confine Pseudomonas aeruginosa Ocular Biofilms and Restrict Brain Invasion. *Cell Host Microbe*. 2019;25(4):526-536.e4. doi:10.1016/j.chom.2019.02.007
85. Kaplan MJ, Radic M. Neutrophil Extracellular Traps: Double-Edged Swords of Innate Immunity. *J Immunol*. 2012;189(6):2689-2695. doi:10.4049/jimmunol.1201719
86. Schmid-burgk JL, Schmidt T, Gaidt MM, et al. Neutrophil Extracellular Traps:

The Biology of Chromatin Externalization. *Dev Cell*. 2018;30(1):1-17. doi:10.1016/j.devcel.2017.10.013
87. Papayannopoulos V, Metzler KD, Hakkim A, Zychlinsky A. Neutrophil elastase and myeloperoxidase regulate the formation of neutrophil extracellular traps. *J Cell Biol*. 2010;191(3):677-691. doi:10.1083/jcb.201006052
88. Amulic B, Knackstedt SL, Abu Abed U, et al. Cell-Cycle Proteins Control Production of Neutrophil Extracellular Traps. *Dev Cell*. 2017;43(4):449-462.e5. doi:10.1016/j.devcel.2017.10.013
89. Van Der Linden M, Westerlaken GHA, Van Der Vlist M, Van Montfrans J, Meyaard L. Differential Signalling and Kinetics of Neutrophil Extracellular Trap Release Revealed by Quantitative Live Imaging. *Sci Rep*. 2017;7(1):1-11. doi:10.1038/s41598-017-06901-w
90. Healy LD, Puy C, Itakura A, et al. Colocalization of neutrophils, extracellular DNA and coagulation factors during NETosis: Development and utility of an immunofluorescence-based microscopy platform. *J Immunol Methods*. 2016;435:77-84. doi:10.1016/j.jim.2016.06.002
91. Albrengues J, Shields MA, Ng D, et al. Neutrophil extracellular traps produced during inflammation awaken dormant cancer cells in mice. *Science (80-)*. 2018;361(6409):eaao4227. doi:10.1126/science.aao4227
92. Pechous RD. With friends like these: The complex role of neutrophils in the progression of severe pneumonia. *Front Cell Infect Microbiol*. 2017;7(MAY). doi:10.3389/fcimb.2017.00160
93. Jones HR, Robb CT, Perretti M, Rossi AG. The role of neutrophils in inflammation resolution. *Semin Immunol*. 2016;28(2):137-145. doi:10.1016/j.smim.2016.03.007
94. Bhatt N, Ghosh R, Roy S, et al. Robust reprogramming of Ataxia-Telangiectasia patient and carrier erythroid cells to induced pluripotent stem cells. *Stem Cell Res*. 2016. doi:10.1016/j.scr.2016.08.006
95. Amirifar P, Ranjouri MR, Yazdani R, Abolhassani H, Aghamohammadi A. Ataxia-telangiectasia: A review of clinical features and molecular pathology. *Pediatr Allergy Immunol*. 2019;30(3):277-288. doi:10.1111/pai.13020
96. Cao J, Shen R, Zhang W, et al. Clinical diagnosis and genetic counseling of atypical ataxia-telangiectasia in a Chinese family. *Mol Med Rep*. 2019;49(5):3441-3448. doi:10.3892/mmr.2019.9992
97. Moin M, Aghamohammadi A, Kouhi A, et al. Ataxia-Telangiectasia in Iran: Clinical and Laboratory Features of 104 Patients. *Pediatr Neurol*. 2007;37(1):21-28. doi:10.1016/j.pediatrneurol.2007.03.002
98. Rothblum-Oviatt C, Wright J, Lefton-Greif MA, McGrath-Morrow SA, Crawford TO, Lederman HM. Ataxia telangiectasia: A review. *Orphanet J Rare Dis*. 2016;11(1):1-21. doi:10.1186/s13023-016-0543-7
99. Fiévet A, Bellanger D, Rieunier G, et al. Functional classification of ATM variants in ataxia-telangiectasia patients . *Hum Mutat*. 2019;40(10):0-3. doi:10.1002/humu.23778
100. Tal E, Alfo M, Zha S, et al. Inactive Atm abrogates DSB repair in mouse cerebellum more than does Atm loss, without causing a neurological phenotype. *DNA Repair (Amst)*. 2018;72(September):10-17. doi:10.1016/j.dnarep.2018.10.001
101. McGrath-Morrow SA, Rothblum-Oviatt CC, Wright J, et al. Multidisciplinary management of ataxia telangiectasia: Current perspectives. *J Multidiscip Healthc*. 2021;14:1637-1643. doi:10.2147/JMDH.S295486

102. Wajid M, Al-baradie RS. Ataxia-telangiectasia : future prospects. 2014:159-167.
103. Connelly PJ, Smith N, Chadwick R, Exley AR, Shneerson JM, Pearson ER. Recessive mutations in the cancer gene Ataxia Telangiectasia Mutated (ATM), at a locus previously associated with metformin response, cause dysglycaemia and insulin resistance. *Diabet Med*. 2016;33(3):371-375. doi:10.1111/dme.13037
104. Nowak-Wegrzyn A, Crawford TO, Winkelstein JA, Carson KA, Lederman HM. Immunodeficiency and infections in ataxia-telangiectasia. *Pediatrics*. 2005;116(2):568. doi:10.1542/peds.2005-0698SSS
105. McGrath-Morrow SA, Ndeh R, Collaco JM, et al. Inflammation and transcriptional responses of peripheral blood mononuclear cells in classic ataxia telangiectasia. *PLoS One*. 2018;13(12):1-16. doi:10.1371/journal.pone.0209496
106. Stracker TH, Roig I, Knobel PA, Marjanović M. The ATM signaling network in development and disease. *Front Genet*. 2013;4(MAR):1-19. doi:10.3389/fgene.2013.00037
107. Blackford AN, Jackson SP. ATM, ATR, and DNA-PK: The Trinity at the Heart of the DNA Damage Response. *Mol Cell*. 2017;66(6):801-817. doi:10.1016/j.molcel.2017.05.015
108. Cara L, Baitemirova M, Follis J, Larios-Sanz M, Ribes-Zamora A. The ATM- and ATR-related SCD domain is over-represented in proteins involved in nervous system development. *Sci Rep*. 2016;6(December 2015):1-8. doi:10.1038/srep19050
109. Udayakumar D, Horikoshi N, Mishra L, Hunt C, Pandita TK. Detecting ATM-Dependent Chromatin Modification in DNA Damage Response. *Chromatin Protoc Third Ed*. 2015:1-487. doi:10.1007/978-1-4939-2474-5_18
110. Shiloh Y, Ziv Y. The ATM protein kinase: regulating the cellular response to genotoxic stress, and more. *Nat Rev Mol Cell Biol*. 2013;14(4):197-210. doi:10.1038/nrm3546
111. Rotman G, Shiloh Y. Ataxia-telangiectasia: is ATM a sensor of oxidative damage and stress? 1997;(4).
112. Berger ND, Stanley FKT, Moore S, Goodarzi AA. ATM-dependent pathways of chromatin remodelling and oxidative DNA damage responses. *Philos Trans R Soc Lond B Biol Sci*. 2017;372(1731):20160283. doi:10.1098/rstb.2016.0283
113. Ortega-Atienza S, Wong VC, DeLoughery Z, Luczak MW, Zhitkovich A. ATM and KAT5 safeguard replicating chromatin against formaldehyde damage. *Nucleic Acids Res*. 2016;44(1):198-209. doi:10.1093/nar/gkv957
114. Tsouroula K, Furst A, Rogier M, et al. Temporal and Spatial Uncoupling of DNA Double Strand Break Repair Pathways within Mammalian Heterochromatin. *Mol Cell*. 2016;63(2):293-305. doi:10.1016/j.molcel.2016.06.002
115. Povea-Cabello S, Oropesa-Ávila M, de la Cruz-Ojeda P, et al. Dynamic reorganization of the cytoskeleton during apoptosis: The two coffins hypothesis. *Int J Mol Sci*. 2017;18(11). doi:10.3390/ijms18112393
116. van Sluis M, McStay B. Nucleolar reorganization in response to rDNA damage. *Curr Opin Cell Biol*. 2017;46:81-86. doi:10.1016/j.ceb.2017.03.004
117. Lemaître C, Grabarz A, Tsouroula K, et al. Nuclear position dictates DNA repair pathway choice. *Genes Dev*. 2014;28(22):2450-2463. doi:10.1101/gad.248369.114
118. Dobbin MM, Madabhushi R, Pan L, et al. SIRT1 collaborates with ATM and HDAC1 to maintain genomic stability in neurons. *Nat Neurosci*.

2013;16(8):1008-1015. doi:10.1038/nn.3460
119. Taylor G, Eskeland R, Hekimoglu-balkan B, Pradeepa MM, Bickmore WA. H4K16 acetylation marks active genes and enhancers of embryonic stem cells , but does not alter chromatin compaction. *Genome Res*. 2013;23:2053-2065. doi:10.1101/gr.155028.113
120. Kastan M, Bakkenist C. DNA damage activates ATM through intermolecular autophosphorylation and dimmer association. *Nature*. 2003;421:499-506.
121. Chakravarty S, Bhat UA, Reddy RG, Gupta P, Kumar A. *Histone Deacetylase Inhibitors and Psychiatric Disorders*. Elsevier Inc.; 2014. doi:10.1016/B978-0-12-417114-5.00025-5
122. Sherrard A, Bishop P, Panagi M, Villagomez MB, Alibhai D, Kaidi A. Streamlined histone-based fluorescence lifetime imaging microscopy (FLIM) for studying chromatin organisation. *Biol Open*. 2018;7(3). doi:10.1242/bio.031476
123. Likhatcheva M, Gieling RG, Brown JAL, Demonacos C, Williams KJ. A Novel Mechanism of Ataxia Telangiectasia Mutated Mediated Regulation of Chromatin Remodeling in Hypoxic Conditions. *Front Cell Dev Biol*. 2021;9(September):1-11. doi:10.3389/fcell.2021.720194
124. Berkovich E, Monnat RJ, Kastan MB. Roles of ATM and NBS1 in chromatin structure modulation and DNA double-strand break repair. *Nat Cell Biol*. 2007;9(6):683-690. doi:10.1038/ncb1599
125. Timashev LA, Babcock H, Zhuang X, de Lange T. The DDR at telomeres lacking intact shelterin does not require substantial chromatin decompaction. *Genes Dev*. 2017;31(6):578-589. doi:10.1101/gad.294108.116
126. Ji S, Zhu L, Gao Y, et al. Baf60b-mediated ATM-p53 activation blocks cell identity conversion by sensing chromatin opening. *Cell Res*. 2017;27(5):642-656. doi:10.1038/cr.2017.36
127. Tresini M, Marteijn JA, Vermeulen W. Bidirectional coupling of splicing and ATM signaling in response to transcription-blocking DNA damage. *RNA Biol*. 2016;13(3):272-278. doi:10.1080/15476286.2016.1142039
128. Kuehne A, Emmert H, Soehle J, et al. Acute Activation of Oxidative Pentose Phosphate Pathway as First-Line Response to Oxidative Stress in Human Skin Cells. *Mol Cell*. 2015;59(3):359-371. doi:10.1016/j.molcel.2015.06.017
129. Gregory MA, D'Alessandro A, Alvarez-Calderon F, et al. ATM/G6PD-driven redox metabolism promotes FLT3 inhibitor resistance in acute myeloid leukemia. *Proc Natl Acad Sci*. 2016;113(43):E6669-E6678. doi:10.1073/pnas.1603876113
130. Alagoz M, Chiang SC, Sharma A, El-Khamisy SF. ATM Deficiency Results in Accumulation of DNA-Topoisomerase I Covalent Intermediates in Neural Cells. *PLoS One*. 2013;8(4). doi:10.1371/journal.pone.0058239
131. Neves-Costa A, Moita LF. Modulation of inflammation and disease tolerance by DNA damage response pathways. *FEBS J*. 2017;284(5):680-698. doi:10.1111/febs.13910
132. Figueiredo N, Chora A, Raquel H, et al. Anthracyclines induce DNA damage response-mediated protection against severe sepsis. *Immunity*. 2013;39(5):874-884. doi:10.1016/j.immuni.2013.08.039
133. Erttmann SF, Härtlova A, Sloniecka M, et al. Loss of the DNA Damage Repair Kinase ATM Impairs Inflammasome-Dependent Anti-Bacterial Innate Immunity. *Immunity*. 2016;45(1):106-118. doi:10.1016/j.immuni.2016.06.018
134. Härtlova A, Erttmann SF, Raffi FAM, et al. DNA Damage Primes the Type I Interferon System via the Cytosolic DNA Sensor STING to Promote Anti-

Microbial Innate Immunity. *Immunity*. 2015;42(2):332-343. doi:10.1016/j.immuni.2015.01.012
135. Rincón E, Rocha-Gregg BL, Collins SR. A map of gene expression in neutrophil-like cell lines. *BMC Genomics*. 2018;19(1):1-17. doi:10.1186/s12864-018-4957-6
136. Schmid-burgk JL, Schmidt T, Gaidt MM, et al. OutKnocker : a web tool for rapid and simple genotyping of designer nuclease edited cell lines. 2014:1719-1723. doi:10.1101/gr.176701.114
137. Frank SB, Schulz V V., Miranti CK. A streamlined method for the design and cloning of shRNAs into an optimized Dox-inducible lentiviral vector. *BMC Biotechnol*. 2017;17(1):1-10. doi:10.1186/s12896-017-0341-x
138. Anheim M. Autosomal recessive cerebellar ataxias. *Prat Neurol - FMC*. 2012;2(4):237-249. doi:10.1016/j.praneu.2011.07.002
139. Schroeder SA, Zielen S. Infections of the respiratory system in patients with ataxia-telangiectasia. *Pediatr Pulmonol*. 2014;49(4):389-399. doi:10.1002/ppul.22817
140. Tong SYC, Davis JS, Eichenberger E, Holland TL, Fowler VG. Staphylococcus aureus infections: Epidemiology, pathophysiology, clinical manifestations, and management. *Clin Microbiol Rev*. 2015;28(3):603-661. doi:10.1128/CMR.00134-14
141. Chambers HF, DeLeo FR. Waves of resistance: Staphylococcus aureus in the antibiotic era. *Nat Rev Microbiol*. 2009;7(9):629-641. doi:10.1038/nrmicro2200
142. O'Neill AJ. Staphylococcus aureus SH1000 and 8325-4: Comparative genome sequences of key laboratory strains in staphylococcal research. *Lett Appl Microbiol*. 2010;51(3):358-361. doi:10.1111/j.1472-765X.2010.02885.x
143. Hiramatsu K, Katayama Y, Matsuo M, et al. Multi-drug-resistant Staphylococcus aureus and future chemotherapy. *J Infect Chemother*. 2014;20(10):593-601. doi:10.1016/j.jiac.2014.08.001
144. Lorenz KS, Athina G, Falko A, et al. Neutrophil extracellular traps drive inflammatory pathogenesis in malaria. *Sci Immunol*. 2019;4(40):eaaw0336. doi:10.1126/sciimmunol.aaw0336
145. Pedruzzi E, Fay M, Elbim C, Gaudry M, Gougerot-Pocidalo MA. Differentiation of PLB-985 myeloid cells into mature neutrophils, shown by degranulation of terminally differentiated compartments in response to N-formyl peptide and priming of superoxide anion production by granulocyte-macrophage colony-stimulating fact. *Br J Haematol*. 2002;117(3):719-726. doi:10.1046/j.1365-2141.2002.03521.x
146. Tucker K, Lilly M, Heck LJ, Rado T. Characterization of a new human diploid myeloid leukemia cell line (PLB- 985) with granulocytic and monocytic differentiating capacity. *Blood*. 1987;70(2):372-378. doi:10.1182/blood.v70.2.372.372
147. Pivot-Pajot C, Chouinard FC, Amine El Azreq M, Harbour D, Bourgoin SG. Characterisation of degranulation and phagocytic capacity of a human neutrophilic cellular model, PLB-985 cells. *Immunobiology*. 2010;215(1):38-52. doi:10.1016/j.imbio.2009.01.007
148. Volk APD, Barber BM, Goss KL, et al. Priming of neutrophils and differentiated PLB-985 cells by pathophysiological concentrations of TNF-α is partially oxygen dependent. *J Innate Immun*. 2011;3(3):298-314. doi:10.1159/000321439
149. Zhen L, King AAJ, Xiao Y, Chanock SJ, Orkin SH, Dinauer MC. Gene targeting of X chromosome-linked chronic granulomatous disease locus in a human

myeloid leukemia cell line and rescue by expression of recombinant gp91(phox). *Proc Natl Acad Sci U S A*. 1993;90(21):9832-9836. doi:10.1073/pnas.90.21.9832
150. Selmeczy Z, Szelényi J, Német K, Vizi ES. The inducibility of TNF-α production is different in the granulocytic and monocytic differentiated forms of wild type and CGD-mutant PLB-985 cells. *Immunol Cell Biol*. 2003;81(6):472-479. doi:10.1046/j.1440-1711.2003.01190.x
151. Chiam LYT, Verhagen MMM, Haraldsson A, et al. Cutaneous Granulomas in Ataxia Telangiectasia and Other Primary Immunodeficiencies: Reflection of Inappropriate Immune Regulation? *Dermatology*. 2011;223(1):13-19. doi:10.1159/000330335
152. Grattarola M, Borghi C, Emionite L, Lulli P, Chessa L, Vergani L. Modifications of nuclear architecture and chromatin organization in ataxia telangiectasia cells are coupled to changes of gene transcription. *J Cell Biochem*. 2006;99(4):1148-1164. doi:10.1002/jcb.20895
153. Herbst S, Gutierrez MG. LRRK2 in Infection: Friend or Foe? *ACS Infect Dis*. 2019;5(6):809-815. doi:10.1021/acsinfecdis.9b00051
154. Moniaga CS, Watanabe S, Honda T, Nielsen S, Hara-Chikuma M. Aquaporin-9-expressing neutrophils are required for the establishment of contact hypersensitivity. *Sci Rep*. 2015;5(October):1-13. doi:10.1038/srep15319
155. Xu Y, Xu C, Price BD. Mechanistic links between ATM and histone methylation codes during DNA repair. *Prog Mol Biol Transl Sci*. 2012;110:263-288. doi:10.1016/B978-0-12-387665-2.00010-9
156. Trojer P, Reinberg D. Facultative Heterochromatin: Is There a Distinctive Molecular Signature? *Mol Cell*. 2007;28(1):1-13. doi:10.1016/j.molcel.2007.09.011
157. Georgopoulos K. In search of the mechanism that shapes the neutrophil's nucleus. *Genes Dev*. 2017;31(2):85-87. doi:10.1101/gad.296228.117
158. Ghiasy S, Leila P, Azizi G, et al. The clinical significance of complete class switching defect in Ataxia telangiectasia patients. *Expert Rev Clin Immunol*. 2017;13(5):499-505. doi:10.1080/1744666X.2017.1292131
159. Dujka ME, Puebla-Osorio N, Tavana O, Sang M, Zhu C. ATM and p53 are essential in the cell-cycle containment of DNA breaks during V(D)J recombination in vivo. *Oncogene*. 2010;29(7):957-965. doi:10.1038/onc.2009.394
160. Libri A, Marton T, Deriano L. The (Lack of) DNA Double-Strand Break Repair Pathway Choice During V(D)J Recombination. *Front Genet*. 2022;12(January):1-10. doi:10.3389/fgene.2021.823943
161. Saunders RA, Michniacki TF, Hames C, et al. Elevated inflammatory responses and targeted therapeutic intervention in a preclinical mouse model of ataxia-telangiectasia lung disease. *Sci Rep*. 2021;11(1):1-15. doi:10.1038/s41598-021-83531-3
162. Gul E, Sayar EH, Gungor B, et al. Type I IFN–related NETosis in ataxia telangiectasia and Artemis deficiency. *J Allergy Clin Immunol*. 2018;142(1):246-257. doi:10.1016/j.jaci.2017.10.030
163. Ashkenazi A, Marks RS. Luminol-dependent chemiluminescence of human phagocyte cell lines: Comparison between DMSO differentiated PLB 985 and HL 60 cells. *Luminescence*. 2009;24(3):171-177. doi:10.1002/bio.1091
164. Manda-Handzlik A, Bystrzycka W, Wachowska M, et al. The influence of agents differentiating HL-60 cells toward granulocyte-like cells on their ability to release

neutrophil extracellular traps. *Immunol Cell Biol*. 2018;96(4):413-425. doi:10.1111/imcb.12015
165. Takishita Y, Yasuda H, Shimizu M, et al. Formation of neutrophil extracellular traps in mitochondrial DNA deficient cells. 2020;66(1):15-23. doi:10.3164/jcbn.19
166. Karlsson A, Nixon JB, McPhail LC. Phorbol myristate acetate induces neutrophil NADPH-oxidase activity by two separate signal transduction pathways: Dependent or independent of phosphatidylinositol 3-kinase. *J Leukoc Biol*. 2000;67(3):396-404. doi:10.1002/jlb.67.3.396
167. Rani R, Kumar S, Sharma A, et al. Mechanisms of concanavalin A-induced cytokine synthesis by hepatic stellate cells: Distinct roles of interferon regulatory factor-1 in liver injury. *J Biol Chem*. 2018;293(48):18466-18476. doi:10.1074/jbc.RA118.005583
168. Unniyampurath U, Crisci A, Krishnan MN. Loss of Function Genetic Screen Identifies ATM Kinase as a Positive Regulator of TLR3-Mediated NF-κB Activation. *iScience*. 2020;23(8):101356. doi:10.1016/j.isci.2020.101356
169. Rincón E, Rocha-Gregg BL, Collins SR. A map of gene expression in neutrophil-like cell lines. *BMC Genomics*. 2018;19(1):1-17. doi:10.1186/s12864-018-4957-6
170. Datta U, Sehgal S, Kumar L, et al. Immune status in ataxia telangiectasia. *Indian J Med Res*. 1991;94:252-254.
171. Zhang Y, Lee JH, Paull TT, et al. Mitochondrial redox sensing by the kinase ATM maintains cellular antioxidant capacity. *Sci Signal*. 2018;11(538). doi:10.1126/scisignal.aaq0702
172. Britt EC, Lika J, Giese MA, et al. Switching to the cyclic pentose phosphate pathway powers the oxidative burst in activated. 2022;4(March). doi:10.1038/s42255-022-00550-8
173. Nordenfelt P, Bauer S, Lönnbro P, Tapper H. Phagocytosis of streptococcus pyogenes by all-trans retinoic acid-differentiated HL-60 cells: Roles of azurophilic granules and NADPH oxidase. *PLoS One*. 2009;4(10). doi:10.1371/journal.pone.0007363
174. Daniel JA, Pellegrini M, Lee BS, et al. Loss of ATM kinase activity leads to embryonic lethality in mice. *J Cell Biol*. 2012;198(3):295-304. doi:10.1083/jcb.201204035
175. Gardet A, Benita Y, Li C, et al. LRRK2 Is Involved in the IFN-γ Response and Host Response to Pathogens. *J Immunol*. 2010;185(9):5577-5585. doi:10.4049/jimmunol.1000548
176. Zhang Q, Pan Y, Yan R, et al. Commensal bacteria direct selective cargo sorting to promote symbiosis. *Nat Immunol*. 2015;16(9):918-926. doi:10.1038/ni.3233
177. Härtlova A, Herbst S, Peltier J, et al. LRRK2 is a negative regulator of Mycobacterium tuberculosis phagosome maturation in macrophages . *EMBO J*. 2018;37(12):1-17. doi:10.15252/embj.201798694
178. Cheng YL, Lin YS, Chen CL, et al. Activation of Nrf2 by the dengue virus causes an increase in CLEC5A, which enhances TNF-α production by mononuclear phagocytes. *Sci Rep*. 2016;6(May):1-15. doi:10.1038/srep32000
179. Huff LA, Yan S, Clemens MG. Mechanisms of ataxia telangiectasia mutated (ATM) control in the DNA damage response to oxidative stress, epigenetic regulation, and persistent innate immune suppression following sepsis. *Antioxidants*. 2021;10(7). doi:10.3390/antiox10071146
180. Xu Y, Ashley T, Brainerd EE, Bronson RT, Meyn MS, Baltimore D. Targeted

disruption of ATM leads to growth retardation, chromosomal fragmentation during meiosis, immune defects, and thymic lymphoma. *Genes Dev*. 1996;10(19):2411-2422. doi:10.1101/gad.10.19.2411
181. Li J, Chen J, Ricupero CL, et al. Nuclear accumulation of HDAC4 in ATM deficiency promotes neurodegeneration in ataxia telangiectasia. *Nat Med*. 2012;18(5):783-790. doi:10.1038/nm.2709
182. Li J, Hart RP, Mallimo EM, Swerdel MR, Kusnecov AW, Herrup K. EZH2-mediated H3K27 trimethylation mediates neurodegeneration in ataxia-telangiectasia. *Nat Neurosci*. 2013;16(12):1745-1753. doi:10.1038/nn.3564
183. Batliner J, Mancarelli MM, Jenal M, et al. CLEC5A (MDL-1) is a novel PU.1 transcriptional target during myeloid differentiation. *Mol Immunol*. 2011;48(4):714-719. doi:10.1016/j.molimm.2010.10.016
184. Arthur RK, Ma L, Slattery M, et al. Evolution of H3K27me3-marked chromatin is linked to gene expression evolution and to patterns of gene duplication and diversification. *Genome Res*. 2014;24(7):1115-1124. doi:10.1101/gr.162008.113
185. Margueron R, Li G, Sarma K, et al. Ezh1 and Ezh2 Maintain Repressive Chromatin through Different Mechanisms. *Mol Cell*. 2008;32(4):503-518. doi:10.1016/j.molcel.2008.11.004
186. Lavin MF. The appropriateness of the mouse model for ataxia-telangiectasia : Neurological defects but no neurodegeneration. *DNA Repair (Amst)*. 2013;12(8):612-619. doi:10.1016/j.dnarep.2013.04.014

Appendix

Table A1 Kits for blood processing, RNA and plasmid purification, and ELISA

Kits	Supplier	Catalogue number
EasySep™ Direct Human Neutrophil Isolation Kit	STEMCELL Technologies	19666
EasyEights™ EasySep™ Magnet	STEMCELL Technologies	18103
Human IL-8/CXCL8 DuoSet ELISA	R&D Systems	DY208
PureLink™ RNA Mini Kit	Thermo Fisher Scientific (Invitrogen)	12183020A
GeneJET Plasmid Miniprep Kit	Thermo Fisher Scientific	K0502
PureLink™ HiPure Plasmid Maxiprep Kit	Thermo Fisher Scientific (Invitrogen)	K210007
Pierce™ BCA Protein Assay Kit - Reducing Agent Compatible	Thermo Fisher Scientific	23250

ELISA, enzyme-linked immunosorbent assay.

Table A2 Cloning and qPCR enzymes

Reagent	Supplier	Catalogue number
Phusion® High-Fidelity DNA Polymerase	New England Biolabs	M0530S
NheI-HF®	New England Biolabs	R3131S
EcoRI-HF®	New England Biolabs	R0101S
SpeI-HF®	New England Biolabs	R3133S
Antarctic Phosphatase	New England Biolabs	M0289S
T4 Polynucleotide Kinase	New England Biolabs	M0201S
Rapid DNA Ligation Kit (T4 DNA ligase/5x Rapid Ligation Buffer)	Thermo Fisher Scientific	K1422
NEB® Stable Competent *E. coli* (High Efficiency)	New England Biolabs	C3040I
5 PRIME Hot Master Mix	Quantabio	2200400
CellTrace™ Violet Cell Proliferation Kit, for flow Cytometry	Thermo Fisher Scientific (Life Technologies)	C34571
pHrodo™ Red Phagocytosis Particle Labeling Kit for Flow Cytometry	Thermo Fisher Scientific (Invitrogen)	A10026
High-Capacity cDNA Reverse Transcription Kit	Thermo Fisher Scientific (Applied Biosystems)	4368814
Fast SYBR™ Green Master Mix	Thermo Fisher Scientific (Applied Biosystems)	4385610

qPCR, quantitative polymerase chain reaction.

Table A3 Media and reagents

Reagent	Supplier	Catalogue number
Phosphate Buffered Saline (PBS)	Thermo Fisher Scientific (Gibco)	10010-023
RPMI 1640 with Phenol red	Thermo Fisher Scientific (Gibco)	21875-034
RPMI 1640 w/o Phenol red	Thermo Fisher Scientific (Gibco)	11835-063
DMEM GlutaMAX™ with Phenol red	Thermo Fisher Scientific (Gibco)	10566-016
Seahorse XF RPMI Medium pH 7.4	Agilent Technologies	103576-100
HBSS with Calcium and Magnessium	Lonza	10-527F
HBSS w/o Calcium Magnessium or Phenol Red	Lonza	10-547F
L-Glutamine 200mM	Thermo Fisher Scientific (Gibco)	25030-081
Penicillin-Streptomycin (10,000U/ml)	Thermo Fisher Scientific (Gibco)	15140-122
Penicillin-Streptomycin-Glutamine (100x)	Thermo Fisher Scientific (Gibco)	10378-016
Fetal Bovine Serum (FBS)	Thermo Fisher Scientific (Gibco)	26140-079
Donkey Serum	Merck (Sigma-Aldrich)	D9663-10ML
Gelatin from cold water fish skin	Merck (Sigma-Aldrich)	G7041-100G
Histopaque-1119	Merck (Sigma-Aldrich)	11191-100ML
Percoll®	VWR (G&E Helathcare)	17-0891-01
HSA-20% solution	VWR (SEQENS)	31020
Histopaque-1077	Merck (Sigma-Aldrich)	10771-100ML
Tris Buffered Saline	Biomedical Sciences media kitchen	
0.5M EDTA	Biomedical Sciences media kitchen	
Tryptic Soy Broth	Biomedical Sciences media kitchen	
Triptic Soy Agar	Biomedical Sciences media kitchen	
LB-Agar plates with Ampicillin	Biomedical Sciences media kitchen	
HEPES buffer solution	Thermo Fisher Scientific (Gibco)	15630-056
Human pooled serum	VWR (SEQENS)	21000P-100ML
Bovine Serum Albumin (BSA)	Fischer Scientific	BP9700-100
Dimethyl sulfoxide (DMSO)	Merck (Sigma-Aldrich)	D2650-100ML
N,N-dimethylformamide (DMF)	Merck (Sigma-Aldrich)	D4551-250ML
Nutridoma-CS	Merck (Roche)	11363743001
Puromycin		
Doxycycline	Merck (Sigma-Aldrich)	
SYTOX Green	Thermo Fisher Scientific (Invitrogen)	S7020
SYTOX Orange	Thermo Fisher Scientific (Invitrogen)	S11368
SYTO Green	Thermo Fisher Scientific (Invitrogen)	S7575
ATM inhibitor (KU55933)	Merck (Sigma-Aldrich)	SML1109-5MG
ATM inhibitor (KU60019)	Merck (Sigma-Aldrich)	5319780001
Horseradish Peroxidase (HRP)	Merck (Sigma-Aldrich)	77332-100MG
Luminol	Merck (Sigma-Aldrich)	123072
Phorbol 12-myristate 13-acetate (PMA)	Merck (Sigma-Aldrich)	P8139-1MG

Table A3 Media and reagents (cont.)

Reagent	Supplier	Catalogue number
Concanavalin A (ConA)	Merck (Sigma-Aldrich)	C5275-5MG
Trehalose-6,6-dibehenate (TDB)	Invivogen	tlrl-tdb
Zymosan A from *Saccharomyces cerevisae*	Merck (Sigma-Aldrich)	Z4250
Lipopolysaccharides (LPS)	Merck (Sigma-Aldrich)	L5668
N-Formyl-Met-Leu-Phe	Merck (Sigma-Aldrich)	F3506-5MG
Recombinant Human TNF	Peprotech	300-01A
S. aureus (JE2)	Massey Lab	N/A
S. Aureus (SH1000)	Massey Lab	N/A
S. aureus (Newman)	Massey Lab	N/A
C. albicans	Diezmann Lab	N/A
96wp white	Appleton woods (Sterilin)	SS246
Glucose	Merck (Sigma-Aldrich)	G8270-1KG
Carbonyl cyanide 4-(trifluoromethoxy) phenylhydrazone (FCCP)	Merck (Sigma-Aldrich)	C2920-10MG
Oligomycin	Alfa Aesar	J61898.MA
Rotenone	Merck (Sigma-Aldrich)	R8875-5G
Antimycin A	Alfa Aesar	J63522.MA
Deoxy-D-glucose (2-DG)	Merck (Sigma-Aldrich)	D8375-5G
Lipofectamine 2000	Thermo Fisher Scientific (Invitrogen)	11668019
Polyethylene glycol (PEG)	Merck (Sigma-Aldrich)	89510-250G-F
Magnessium Chloride	Merck (Sigma-Aldrich)	M8266-100G
Ethyl alcohol Pure	Merck (Sigma-Aldrich)	459836-2L
Methanol	Merck (Sigma-Aldrich)	322415-100ML
Potassium Acetate	Merck (Sigma-Aldrich)	P1190-100G
β-mercaptoethanol	Merck (Sigma-Aldrich)	M6250-100ML
Sodium Acetate	Merck (Sigma-Aldrich)	S2889-250G
Trisodium citrate dihydrated	Merck (Sigma-Aldrich)	S1804-500G
Pierce Protease and Phosphatase Inhibitor Mini Tablets, EDTA-free	Thermo Fisher Scientific	A32961
Bay-678 (human neutrophil elastase inhibitor)	Merck (Sigma-Aldrich)	SML1563-5MG
Cathepsin G Inhibitor	Alfa Aesar	J65957
NuPAGE™ LDS Sample Buffer (4x)	Thermo Fisher Scientific (Invitrogen)	NP0007
NuPAGE™ 4 to 12%, Bis-Tris, 1.0 mm, Mini Protein Gels	Thermo Fisher Scientific (Invitrogen)	NP0321BOX
NuPAGE™ 3 to 8%, Tris-Acetate, 1.0 mm, Mini Protein Gels	Thermo Fisher Scientific (Invitrogen)	EA0375BOX
NuPAGE™ MES SDS Running Buffer (20x)	Thermo Fisher Scientific (Invitrogen)	NP0002
NuPAGE™ MOPS SDS Running Buffer (20x)	Thermo Fisher Scientific (Invitrogen)	NP0001
NuPAGE™ Tris-Acetate SDS Running Buffer (20x)	Thermo Fisher Scientific (Invitrogen)	LA0041
RIPA Buffer	Merck (Sigma-Aldrich)	R0278-50ML

Table A3 Media and reagents (cont.)

Reagent	Supplier	Catalogue number
Phenylmethanesulfonyl fluoride (PMSF)	Merck (Sigma-Aldrich)	P7626-250MG
Tris(2-carbocyethyl)phosphine hydrochloride (TCEP)	Merck (Sigma-Aldrich)	C4706-2G
Halt™ Phosphatase Inhibitor Cocktail	Thermo Fisher Scientific	78420
DAPI	Merck (Sigma-Aldrich)	D9542-1MG
Mowiol® 4-88	Merck (Sigma-Aldrich)	81381-50G
16% Paraformaldehyde Aqueous Solution, EM Grade	Electron Microscopy Sciences	50-980-487

Table A4 Antibodies

Antibodies	Supplier	Catalogue number	Concentration
PE anti-human CD10 Antibody clone HI10a	Biolegend	312204	1 in 50
PE/Cyanine7 anti-mouse/human CD11b Antibody Clone M1/70	Biolegend	101216	1 in 50
Brilliant Violet 785™ anti-human CD14 Antibody Clone M5E2	Biolegend	301840	1 in 50
Alexa Fluor® 700 anti-human CD15 (SSEA-1) Antibody Clone HI98	Biolegend	301920	1 in 50
FITC anti-human CD16 Antibody Clone 3G8	Biolegend	302006	1 in 50
PE/Cyanine7 anti-human CD62L Antibody Clone DREG-56	Biolegend	304822	1 in 50
Brilliant Violet 421™ anti-human CD63 Antibody H5C6	Biolegend	353030	1 in 50
APC anti-human CD66b Antibody Clone G10F5	Biolegend	305118	1 in 50
CD125 (IL-5R) Antibody, anti-human, REAfinity™ Clone REA705	Miltenyi Biotec	130-110-543	1 in 25
Brilliant Violet 605™ anti-human CD184 (CXCR4) Antibody Clone 12G5	Biolegend	306522	1 in 50
PE/Dazzle™ 594 anti-human CD182(CXCR2) Antibody Clone 5E8/CXCR2	Biolegend	320722	1 in 50
PerCP/Cyanine5.5 Streptavidin	Biolegend	405214	1 in 200
Human TruStain FcX™ (Fc Receptor Blocking Solution)	Biolegend	422302	1 in 200
Rat anti-Calgranulin A (S100A8) Clone 8H6	in-house made (Max Planck Institute for Infection Biology, Berlin)	N/A	1 in 100
Anti-Lamin A+ Lamin C antibody [JOL2]	Abcam	ab40567	1 in 500
Histon H3 (D1H2) XP® Rabbit mAb	Cell Signaling	4499	1 in 1000

Table A4 Antibodies (cont.)

Antibodies	Supplier	Catalogue number	Concentration
H3K9me3 Polyclonal Antibody	Thermo Fisher Scientific (Invitrogen)	720093	1 in 1000
Tri-Methyl-Histon H3 (Lys27)(C36B11) Rabbit mAb	Cell Signaling	9733	1 in 1000
Recombinant Anti-Lamin B1 antibody [EPR8985(B)]	Abcam	ab133741	1 in 1000
GAPDH (D16H11) XP® Rabbit mAb	Cell Signaling	5174	1 in 1000
alpha Tubulin monoclonal antibody (DM1A)	Thermo Fisher Scientific (Invitrogen)	62204	1 in 1000
Donkey anti-Rat IgG (H+L) Highly Cross-Adsorbed Secondary Antibody, Alexa Fluor™ 488	Thermo Fisher Scientific (Invitrogen)	A-21208	1 in 200
Anti-rabbit IgG HRP-linked Ab	Cell Signaling	7074P2	1 in 2000
Anti-mouse IgG HRP-linked Ab	Cell Signaling	7076P2	1 in 2000

Table A5 Primers used

Primers	Supplier	Target
ACACTCTTTCCCTACACGACGctcttccgatctCAGGCTCTATCTGAAACCTTCAC	Eurofins	FWD-ATMcr1
TGACTGGAGTTCAGACGTGTGctcttccgatctACTGAGTCTAAAACATGGTCTTG	Eurofins	REV-ATMcr1
ACACTCTTTCCCTACACGACGctcttccgatctTACAGACAGTGATGTGTGTTCTG	Eurofins	FWD-ATMcr2
TGACTGGAGTTCAGACGTGTGctcttccgatctTTCAGGATCTCGAATCAGGCGCT	Eurofins	REV-ATMcr2
AATGATACGGCGACCACCGAGATCTACACTATAGCCTACACTCTTTCCCTACACGACGCT	Eurofins	Illumina FWD 1
AATGATACGGCGACCACCGAGATCTACACATAGAGGCACACTCTTTCCCTACACGACGCT	Eurofins	Illumina FWD 2
AATGATACGGCGACCACCGAGATCTACACCCTATCCTACACTCTTTCCCTACACGACGCT	Eurofins	Illumina FWD 3
AATGATACGGCGACCACCGAGATCTACACGGCTCTGAACACTCTTTCCCTACACGACGCT	Eurofins	Illumina FWD 4
AATGATACGGCGACCACCGAGATCTACACAGGCGAAGACACTCTTTCCCTACACGACGCT	Eurofins	Illumina FWD 5
AATGATACGGCGACCACCGAGATCTACACTAATCTTAACACTCTTTCCCTACACGACGCT	Eurofins	Illumina FWD 6

Table A5 Primers used (cont.)

Primers	Supplier	Target
AATGATACGGCGACCACCGAGATCTACAC CAGGACGTACACTCTTTCCCTACACGACGC T	Eurofins	Illumina FWD 7
AATGATACGGCGACCACCGAGATCTACAC GTACTGACACACTCTTTCCCTACACGACGC T	Eurofins	Illumina FWD 8
CAAGCAGAAGACGGCATACGAGATCGAGT AATGTGACTGGAGTTCAGACGTGTGCT	Eurofins	Illumina REV 1
CAAGCAGAAGACGGCATACGAGATTCTCC GGAGTGACTGGAGTTCAGACGTGTGCT	Eurofins	Illumina REV 2
CAAGCAGAAGACGGCATACGAGATAATGA GCGGTGACTGGAGTTCAGACGTGTGCT	Eurofins	Illumina REV 3
CAAGCAGAAGACGGCATACGAGATGGAAT CTCGTGACTGGAGTTCAGACGTGTGCT	Eurofins	Illumina REV 4
CAAGCAGAAGACGGCATACGAGATTTCTG AATGTGACTGGAGTTCAGACGTGTGCT	Eurofins	Illumina REV 5
CAAGCAGAAGACGGCATACGAGATACGAA TTCGTGACTGGAGTTCAGACGTGTGCT	Eurofins	Illumina REV 6
CAAGCAGAAGACGGCATACGAGATAGCTT CAGGTGACTGGAGTTCAGACGTGTGCT	Eurofins	Illumina REV 7
CAAGCAGAAGACGGCATACGAGATGCGCA TTAGTGACTGGAGTTCAGACGTGTGCT	Eurofins	Illumina REV 8
CAAGCAGAAGACGGCATACGAGATCATAG CCGGTGACTGGAGTTCAGACGTGTGCT	Eurofins	Illumina REV 9
CAAGCAGAAGACGGCATACGAGATTTCGC GGAGTGACTGGAGTTCAGACGTGTGCT	Eurofins	Illumina REV 10
CAAGCAGAAGACGGCATACGAGATGCGCG AGAGTGACTGGAGTTCAGACGTGTGCT	Eurofins	Illumina REV 11
CAAGCAGAAGACGGCATACGAGATCTATC GCTGTGACTGGAGTTCAGACGTGTGCT	Eurofins	Illumina REV 12
TCTTATGGACTGTTGCTGGGA	Eurofins	FWD-CLEC4E
TCCATAATTGTAGCAGGAGAGC	Eurofins	REV-CLEC4E
TCTTGGAATGAAAGCAGGGAC	Eurofins	FWD-CLEC5A
CCACCTTTTCTCTTCACGATGG	Eurofins	REV-CLEC5A
AAAAGAGGCTGGTTGTCCCT	Eurofins	FWD-CLEC6A
GCACCTTTGTCCCTTCACTG	Eurofins	REV-CLEC6A

Table A5 Primers used (cont.)

Primers	Supplier	Target
ACTGAGGTACCATGGCTCTG	Eurofins	FWD-CLEC7A
CTTCTCCACCCTTCCTCTTACA	Eurofins	REV-CLEC7A
CTCTCCACCACACTGCAAAC	Eurofins	FWD-CLEC12A
GGCCATTTTACTCTCCTGCC	Eurofins	REV-CLEC12A
GGCCACCAACAGTACAGTCC	Eurofins	FWD-CSF3R
GTTCCACAGAGGCAGGTGAG	Eurofins	REV-CSF3R
TCCTGGTGCGAGAAGACTTT	Eurofins	FWD-CTSG
GTGATGTGTTGCTGGGTGTT	Eurofins	REV-CTSG
CAACTTCGTCATGTCGGCC	Eurofins	FWD-ELANE
CGAGAGGTTATGGGCTCCC	Eurofins	REV-ELANE
CTGACGATGAAAGTGGCCAG	Eurofins	FWD-PADI4
GATGTCTGCGCACAAGGAG	Eurofins	REV-PADI4
CTAGCCAAACGAAATCTCAGTGATATTACT AGTATATCACTGAGATTTCGTTTGTTTTTG	Eurofins	FWD-ATMshRNA1
AATTCAAAAACAAACGAAATCTCAGTGATAT ACTAGTAATATCACTGAGATTTCGTTTGG	Eurofins	REV-ATMshRNA1
CTAGCGCCTCCAATTCTTCACAGTAATACT AGTTTACTGTGAAGAATTGGAGGCTTTTTG	Eurofins	FWD-ATMshRNA2
AATTCAAAAAGCCTCCAATTCTTCACAGTAA ACTAGTATTACTGTGAAGAATTGGAGGCG	Eurofins	REV-ATMshRNA2
CTAGCCCAAGGTCTATGATATGCTTATACT AGTTAAGCATATCATAGACCTTGGTTTTTG	Eurofins	FWD-ATMshRNA3
AATTCAAAAACCAAGGTCTATGATATGCTTA ACTAGTATAAGCATATCATAGACCTTGGG	Eurofins	REV-ATMshRNA3
QuantiTect® Primer Assay (Hs_MPO_1_SG)	Qiagen	MPO
QuantiTect® Primer Assay (Hs_LRRK2_1_SG)	Qiagen	LRRK2
QuantiTect® Primer Assay (Hs_GAPDH_1_SG)	Qiagen	GAPDH

Table A6 Equipment used

Equipment	Supplier	Catalogue number
FLUOstar plate reader	BMG Labtech	N/A
IncuCyte ZOOM	Essen Bioscences	N/A
EVOS confocal microscope	Invitrogen	N/A
Seahorse XFe96 Analyzer	Agilent Technologies	N/A
SimpliAmp™ Thermal Cycler	Thermo Fisher Scientific (Applied Biosystems)	N/A
QuantStudio™ 3 Real-Time PCR System	Thermo Fisher Scientific (Applied Biosystems)	N/A
NanoDrop™ Lite Spectrophotometer	Thermo Fisher Scientific	N/A
BD LSRFortessa™ Cell Analyzer	BD Biosciences	N/A
Q125 Sonicator	QSONICA	N/A
iBlot 2 Dry Blotting System	Thermo Fisher Scientific (Invitrogen)	N/A
Power Blotter-Semi-dry Transfer System	Thermo Fisher Scientific (Invitrogen)	N/A
Leica DMI6000	Leica Microsystems	N/A
LI-COR Odyssey® XF	LI-COR, Inc	N/A
Tecnai 12-FEI 120kV BioTwin Spirit		

N/A, non-applicable.

Table A7 Software used

Software	Supplier	Catalogue number
FIJI image analysis	imagej.net	N/A
FlowJo	BD (FlowJO, LLC)	N/A
Wave Controller	Agilent Technologies	N/A
OutKnocker 2.0	Outknocker.org	N/A
Graphpad Prism	GraphPad by Dotmatics	N/A
BioRender	BioRender	N/A
Leica LASX	Leica Microsystems	N/A

N/A, non-applicable.